Diplomarbeit

Advanced treatment of municipal wastewater by ozonation and activated carbon adsorption

Ausgeführt am Institut für Wassergüte und Ressourcenmanagement

der Technischen Universität Wien

Unter der Anleitung von

Ass.Prof. Mag.rer.nat. Dr.rer.nat Norbert Kreuzinger

und

Dipl. -Ing. Dr.techn. Heidemarie Schaar

Dipl. -Ing. Daniela Reif

durch

Liad Weisz, BSc.

1549242

Wien

Datum   Unterschrift

Eidesstattliche Erklärung

Ich erkläre an Eides statt, dass die vorliegende Arbeit nach den anerkannten Grundsätzen für wissenschaftliche Abhandlungen von mir selbstständig erstellt wurde. Alle verwendeten Hilfsmittel, insbesondere die zugrunde gelegte Literatur, sind in dieser Arbeit genannt und aufgelistet. Die aus den Quellen wörtlich entnommenen Stellen sind als solche kenntlich gemacht.

Das Thema dieser Arbeit wurde von mir bisher weder im In- noch Ausland einer Beurteilerin / einem Beurteiler zur Begutachtung in irgendeiner Form als Prüfungsarbeit vorgelegt. Diese Arbeit stimmt mit der von den Begutachterinnen / Begutachtern beurteilten Arbeit überein.

Wien, am 29.10.2021

_____

Unterschrift

Acknowledgments

I wish to express my sincere gratitude to my advisors, DI Dr. Heidemarie Schaar, and DI Daniela Reif, for their valuable insights and guidance in the past months. I appreciate the great support throughout this thesis very much. Furthermore, I would like to thank M.Eng Lam Thanh Phan for his experimental assistance. A special thank-you goes to DI Zdravka Saracevic for her practical support and Dr. Ernis Saracevic for his constructive feedbacks and interesting discussions.

Last but not least, I would like to thank the Institute for Water Quality and Resource Management, especially Ass. Prof. Norbert Kreuzinger, for giving me the opportunity to write my master thesis in his research group.

Kurzfassung. Organische Spurenstoffe (OS) sind potenziell toxische, niedermolekulare Verbindungen, die in der aquatischen Umwelt ubiquitär sind. Die Einleitung von Abwasser in Oberflächengewässer gilt als wesentlicher Faktor für ihre Allgegenwart. Begründet wird dies damit, dass die herkömmliche Abwasserreinigung viele dieser Verbindungen nicht entfernen kann. Zwecks ihrer Minderung hat sich in zahlreichen Studien die Einführung einer weitergehenden Behandlungsstufe als effizient erwiesen.

In dieser Diplomarbeit wird die Anwendung von Ozonung und Aktivkohle (AK) Adsorption auf Ablaufproben untersucht. Hierfür wurden im Labormaßstab Ozon- und Aktivkohle-Batch-Tests durchgeführt. Der Fokus liegt auf der Minderung von neun OS, bestehend aus sieben Arzneimitteln, einem Korrosionsinhibitor und einem Herbizid. Zusätzlich wurden nach der Ozonung die Parameter Bromat und BSB_5 gemessen. Aufgrund der Anwendbarkeit des Surrogatparameters für Online-Monitoring wurde eine Korrelation von ΔSAC_{254} mit der spezifischen Ozon- und AK-Dosis, und damit mit OS-Minderung, untersucht. Zur Untersuchung der Entfernungsleistung der Ozonung wurden drei verschiedene spezifische Ozondosen im Bereich von 0,40-0,88 g O_3 g^{-1} DOC in Proben aus der Kläranlage A eingesetzt. Um die Entfernungsleistung der kommerziell erhältlichen Pulveraktivkohle (PAK) Epibon A zu testen, wurde eine kombinierte Behandlung, bestehend aus Ozonung und einem anschließenden PAK Adsorptionsschritt, mit den Dosen 1,0-2,0 g AK g^{-1} DOC, auf ozonierten Ablaufproben aus der Kläranlage A angewendet. Darüber hinaus wurde die Entfernungsleistung eines neuartigen Produkts beim AK-Dosisbereich 0,8-2,3 g AK g^{-1} DOC in den Kläranlagen A, B und C untersucht. Bei den Adsorptionsexperimenten wurde die Korrelation der linearisierten Adsorptionsisothermen an den Langmuir- und Freundlich-Modellen analysiert.

Es war ersichtlich, dass Verbindungen mit höheren Reaktionskonstanten k_{O_3} bereits bei niedrigeren spezifischen Ozondosen effizient entfernt werden konnten. Obwohl Sulfamethoxazol (SMX) eine hohe Reaktionskonstante aufweist, zeigte es überraschenderweise bei niedriger und mittlerer spezifischen Ozondosis nur eine mittlere Entfernung. Bei 0,88 g O_3 g^{-1} DOC wurde Bromat mit einer Konzentration von 18.4 ± 1.2 µg L^{-1} gebildet, welche den Trinkwasser-Grenzwert von 10 µg L^{-1} überschritt. Der Einfluss der Ozonung auf den Summenparameter BSB_5 zeigte keine eindeutigen Ergebnisse, sodass weitere Untersuchungen erforderlich wären. Als Ozonung und PAK-Adsorption kombiniert wurden, hatten die Verbindungen Carbamazepin (CBZ), Diclofenac (DCF) und Bezafibrat (BZF) bereits bei der niedrigsten angewendeten spezifischen AK-Dosis hohe Entfernungen von über 80 %. Ein Vergleich von Ozonung, PAK-Adsorption und einer Kombination davon führte zu unterschiedlichen Entfernungen, wobei die Letztgenannte eine bessere Leistung für die meisten Verbindungen aufwies. In den ozonierten, PAK-behandelten Proben zeigte nur die linearisierte Adsorptionsisotherme von BZF eine hohe Korrelation (R^2 = 0,89) mit dem Langmuir-Modell. Bezüglich der Entfernungsleistung des Produkts war eine spezifische AK-Dosis von 1,5 g AK g^{-1} DOC für eine hohe Entfernung über 80 % in Probe C erforderlich, während 2,25 g AK g^{-1} DOC für die Entfernung der meisten Verbindungen in Probe B nicht ausreichte. Ein Vergleich mit dem PAK CARBOPAL® zeigte eine schlechtere Leistung des Produkts. Bei Anwendung des Produkts wies die linearisierte Adsorptionsisotherme von CBZ eine hohe Korrelation (R^2 = 0,92) mit dem Langmuir-Adsorptionsmodell auf. Für eine genauere Untersuchung der Adsorptionsmodelle wären jedoch mehr Datenpunkte notwendig. Für die Kläranlage A wurde eine hohe lineare Korrelation (R^2 = 0,94) zwischen dem Surrogatparameter ΔSAC_{254} und der spezifischen Ozondosis festgestellt. Eine lineare Korrelation zwischen ΔSAC_{254} und der spezifischen AK-Dosis zeigte unterschiedliche Resultate, wenn das Produkt angewendet wurde.

Schlagwörter: weitergehende Abwasserreinigung, Organische Spurenstoffe, Ozonung, Aktivkohle Adsorption

Abstract. Organic micropollutants (OMPs) are potentially toxic, low molecular compounds that are ubiquitous in the aquatic environment. The discharge of wastewater effluents to surface waters is considered a major contributing factor to their omnipresence. This lies in the fact that the typical wastewater treatment train is incapable to remove many of these compounds. The introduction of an enhanced treatment stage for the abatement of OMPs has been proven efficient by numerous studies.

In this thesis, the application of ozonation and activated carbon (AC) adsorption to wastewater effluent samples is explored. For this purpose, lab-scale ozone and activated carbon batch tests were carried out. The focus lies on the abatement of nine OMPs, consisting of seven pharmaceuticals, a corrosion inhibitor, and a herbicide. In addition, the parameters bromate and BOD_5 were measured following ozonation. A correlation of ΔSAC_{254} with the specific ozone and AC dose was performed due to the applicability of the surrogate parameter for online monitoring. To investigate the removal performance of ozonation, three different specific ozone doses at the range of 0.40-0.88 g O_3 g^{-1} DOC were applied on samples from wastewater treatment plant A. To test the removal performance of the commercially available PAC Epibon A, a combined treatment of ozonation and a subsequent powdered activated carbon (PAC) adsorption step, consisting of 1.0-2.0 g AC g^{-1} DOC, was applied on ozonated effluent samples from WWTP A. Moreover, the removal performance of a novel product was analyzed at the specific AC dose range of 0.8-2.3 g AC g^{-1} DOC in three different WWTPs, A, B, and C. Concerning the adsorption experiments, the fit of the linearized adsorption isotherms to the Langmuir and Freundlich models was analyzed.

Consistent with compound reactivity, it could be shown that compounds with a higher second-order rate constant are efficiently removed already at a lower specific ozone dose. Surprisingly, although sulfamethoxazole (SMX) has a high second-order rate constant, it exhibited only intermediate removal at the low and intermediate specific ozone dose. Bromate formation could be observed only at the highest specific ozone dose of 0.88 g O_3 g^{-1} DOC, which exceeded the drinking water threshold of 10 µg L^{-1}. The effect of ozonation on the sum parameter BOD_5 showed inconclusive results, thereby requiring further investigations. When ozonation and PAC adsorption were combined, the compounds carbamazepine (CBZ), diclofenac (DCF) and bezafibrate (BZF) had high removal percentages above 80% already at the lowest specific AC applied. A comparison of ozonation, PAC adsorption, and a combination thereof resulted in different removals among the compounds, whereas the latter had a superior performance for most compounds. A correlation of the ozonated, AC-treated samples to the adsorption isotherms showed a high fit ($R^2 = 0.89$) of bezafibrate to the Langmuir model. Concerning the product performance, a specific AC dose of 1.5 g AC g^{-1} DOC was required for a high removal above 80% in sample C, whereas 2.25 g AC g^{-1} DOC was not sufficient for the removal of most compounds in sample B. A comparison of the product with the PAC CARBOPAL® showed an inferior performance of the product. CBZ had a high fit ($R^2 = 0.92$) to the Langmuir adsorption model. However, further investigations are necessary. A high linear correlation of $R^2 = 0.94$ between the surrogate parameter ΔSAC_{254} and the specific ozone dose was obtained for WWTP A. A linear correlation between ΔSAC_{254} and the specific AC dose showed different results for the product in different WWTPs.

Keywords: enhanced wastewater treatment, organic micropollutants, ozonation, activated carbon adsorption

Table of contents

List of figures

List of tables

List of abbreviations and notations

AC	*Activated carbon*
AMO	*Ammonium oxygenase*
AOB	*Ammonium oxidizing bacteria*
ATU	*Allthiourea*
BDOC	*Biodegradable dissolved organic compounds*
BOD5	*Biological oxygen demand over 5 days*
BTA	*Benzotriazole*
BZF	*Bezafibrate*
CAS	*Conventional activated sludge*
CBZ	*Carbamazepine*
DCF	*Diclofenac*
DI water	*Deionized water*
DIU	*Diuron*
DOM	*Dissolved organic matter*
D_{spec}	*Specific ozone dose*
ESI-MS	*Electrospray ionization - mass spectroscopy*
HPLC	*High performance liquid chromatography*
IBP	*Ibuprofen*
KI	*Potassium iodide*
$\log D_{OW}$	*pH-dependent n-octanol water distribution ratio*
MTP	*Metoprolol*
online SPE	*Online solid-phase extraction*
PAC	*Powdered activated carbon*
PACl	*Polyaluminum chloride*
PNEC	*Predictive No Effect Concentration*
R_{ct}	*Ratio of ozone to OH radical concentration*
SAC_{254}	*Spectral absorption coefficient at 254 nm*
SMX	*Sulfamethoxazole*
SUV_{254}	*Specific UV254*
t_{eq}	*Equilibration time*
TMP	*Trimethoprim*
π-π EDA	*π-π electorn donating accepting interactions*

1 Introduction

1.1 Organic micropollutants

Organic micropollutants (OMPs) are a group of potentially harmful compounds which are present in municipal wastewater in concentration ranges of $\mu g\,L^{-1}$ to $ng\,L^{-1}$. The umbrella term organic micropollutants comprises a large group of chemicals including pharmaceuticals, personal care products, steroid hormones, industrial chemicals, and pesticides. Many of these compounds can be quantified by established target analysis approach. However, the majority of OMPs present in wastewater consists of unknown compounds, including metabolites or transformation products. With over 10.000 prescription drugs and 300 over-the-counter drugs currently produced in the USA, it appears impossible to target all those compounds (Rogowska et al., 2020). The detection of OMPs is conducted by separation methods combined with mass spectrometry, which include LC-MS or GC-MS. A target analysis such as MRM is established for certain OMPs of interest, while a full-scan mode allows measuring a large spectrum of compounds. While a full-scan mode provides qualitative information about existing OMPs, target analysis allows a sensitive quantification of selected OMPs (Rogowska et al., 2020).

Certain OMPs are resistant to biological degradation during the activated sludge process. Therefore, the discharge of effluents from wastewater treatment plants (WWTPs) to receiving water bodies is an important contributor to the ubiquitous occurrence of OMPs in aquatic systems, especially in surface waters (Luo et al., 2014; Rizzo et al., 2019). In comparison, ground water is found to be less contaminated in studies conducted in Europe and the USA. A few sources for the occurrence of OMPs in groundwater include landfill leachate, contaminated surface waters, and infiltration from septic tanks and agricultural land (Lapworth et al., 2012).

Because OMPs are used regularly, long-term exposure to them is related to chronic effects of aquatic organisms, which directly affects their sustainability. These effects may be negligible during the life cycle of an organism, but they may become evident long-term (Santos et al., 2010). For example, it has been documented that male fish in waterways downstream of municipal effluents undergo feminization, which is linked with the presence of estrogenic substances in wastewater (Grieshaber et al., 2018). Diclofenac (DCF) is a recalcitrant OMP and one of the most commonly found nonsteroidal anti-inflammatory drugs (NSAIDs) within the aquatic environment, with a reported median concentration of 0.15 µg/L and maximal concentration of 2 µg/L in surface waters. According to Schwaiger et al. (2004), a 4-week exposure of rainbow trout to DCF in environmentally relevant concentrations (5 µg/L) can induce renal lesions, which indicates a potential toxic effect for fish in the environment. Due to the risks posed by pharmaceuticals, ecotoxicological research has established a hazard quotient (HQ), which is calculated for each compound by the quotient of the highest concentration ever measured in hospital wastewaters and the predicted no effect concentration (PNEC) (Frédéric & Yves, 2014).

Despite the environmental and toxicological concerns arising from OMPs discharged into the aquatic environments, there are currently no discharged limits regulated on an EU level. In 2013, the European Union Directive 2013/39/EU recommended monitoring and treatment options for a list of 45 priority substances (PS). Two years later, Decision 2015/495/EU was reported. The decision established a watchlist for monitoring 17 pollutants, and according to the risk posed Environmental Quality

Standards (EQS) should be set at the EU level. According to the EQS Directive, the list should be updated every two years. The watchlist includes five neonicotinoid pesticides (imidacloprid, thiacloprid, thiamethoxam, clothianidin, acetamiprid), three non-neonicotinoid pesticides (methiocarb, oxadiazon, triallate), three macrolide antibiotics (azithromycin, clarithromycin, erythromycin), two natural hormones (17-β-estradiol and estrone), and a synthetic hormone (17-α-ethinylestradiol), a pharmaceutical (DCF), a UV-filter (2-ethylhexyl-4-methoxycinnamate) and an antioxidant (2,6-di-*tert*-butyl-4-methylphenol). In 2018, Decision 2018/840/EU was reported, which concluded that five substances should be removed from the list since high-quality monitoring data has been gathered (DCF, oxadiazon, triallate, 2-ethylhexl-4-methoxycinnamate and 2,6-di-*tert*-butyl-4-methylphenol), while a pesticide (metaflumizone) and two antibiotics (amoxicillin, ciprofloxacin) were added (Barbosa et al. (2016); Directive 2013/39/EU).

1.1.1 Factors affecting removal efficiency in conventional WWTPs

Since the term OMPs comprises many chemicals with varying physicochemical properties, different factors influence their removal efficiency and detection. Besides the operating conditions in the WWTP (e.g., sludge retention, hydraulic retention time, temperature, presence of growth substrates, redox conditions) and wastewater matrix (e.g., pH, ionic strength), the physicochemical properties of OMPs are regarded as the most important factors (Chavoshani et al., 2020).

During primary treatment OMPs can be removed by sedimentation and flotation, for which the mechanism of action is sorption. The exact sorption interaction of hydrophobic OMPs to activated sludge is characterized by absorption, which takes place by hydrophobic interactions of aliphatic and aromatic groups with the lipophilic cell membrane of microorganisms and lipid fractions of the sludge (Suarez et al., 2009). As a general rule, the sorption capacity depends on the *n*-octanol-water partition coefficient (log K_{OW}) of the compounds: log K_{OW} < 2.5 indicates a low sorption capacity, 2.5 < log K_{OW} < 4 indicates a medium sorption capacity, and log K_{OW} > 4 indicates a high sorption capacity (Rogers, 1996). As such, compounds with log K_{OW} < 2.5 are not expected to sorb to sludge and may not be removed during primary sludge withdrawal. Depending on the pKa of a compound and the pH of the water, a compound can be neutral or charged. The charge leads to electrostatic interaction with the charged sludge. Negatively charged molecules are expected to experience a charge repulsion with the negatively charged microorganisms of the activated sludge, whereas positively charged compounds may undergo adsorption onto the sludge surface (Suarez et al., 2009). Charged species can also undergo hydrophobic interactions with the sludge matrix, leading to their sorption (Cirja et al., 2008).

Biological treatment refers to the cellular uptake processes by microorganisms and their biodegradation by enzymes during conventional activated sludge (CAS) treatment. Some microorganisms can assimilate OMPs as biomass or maintenance substrates leading to their abatement. The levels of removal are reported to vary from a few percent for recalcitrant compounds to 100 % for readily biodegradable compounds (Kamaz et al., 2019). The biodegradative fate of a compound depends on its structure, concentration, and microbial populations. Concerning chemical structures, linear molecules with short side chains are considered easily biodegradable, as well as unsaturated aliphatic molecules and molecules possessing electron-donating function groups. Conversely, persistent molecules are structurally long with highly branched side chains, saturated/polycyclic molecules, as well as molecules possessing sulfate, halogen, or electron-withdrawing functional groups (Luo et al., 2014). Since biodegradability of most compounds requires an enzyme-saturating substrate concentration (copiotrophic metabolism), it is more likely that biotransformation occurs due to co-metabolism. It was suggested that the enzyme ammonium oxygenase (AMO) present in ammonium oxidizing bacteria (AOBs) is responsible for catalyzing the

degradation of OMPs co-metabolically with ammonia (Alvarino et al., 2018; Daughton & Ternes, 1999). Redox conditions are another important factor as they influence which microbial population develops. In general, aerobic processes are regarded as more effective for the biotransformation of most substances, consistent with AOBs role in OMPs' degradation. Nevertheless, some substances are reportedly better eliminated under anaerobic conditions, such as sulfamethoxazole (SMX) and trimethoprim (TMP) (Alvarino et al., 2018; Ngo et al., 2020).

1.2 Advanced wastewater treatment for OMP removal

Advanced wastewater treatment encompasses many techniques, including ozonation, AC adsorption, membrane filtration, and advanced oxidation processes (AOPs). Abegglen & Siegrist (2012) set four criteria for the feasibility of advanced wastewater treatment:

   (1) the technique should target a broad spectrum of substances.

   (2) by-products should be avoided.

   (3) the treatment unit should be integrated into the existing system.

   (4) expenditures regarding material, energy, personnel must be justifiable.

They applied these four criteria on 13 advanced techniques and, accordingly, only ozonation and powdered activated carbon (PAC) adsorption were rated as broadly suitable techniques for the removal of OMPs. Details are shown in Table 1. It should be noted that at the time the report has been published (2012) the use of granular activated carbon (GAC) still lacked data for its evaluation, however, since then it has become popular.

Table 1: Comparison of ozonation and PAC adsorption in view of the four criteria (Abegglen & Siegrist, 2012)

Criteria	Ozonation	PAC adsorption
Dose for > 80 % abatement	3-5 g O_3 m^{-3} 0.4-0.6 g O_3 g^{-1} DOC[a]	12-15 g m^{-3} 1.5-3.0 g AC g^{-1} DOC[a]
By-products/waste	Oxidation by-products require a downstream installation of a biological treatment unit	5-10 % increase of sludge production, PAC must be incinerated
Integrability	good	good
Increase of energy consumption	0.05-0.1 kWh m^{-3}	0.01-0.04 kWh m^{-3}

[a]Rizzo et al. (2019)

1.2.1 Ozonation

Ozonation as water treatment technology was already applied more than a century ago for the purpose of disinfection and prevention of waterborne disease. Other fields of application include bleaching and oxidation of iron and manganese. Nowadays ozonation finds use in both industrial and municipal WWTPs. Objectives for the application of ozone as a wastewater treatment technique include the requirement to meet higher quality standards of effluent and for water recycling. Such standard parameters encompass disinfection, decrease in sum parameters (DOC, SUV$_{254}$), DOM

removal, color removal, and transformation of OMPs (Gottschalk et al., 2009; Paraskeva & Graham, 2002).

Ozonation is usually applied after tertiary wastewater treatment to reduce ozone consumption by the CAS process. Downstream of the ozonation unit a biological post-treatment (e.g. sand or GAC filter) should be installed for Assimilable Organic Carbon (AOC) removal, as these compounds are of ecotoxicological concern (Von Sonntag & Von Gunten, 2012). A typical treatment train is shown in Figure 1.
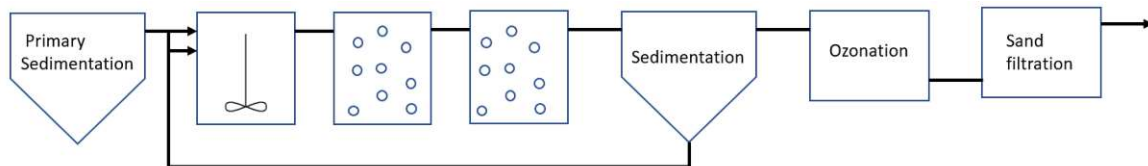
Figure 1: Typical treatment train for wastewater ozonation, adapted from Von Sonntag & Von Gunten (2012)

1.2.1.1 Physicochemical properties of ozone

Ozone (O_3) is a triatomic, polar molecule consisting of oxygen atoms. From the point of view of molecular geometry, O_3 has a trigonal planar structure. Considering the electron pair geometry, it has a bent shape due to the lone pair of electrons in the central oxygen atom. This reduces the bond angle to 116.78°.

According to the molecular orbital theory, the positively charged oxygen atom and the neutral end oxygen atom are sp^2 hybridized, whereas the negatively charged oxygen atom is sp^3 hybridized. Therefore, the σ framework consists of an sp^3-sp^2 and an sp^2-sp^2 σ bonds, while the remaining two p orbitals form a π molecular orbital. However, the electrons in the π molecular orbital are considered delocalized across orbitals throughout the molecule, resulting in each end oxygen atom carrying a formal charge of -0.5. This corresponds to the observed bond length (1.278 Å) of O_3, which is intermediate between a double and a single bond. Due to the 1,3-dipole structure, O_3 can act both as a nucleophile and as an electrophile (Bailey, 1958; Trambarulo et al., 1953). In addition, O_3 has a high oxidation potential of 2.07 V which makes it highly reactive, a property that led to its wide use in the field of water treatment (Paraskeva & Graham, 2002).
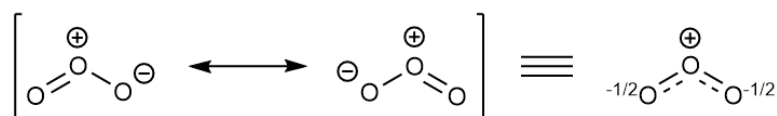
Figure 2: Mesomeric O_3 states

1.2.1.2 Kinetics

As a highly reactive molecule, O_3 may oxidize both organic and inorganic molecules. However, the removal of organics is of special interest in water and wastewater treatment. Many studies focusing on OMP removal by O_3 in advanced wastewater treatment have been conducted. These studies have published rate constants of OMPs, allowing to assess their reactivity with O_3 and classify them according to their removal efficiency. Nevertheless, it must be kept in mind that the unique composition of wastewaters impacts both the removal efficiency as well as the formation of undesired oxidation by-products (Gottschalk et al., 2009).

1.2.1.2.1 Reactions

The oxidation of OMPs by O_3 is characterized by second-order kinetics (Gottschalk et al., 2009). According to (Jekel & Dott, 2013), compounds with k_{O_3} higher than 10^4 are regarded as highly reactive, those with $10^4 < k_{O_3} < 10$ are considered moderately reactive, while those with $k_{O_3} < 10$ show a low reactivity. Compared to the O_3 second-order rate constant, the $\cdot OH$ second-order rate constant is higher by a few orders of magnitude when regarding polar organic compounds. Their value distribution is, except for diuron (DIU), narrower, ranging from 10^9 $M^{-1}s^{-1}$ to diffusion-controlled 10^{10} $M^{-1}s^{-1}$. Due to its high reactivity, $\cdot OH$ is also rapidly consumed by scavengers found in the wastewater matrix. The lower rate constant values of O_3 reflect its selectivity, targeting specific electron-rich moieties, versus the non-selectivity of $\cdot OH$, which reacts readily with aliphatics, olefines, or aromatics. In addition, this difference indicates that while substances possessing electron-rich moieties may be eliminated by both oxidative pathways, those with low reaction rates are mainly subject to the $\cdot OH$ oxidative pathway (Lee et al., 2013).

There are two types of reactions involving O_3 and organics: the direct reactions and reactions of $\cdot OH$, formed by the decomposition of O_3. Often both reactions occur during ozonation. As shown in Equation (1), the temporal abatement of a target compound is a function of oxidant and reactant concentrations, and the respective rate constant (Gottschalk et al., 2009). To solve for the reactant concentration, also the oxidant exposure time must be known, as described in Equation (2) (Buffle et al., 2006).

$$-\frac{d[M]}{dt} = k"_{O_3}[M][O_3] + k"_{\cdot OH}[M][\cdot OH] \tag{1}$$

$$[M] = [M]_0 * e^{-k"_{O_3} \cdot \int_0^{tR}[O_3]\cdot dt - k"_{\cdot OH} \cdot \int_0^{tR}[\cdot OH]\cdot dt} \tag{2}$$

Whether the direct or indirect reaction is favored depends on different factors. In the context of drinking water, factors such as low DOM levels, acidification, and the presence of $\cdot OH$ scavengers, which include bicarbonate and carbonate, stabilize O_3 and thus favor the direct reaction (Von Sonntag & Von Gunten, 2012).

1.2.1.2.1.1 Direct reactions

Direct reactions are characterized by their high selectivity and relative slowness (k_{O_3} = 1.0-10^6 $M^{-1}s^{-1}$) (Gottschalk et al., 2009). Various direct reactions have been described, which include H abstraction, hydride transfer, insertion, and electron transfer. Equations (3) and (4) show possible direct reaction mechanisms involving DOM (Von Gunten, 2003).

$$O_3 + DOM_{direct,1} \Longrightarrow DOM_{ox} \tag{3}$$

$$O_3 + DOM_{direct,2} \Longrightarrow DOM^{+\cdot} + O_3^{-} \tag{4}$$

Due to its electrophilic character, O_3 reacts selectively with electron-rich moieties in DOM, such as phenols, activated benzene rings, and neutral amines. In contrast, saturated compounds lacking heteroatoms are O_3-refractory and their elimination is dependent on the indirect reaction (Von Sonntag & Von Gunten, 2012).

1.2.1.2.1.2   Indirect reactions

Those reactions involve $\cdot$OH, which reacts with target molecules non-selectively and immediately ($k_{\cdot OH} = 10^8\text{-}10^{10}$ $M^{-1}s^{-1}$). Being radical species, the overall reaction can be broken down into three steps: initiation, chain propagation, and termination (Gottschalk et al., 2009). Equations (5) and (6) describe the initiation step, which involves the formation of superoxide and hydroperoxyl radical intermediates, induced by OH$^-$ and DOMs possessing electron-rich moieties. Hydroxyperoxyl radical is in acid-base equilibrium with superoxide anion, as shown by Equation (7). The pH of the water is an important factor since increasing alkalinity initiates $\cdot$OH formation. However, because of the low rate constant of Equation (5), initiation by EfOM, with a reported rate constant of $\sim 2 \times 10^4$ $M^{-1}s^{-1}$, is expected to play a bigger role in wastewater effluents (Buffle et al., 2006; Nöthe et al., 2009; Park et al., 2001; Von Gunten, 2003). Nöthe et al. (2009) observed an almost linear increase of $\cdot$OH concentration with increasing O_3 concentrations until 9.6 mg L^{-1}. They suggested that the increase is linked with the breakdown of macromolecules such as humic compounds accompanied by the formation of phenolic compounds. These serve as $\cdot$OH-generating intermediates given their high O_3 reactivity. Therefore, Equation (5) is only relevant in the context of drinking water, while Equation (6) reflects the actual $\cdot$OH formation in wastewaters. In addition to OH$^-$, also the application of O_3/H_2O_2 as an AOP for wastewater treatment did not result in increased $\cdot$OH formation. It should be noted that wastewater ozonation is intrinsically an AOP given that the R_{ct} values in wastewater are higher than those achieved in drinking water (Buffle et al., 2006).

$$O_3 + OH^- \xrightarrow{k=70M^{-1}s^{-1}} HO_2^- + O_2^{\cdot -} \tag{5}$$

$$O_3 + DOM_{Initiator} \Longrightarrow HO_2^{\cdot} \tag{6}$$

$$HO_2^{\cdot} \xleftrightarrow{pKa=4.8} O_2^{\cdot -} + H^+ \tag{7}$$

Equations (8)-(11) describe the chain propagation, which further consumes O_3 molecules by reaction with superoxide anion and by the formation of ozonide radical anion. At pH $<\approx$ 8, the ozonide is protonated to form hydrogen trioxide radical, which decomposes to $\cdot$OH and oxygen. DOM promoters include aryl groups, primary and secondary alcohols, and humic acids (Gottschalk et al., 2009). Promoters propagate the reaction chain by converting $\cdot$OH to superoxide anion and hydroperoxyl radical intermediates, which refeed into Equation (7) (Park et al., 2001; Von Gunten, 2003).

$$O_2^{\cdot -} + O_3 \xrightarrow{k=1.6\cdot10^9M^{-1}s^{-1}} O_3^{\cdot -} + O_2 \tag{8}$$

$$O_3^{\cdot -} + H^+ \Longleftrightarrow HO_3^{\cdot} \tag{9}$$

$$HO_3^{\cdot} \xrightarrow{k=1.4\cdot10^5 s^{-1}} \cdot OH + O_2 \tag{10}$$

$$\cdot OH + DOM_{Promoter} \Longrightarrow ... \Longrightarrow O_2^{\cdot -} \tag{11}$$
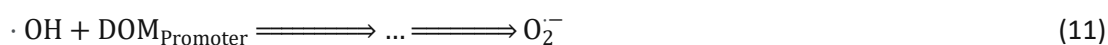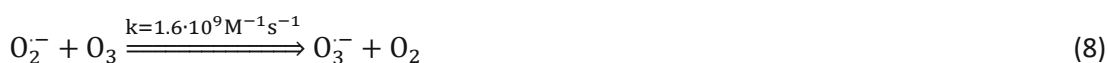
The quickly formed ·OH is also quickly consumed by scavengers, thus terminating the indirect reaction, as shown by Equations (12)-(13) (Von Gunten, 2003). DOM scavengers include bicarbonate/carbonate, humic acids, and phosphate (Gottschalk, Libra, & Saupe, 2009). In the context of wastewater, the abundantly found EfOM is the main ·OH scavenger (Von Sonntag & Von Gunten, 2012).

$$\cdot\,OH + DOM_{Scavenger} \xRightarrow{\hspace{2cm}} DOM \cdot + H_2O \tag{12}$$

$$\cdot\,OH + DOM_{Scavenger} \xRightarrow{\hspace{2cm}} DOM \cdot + OH^- \tag{13}$$

1.2.1.3 Oxidation by-products and transformation products

Ozonation involves the formation of oxidation by-products and transformation products. The former refers to the formation of undesirable and unavoidable reactions with non-target compounds, while the latter refers to reactions of O_3 with the target compounds.

During wastewater ozonation, EfOM undergoes oxidation to more polar and lower molecular weight oxidation by-products. DOC as a measure of the state of mineralization is essentially not affected at the conventional specific O_3 doses applied in urban WWTPs (Gottschalk et al., 2009).

The formation of oxidation by-products is evident by the shift from larger to lower molecular size distribution, which was reported by Imai et al. (1998) in the case of refractory leachate organics. Using high-performance gel filtration chromatography with UV detection, they correlated a higher ozonation exposure time with lower molecular size distribution.

In the context of pharmaceuticals, ozonation targets biologically active molecules and changes their chemical structure, which could result in reduced biological activity. This has been demonstrated for the steroid hormone 17-α-ethinylestradiol, which loses its estrogenic effects by reaction with a phenol moiety (Dodd et al., 2006).

Conversely, structural modifications by ozonation can also be detrimental. Nitrosamines are a group of carcinogenic chemicals with the chemical structure $R_1R_2N\text{-}N=O$, with N-nitrosodimethylamine (NDMA) being the simplest representative. Schmidt & Brauch (2008) investigated the transformation products of plant protection compounds with an N-N moiety and showed that NDMA is formed upon ozonation of N,N-Dimethylsulfamide (DMS), which is the metabolite of the popular fungicide tolyfluanid. DMS bears a sulfonamide moiety which may undergo intramolecular rearrangement and SO_2 extrusion upon ozonation. On the contrary, the urea-based herbicide DIU did not produce NMDA. The difference may be explained by deprotonation of sulfonamide, forming an O_3 adduct on a nitrogen atom, and SO_2 serving as a better leaving group than a carboxyl group (Von Gunten et al., 2010).

1.2.1.3.1 Bromate

Bromate is an oxidation by-product and a potential carcinogen. Additionally, it is a regulated disinfection by-product in drinking waters with a maximum contaminant level of 10 µg L^{-1} in the EU and USA. The Swiss Federal Institute of Aquatic Science and Technology defined an acute and chronic quality criterion of 50 µg L^{-1} for water protection. Therefore, discharge of ozonated effluent containing bromate may be toxicologically problematic (Gottschalk et al., 2009). Although there are no regulations regarding bromate discharge from WWTPs, its formation should be minimized (Bahr et al., 2007).

As a precursor to bromate, bromide concentrations should be considered when assessing the feasibility of ozonation as an upgrade to a WWTP. Data from Soltermann et al. (2016) about Swiss WWTPs effluents showed that bromide concentrations in municipal effluents are higher than 100 µg L^{-1}. Effluents from industrial WWTPs showed higher bromide concentrations in the range of 100-300 µg L^{-1}, while effluent originating from chemical industries or the special waste industry had concentrations higher than 400 µg L^{-1}. Concentrations below 100 µg L^{-1} are considered unproblematic at the conventionally applied specific doses in WWTPs (0.4-0.6 g O_3 g^{-1} DOC). These specific O_3 doses result in a bromate yield lower than 3 %, which is significantly less than the maximum contaminant level and the Swiss quality criteria (Rizzo et al., 2019; Soltermann et al., 2016).

Chon et al. (2015) reported that bromate is generated at $D_{spec} > 0.25$ g O_3 g^{-1} DOC at the same time as electron-rich moieties are oxidized. At $0.25 < D_{spec} < 1.45$ g O_3 g^{-1} DOC the increase is almost linear, which correlates with the decline of electron-rich moieties and results in higher residual O_3 concentration. Nevertheless, bromate formation is multifactorial and depends on temperature, pH, DOC, ammonia, O_3, and ·OH concentrations. Generally, bromate formation correlates with the specific O_3 dose, however, ·OH concentrations should also be regarded. When the ·OH concentrations are too high due to high DOC levels bromide may not fully be oxidized to bromate. Instead, reaction intermediates may occur, resulting in low bromate levels (Schindler Wildhaber et al., 2015).

Mechanistically, bromate (BrO_3^-) occurs as a result of a complex multistep reaction mechanism involving a combination of O_3 and ·OH. Pinkernell & Von Gunten (2001) illustrate the interplay of the possible reaction pathways. Accordingly, bromide (Br$^-$) can be directly oxidized by O_3 to hypobromous acid (HOBr), which is in chemical equilibrium with bromamine (NH_2Br) in the presence of ammonia (NH_3). Hypobromous acid may be oxidized by ·OH to BrO· or by O_3 to bromite (BrO_2^-), which is rapidly oxidized by O_3 to bromate. Alternatively, bromide can be oxidized by ·OH to ·Br, which is further oxidized by O_3 to BrO·. The latter may undergo disproportionation to hypobromous acid and bromite, which again feeds into bromate.

1.2.1.4 Parameters affecting OMP degradation during ozonation

1.2.1.4.1 EfOM and nitrite

EfOM is the most important factor considered during ozonation since it contains numerous O_3 reactive species which contribute to rapid O_3 depletion (Rizzo et al., 2019). For this reason, the dosed O_3 amount is calculated as a function of DOC called specific O_3 dose (D_{spec} in g O_3 g^{-1} DOC). Furthermore, nitrite is another component that can occur due to incomplete nitrification. As shown in Equation (14), it consumes O_3 rapidly ($k_{O_3} = 3.7 \times 10^5$ M^{-1}s^{-1}) in a 1:1 molar ratio, forming nitrate and $^1O_2$ (Naumov et al., 2010). Because of its high reactivity, it competes with compounds of an intermediate O_3 reactivity and decreases their removal efficiency. Therefore, the specific O_3 dose is nitrite compensated, considering consumption of 3.43 g O_3/g NO_2-N. The nitrite-compensated specific O_3 dose is denoted in Equation (15).

$$NO_2^- + O_3 \Longrightarrow NO_3^- + O_2 \tag{14}$$
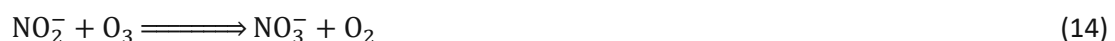
$$NO_2^- - \text{compensated } D_{spec} = \frac{[O_3 - (NO_2 - N) \cdot 3.43]}{DOC} \tag{15}$$

1.2.1.4.2 Temperature

The temperature effect on the reaction rate can be expressed by Arrhenius law, as shown in Equation (16). It can also be expressed by the general Van't Hoff rule, stating that the speed of chemical reactions is increased at least twofold for every 10° C rise in temperature.

$$k = A \cdot e^{-\frac{Ea}{RT}}$$

(16)

When calculating activation energies, the solubility of O_3 in water should be taken into account as increasing temperature results in lower solubility. O_3 solubility at room temperature is 10-15 mM, while at 0° C is 20-25 mM. Therefore, to increase solubility, ice cooling the O_3 stock solution may be necessary thus allowing a lower sample dilution (Gottschalk et al., 2009). Elovitz (2000) showed that O_3 decay rates are approximately first order, and they increase more than an order of magnitude in the range 5° C-35° C. The temperature range resulted in a 14-fold increase in R_{ct}, which indicates that although O_3 is highly sensitive to temperature, ·OH exposure is left unaffected.

1.2.1.4.3 pH and carbonate alkalinity

The effect of pH and the role of carbonate alkalinity in ·OH scavenging is relevant in the context of drinking water/natural water (Schaar, 2015). On the one hand, an elevated pH in natural water depletes O_3 due to the reaction with hydroxyl ions initiating the indirect radical chain reaction. On the other hand, many acidic functional groups found in DOM are deprotonated at higher pH, which increases O_3 electrophilic reactivity (Gottschalk et al., 2009). Buffle et al. (2006) found that in wastewater there is a significant increase of ·OH concentration when the pH is raised from 2 to 6.7. However, higher pH values relevant to wastewater effluents did not result in higher ·OH concentrations. Likewise, Lee et al. (2013) reported that pH values ranging from 6.9 to 7.6 in 10 different wastewater effluents did not have an effect on OMP elimination efficiency.

Carbonate is an important ·OH scavenger in natural water, as its decrease results in an increase of ·OH exposure. The carbonate/bicarbonate chemical equilibrium of natural waters is pH-dependent, whereas higher pH of 8.5-9 shifts the equilibrium towards carbonate (Gottschalk et al., 2009). As these pH values are not relevant for wastewater effluents, carbonate does not play a major role as an ·OH scavenger. Buffle et al. (2006) compared wastewater effluents from two different WWTPs treated with similar specific O_3 doses. Accordingly, although the ·OH exposures were significantly different, O_3 decomposition in both samples was similar. If alkalinity played a major role in ·OH scavenging, then higher alkalinity would have resulted in lower O_3 decomposition and lower ·OH exposure. This indicates that the EfOM as ·OH scavenger is far more important than carbonate/bicarbonate in wastewater.

1.2.1.5 Reactivity of functional groups

OMPs contain particular elements in their molecular structure which may be crucial for their functionality. For their degradation by O_3, the relative reactivities of the different potential sites of attack must be considered. This allows one to estimate the mechanistic degradation of OMPs. In the following subsections, the reaction mechanisms of O_3 with certain functional groups of importance are discussed. Further details are described by Von Sonntag & Von Gunten, (2012).

1.2.1.5.1 Olefines

The ozonolysis of olefines is generally described as cyclo-addition according to the Criegee mechanism. This reaction is regarded as concerted, stereospecific, and regioselective. As depicted in figure 3, the reaction proceeds via electrophilic attack, which leads to the formation of an unstable ozonide (molozonide). This is followed by a thermodynamically determined, heterolytic cleavage of an O-O bond and splitting of the C-C single bond, yielding a zwitterionic structure and a carbonyl compound. The zwitterionic structure is hydrated and produces α-hydroxyalkylhydroperoxide, which is in equilibrium with hydrogen peroxide and a carbonyl compound (Von Sonntag & Von Gunten, 2012). In case the ozonide formation is not concerted, a zwitterionic structure is formed (not shown in Figure 3). This can be intercepted by water, thus hindering C-C cleavage and resulting in partial oxidation (Von Sonntag & Von Gunten, 2012).
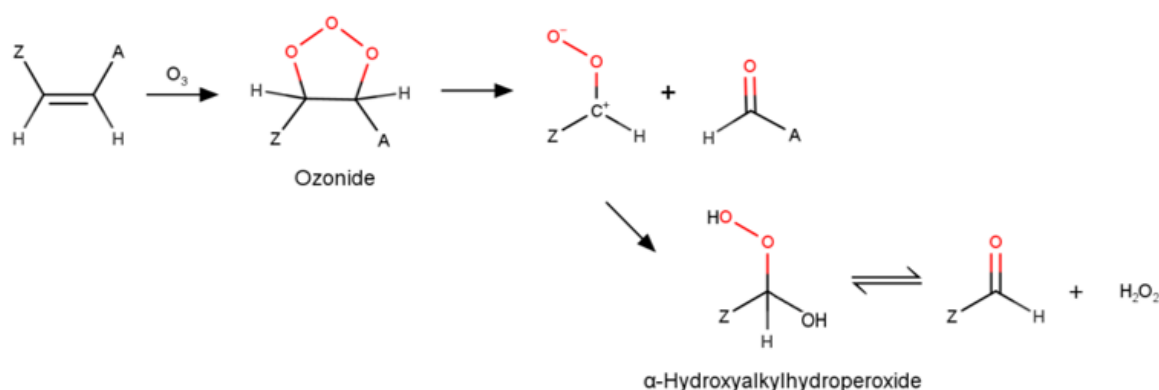
Figure 3: Ozonolysis reaction of olefines, adapted from Von Sonntag & Von Gunten (2012)

Non-symmetric olefine substituents, which are electron-withdrawing, such as halogens or cyano, acetyl, and diethyl phosphonate groups, form preferentially the products α-hydroxyalkylhydroperoxide and the corresponding formyl derivative (Von Sonntag & Von Gunten, 2012).

1.2.1.5.2 Aromatic compounds

A few reaction mechanisms are possible for aromatic compounds. Cyclo-addition is generally exergonic and occurs regularly in all aromatic compounds. It involves an electrophilic attack of an olefine to a zwitterionic adduct with a subsequent ozonide formation, followed by its decomposition and C-C cleavage. Since the positive charge of the adduct is stabilized by the mesomeric effect over the entire ring, ozonide closure is retarded, allowing different reactions to proceed. Hydroxylation is another standard reaction for aromatic compounds, the O_3 adduct releases singlet oxygen followed by protonation of the phenolate ion. It has also been suggested that oxygen is cleaved homolytically, forming an aryl radical. Alternatively, the O_3 adduct can undergo electron transfer, which proceeds by homolytic cleavage of the C-O bond, producing aryl radical cation and ozonide radical anion. Electron transfer has been reported to be exergonic by methoxy-substituted benzenes, while for benzene the reaction is endergonic, which may indicate that electron-donating groups are required (Von Sonntag & Von Gunten, 2012).

O_3 reactivity towards aromatic compounds is largely dependent on the substituents. Electron-donating substituents lead to high reaction rates, while aromatic compounds with electron-withdrawing substituents mainly rely on the ·OH route (Von Sonntag & Von Gunten, 2012). The pH also plays a major role, as it determines to which extent the compound lies in its dissociated form. As an example, phenol is moderately reactive with O_3, but the reactivity of phenolate ion is six orders of magnitude faster (Muñoz et al., 2001). As such, phenolate is the dominant reactive species at pH > 4 and the only relevant species at pH 7. Activated phenols increase the pKa value of the phenolate and therefore decrease O_3 reactivity. In contrast, deactivated phenols increase compound acidity, making them highly reactive also at lower pH values. As an example, 2,6-dibromophenolate is the only relevant species at pH 3 (Tentscher et al., 2018).

1.2.1.5.3 Nitrogen-containing groups

The reaction mechanism of O_3 with aliphatic amines proceeds via addition at the nitrogen atom. The addition is dependent on the availability of the lone electron pair of the nitrogen. For example, amides and sulfonamides have low second-order reaction rate constants because of the electron-withdrawing carbonyl and sulfonyl groups, respectively. On the contrary, an addition to a deprotonated amine is highly favored. The O_3 adduct formed may release $^1O_2$ and generate hydroxylamine or N-oxide, depending on whether the amine is secondary or tertiary. Alternatively, O_3 may cleave homolytically and form amine radical cation, but because of the cage effect of the water medium, N-oxide or hydroxylamine and $^3O_2$ are the expected products (Von Sonntag & Von Gunten, 2012). In the case of aromatic amines, addition to the ring is highly exergonic and therefore most likely. On the one hand, the O_3 adduct may undergo cycloaddition and produce a pyridine derivative. On the other hand, the formation of aniline radical is also possible (Von Sonntag & Von Gunten, 2012).

1.2.1.5.4 Sulfur-containing groups

O_3 reactivity relies on the oxidation state of the sulfur atom, with lower oxidation states being favored. As to sulfides, disulfides, and sulfinic acids, an oxygen atom transfer takes place and the O_3 adduct then decomposes to sulfoxide and $^1O_2$. Despite the electron-withdrawing oxygens of sulfinic acid, the sulfur is considered a nucleophile because it is deprotonated at pH 7. In contrast, sulfoxide is considered O_3-refractory as it exists as a zwitterion, with the sulfur acting as an electrophile (Von Sonntag & Von Gunten, 2012).

1.2.2 Adsorption

1.2.2.1 Background

Adsorption describes the transfer of adsorbate from the fluid phase onto the surface or interface of an adsorbent. Per definition, adsorption is a surface process. In contrast, absorption describes the transfer from the fluid phase into the material bulk and is, therefore, a volume process. Both adsorption and absorption describe a phase transfer from the bulk fluid to the solid phase and thus comprise the umbrella term "sorption". The process of adsorption is highly complex since it involves an interplay of the chemical, physical and textural properties of the adsorbent as well as chemical and physical features of the adsorbates (Worch, 2012).

In adsorption theory, the Gibbs free energy is not only dependent on pressure, temperature, and the number of moles but is also a function of surface area. The phase transfer from the solute-fluid interface to the solute-solid interface leads to a reduction of the surface free energy. The total change of the Gibbs free energy upon adsorption is driven by the change of enthalpy of adsorption and entropy as denoted in Equation (17). During adsorption, adsorbate molecules gain energy due to stabilizing interactions with the adsorbent surface, which results in a reduction of enthalpy. Conversely, due to the restricted motion of adsorbates and confinement within pores, the entropy is reduced. Therefore, the change of enthalpy favors adsorption while the change of entropy counters that effect. For spontaneous adsorption to take place, a compensation exchange rate must be measured (Dauenhauer & Omar, 2018; Worch, 2012).

$$\Delta G_{ads} = \Delta H_{ads} - T\Delta S_{ads} < 0 \qquad\qquad\qquad (17)$$

The driving forces of adsorption can be either of physical or chemical nature. Physisorption occurs due to weak van der Waals interactions such as dipole-dipole, dispersion, and induction forces. These forces lie energetically low with a change of adsorption enthalpy of typically less than 50 kJ mol^{-1}. Chemisorption is associated with electron exchange and the formation of covalent bonds between adsorbate and adsorbent. The amount of energy release during chemisorption is therefore in the order of magnitude of chemical reactions. Physisorption is further characterized as an unspecific, reversible adsorption process and can form more than one layer. In contrast, chemisorption is considered a specific, irreversible adsorption process and it involves the formation of a single layer (Böhme, 2000; Worch, 2012).

1.2.2.2 Activated carbon

The high popularity of AC used as an adsorbent in all water treatment processes is attributed to its high porosity and non-specific interactions including van der Waals forces, π-π bonds, and electrostatic interactions. Its porosity is explicit by its large internal surface area of 10^2-10^3 m^2 g^{-1} and a comparably marginal external surface area lower than 1 m^2 g^{-1} (Worch, 2012).

AC constitutes a microcrystalline structure consisting of graphene layers. The carbon atoms in each layer are sp^2 hybridized. Every carbon atom of a graphene layer is joined by a σ bond with three neighboring carbon atoms while the fourth electron is delocalized over the whole layer. Both AC and graphite contain graphene layers but due to the larger interlayer spacings of AC compared to graphite, many crystallites are tilted with respect to one another. This non-parallel orientation compared to graphite generate voids that are de facto the micropores (Çeçen & Aktaş, 2011; Coughlin & Fouad, 1968).

AC is produced from both carbonized materials such as coals or organic materials such as coconut shells, wood, and sawdust. In recent years, biochar has received growing attention due to its production from different wastes and its low cost (Inyang et al., 2016). AC production consists of two steps, carbonization, and activation. The carbonization step involves drying and heating at 400-600° C in a pyrolytic atmosphere. This allows removing hydrogen, oxygen, and volatile low molecular weight fractions. At the end of the carbonization step, a carbon skeleton remains. The consequent activation generates the micropore structure. Based on the raw materials used the following activation processes are applied (Çeçen & Aktaş, 2011; Worch, 2012).

- Chemical activation involves the impregnation of dehydrating chemicals in the raw carbonaceous material followed by carbonization. This is succeeded by an extraction step of the dehydrating chemicals.

- Physical activation involves the use of oxidizing gases at 800-1000° C. This allows to increase the pore volume and to open new pores due to oxidation of the carbonaceous material.

1.2.2.3 Factors affecting adsorption capacity

1.2.2.3.1 Porosity

According to the definition of the International Union of Pure and Applied Chemistry (IUPAC), three pore types are classified: macropores with a pore width larger than 50 nm, mesopores with a pore width in the range of 2-50 nm, and micropores with a pore width not exceeding 2 nm. Due to its molecular size, the relevant pore type for the adsorption of OMPs is the micropore. As such, the minimal projection area of a molecule should have similar dimensions as the micropore. Meso- and macropores are mostly relevant for mass transfer (Worch, 2012). The importance of mesopores in OMPs adsorption relates to DOM adsorption. A low mesoporous volume negatively affects the adsorption capacity of OMPs due to micropore blockage by DOM (Li et al., 2003; Newcombe et al., 2002).

1.2.2.3.2 Chemical structure of adsorbate

In general, the adsorption affinity of OMPs increases with increasing aromaticity, the number of functional groups such as halogens, and polarizability (Cheremisinoff, 2002). In addition, log D_{OW} is an important factor, considering the hydrophobic interactions between adsorbate and AC. Larger molecules have a better adsorption capacity at a large enough pore size. Branched side chains of polymers are better adsorbable than polymers with straight chains (Çeçen & Aktaş, 2011).

1.2.2.3.3 Surface oxides

AC contains oxygen atoms in the form of different acidic and basic functional groups called surface oxides. This has a negative effect on the adsorption of most organic compounds, which is attributed to their lowering of the π electron density of the graphene layer resulting in a decrease of dispersion forces. Moreover, the higher polarity can result in the pore filling of water molecules and the formation of water complexes therein. As a consequence, adsorption can be hindered (Coughlin & Fouad, 1968; García-Araya et al., 2003).

1.2.2.3.4 Temperature

A lower temperature is generally favored for adsorption as it is an exothermic process. In addition, for many compounds, the solubility increases with temperature. On the contrary, the temperature can also favor adsorption in the liquid phase by increasing the diffusion rate into the pores (Worch, 2012).

1.2.2.3.5 pH

The pH determines the predominant species of a compound. Generally, at low pH organic compounds are positively charged, at intermediate pH they are neutral, and at high pH, they are negatively

charged. Since the main interactions between organic compounds and AC are hydrophobic, intermediate pH is favored. In relation to the adsorbent, a lower pH is favored for adsorption. This lies on the negatively charged surface area of the activated carbon which is neutralized at low pH (Çeçen & Aktaş, 2011).

1.2.2.4 Isotherms

The adsorption affinity of adsorbates can be characterized by different isotherm models. The data for modeling must be collected in lab experiments at different AC concentration levels and a constant temperature. An isotherm reflects the adsorption capacity after equilibrium has been reached, meaning that the liquid phase concentration and the solid phase concentration of a solute are constant (DWA, 2019). The data is plotted with the residual liquid phase concentration on the x-axis and the uptake of solute by the adsorbent, referred to as loading, on the y axis. Equation (18) defines the loading, from which one data point is calculated. By changing either the adsorbent mass at a constant initial solute concentration or the initial solute concentration at a constant adsorbent mass, further data points are plotted (Worch, 2012).

$$q = \frac{V}{m} * (c_0 - c_{eq})$$
(18)

q   Loading (ng g^{-1} for OMPs)

V   Volume (L)

c_0 Initial solute concentration (ng L^{-1})

c_{eq} Equilibrium concentration (ng L^{-1})

m   Mass of adsorbent (g)

Isotherm can be characterized according to different adsorption models. These vary according to the number of parameters included that have to be determined from the experimental data. The higher the number of parameters included the better is the fitting but the more complex is the equation and its application in adsorption models. Giles et al. (1974) classified the adsorption isotherms into four classes and four subgroups. The four classes are S, L ("Langmuir"), H ("high affinity"), and C ("constant partition").

- S class: the molecules are vertically oriented on the surface. The shape results from a combination of adsorption inhibition of the solute and attractive interactions of the adsorbates (Inglezakis et al., 2018).
- L class: the molecules are horizontally oriented on the surface. Adsorption is fast in the beginning and levels off with increased occupation of adsorption sites. For an aqueous solution, the L class is most relevant.
- H class: the molecules are strongly adsorbed to the surface. The interactions between the adsorbates are insignificant.
- C class: the C class isotherm is a linear isotherm that arises from a steady penetration of solutes into micropores.

The simplest adsorption models include the zero-parametric irreversible isotherm and the one-parametric Henry adsorption model, which mostly describes a limited isotherm range. The irreversible isotherm describes adsorption when saturation has been reached and is, therefore, only temperature-dependent. The Henry model describes a linear dependence between concentration and

loading and is dependent on the Henry coefficient, K_H. For the description of broader isotherm ranges the 2-parametric Langmuir and Freundlich isotherms are applied (Çeçen & Aktaş, 2011; Worch, 2012).

1.2.2.4.1 Langmuir Isotherm

The Langmuir model was first used to describe the adsorption of gases on solid surfaces. It assumed that inelastic collisions of the gas with a surface led to a residence time of the gas in the location of incidence until leaving the surface back to the gas phase. The Langmuir adsorption model is based on the following fundamental assumptions:

- The adsorbent surface is uniform and all adsorption sites are energetically equivalent.
- Each adsorption site is occupied by a single molecule leading to the formation of a single monolayer.
- There are no lateral interactions between adjacent adsorbing molecules.
- At equilibrium adsorption and desorption are equal.

The Langmuir isotherm equation is calculated according to Equation (19).

$$q = \frac{q_{max}bc}{1+bc}$$
(19)

q_{max} Maximum adsorption capacity (ng g^{-1} for OMPs)

b Adsorption coefficient (L ng^{-1})

c Equilibrium concentration (ng L^{-1})

The Langmuir isotherm can describe saturation of the adsorbent at very high concentrations when $bc \gg 1$. Then the loading is independent of the concentration and the isotherm becomes irreversible (q = constant). For $bc \ll 1$ the Langmuir equation describes a linear relationship between concentration and loading, which is the linear Henry isotherm ($q = q_{max}bc = K_Hc$). In case of $b = c^{-1}$, half of the adsorption sites are occupied ($q = 0.5q_{max}$) (Swenson & Stadie, 2019).

The adsorption coefficient (b) is a function of the heat of adsorption, which is an indicator of the strength of the interaction between an adsorbate and an adsorbent. According to the Langmuir model, the heat of adsorption is assumed to be equal for all adsorption sites. This model is suitable to describe chemisorption but can also describe systems with low coverage. However, the model assumptions of energetically equal adsorption sites and monolayer coverage are often not satisfying for the description of adsorption in aqueous systems (Çeçen & Aktaş, 2011; Worch, 2012).

1.2.2.4.2 Freundlich Isotherm

Unlike the Langmuir model, the Freundlich model is based purely on an empirical relation between the concentration of a solute in the liquid phase and its loading at the adsorbent. Despite it being empirical, it is used widely to describe adsorption in aqueous systems. The Freundlich model applies to heterogeneous surfaces and is described as a non-ideal, multilayer reversible adsorption process. It assumes that the heat of adsorption decreases logarithmically with increased loading. As such, it relates q and c using a power function, as described in Equation (20) (Çeçen & Aktaş, 2011; Sahoo & Prelot, 2020; Worch, 2012).

$$q = K_F c^n \tag{20}$$

K_F   Adsorption coefficient ((ng^{1-n} L^n)/g)

n   Adsorption coefficient ()

c   Equilibrium concentration (ng L^{-1})

The adsorption coefficient K_F characterizes the adsorption strength and thus leads to higher loadings at higher K_F values. The adsorption coefficient n determines the curvature of the isotherm and is dependent on the heterogeneity of the adsorbent surface. At n < 1 the isotherm is referred to as favorable. Because it is concave towards the x-axis high loadings are provided at low concentrations. If n > 1 the isotherm is unfavorable since high loadings can be reached only at high concentrations.

Whereas the Langmuir model is suitable to describe the extreme concentration ranges, the Freundlich model best describes the intermediate concentration range. At very high concentrations the adsorption sites are not saturated. Instead, the surface is assumed to have infinite adsorption sites, which leads to an overestimation of the adsorption process (Çeçen & Aktaş, 2011; Worch, 2012).

1.2.2.5 PAC application in WWTPs

The application of PAC in WWTPs is known as the PACT process, originally developed in the 1970s by DuPont. The PACT process has broad wastewater applicability including municipal and industrial wastewaters and landfill leachate. Moreover, it is widely applied in the refinery and petrochemical industries (Çeçen & Aktaş, 2011).

PAC can be either applied directly in the biological treatment stage or a subsequent contact reactor following the secondary clarifier. Figure 4 depicts a direct addition of PAC into the mixed liquor of the aeration basin, which allows the integration of PAC into the activated sludge flocs. Once aeration is complete, the combined PAC-mixed liquor enters the secondary clarifier. After sedimentation, the PAC is continuously recirculated back to the aeration basin while a portion of it is wasted together with the excess sludge. By adding the PAC directly into the activated sludge tank its retention time in the system is equal to the sludge age, which allows the PAC to reach a high loading. A downstream installation of a filter is recommended to prevent the loaded PAC particles to enter the effluent (Çeçen & Aktaş, 2011; DWA, 2019).

Advantages of the process include (Çeçen & Aktaş, 2011):

- Synergism between the biomass of the activated sludge and the PAC. This allows an improved removal of OMPs both by biodegradation and by adsorption.
- Low capital investment costs.
- PAC dosing can be changed according to the influent properties.

The drawbacks include the larger amounts of excess sludge. However, the settling and dewatering properties of the PACT sludge are improved.
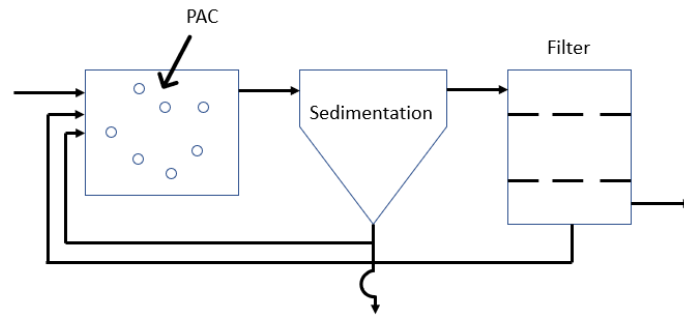
Figure 4: PAC addition to the aeration tank, adapted from DWA (2019)

The main drawback of the direct addition to the aeration basin is the high presence of the EfOM, which acts as a competitor for the adsorption sites. In addition, mostly biodegradable compounds are targeted. These are made available to the microorganisms by adsorption and desorption. To overcome these, PAC can also be added to a contact reactor after the secondary sedimentation, as depicted in Figure 5 (Çeçen & Aktaş, 2011; DWA, 2019).
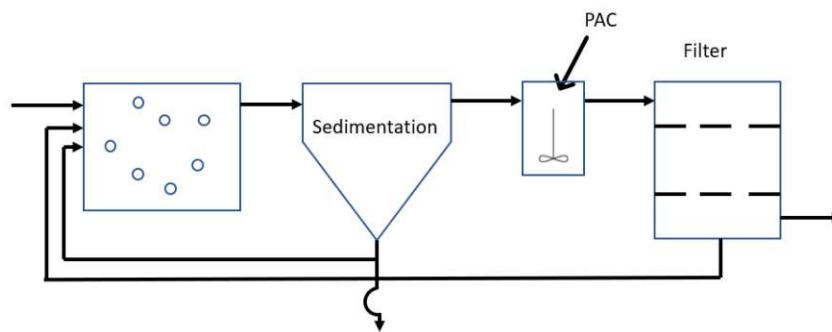
Figure 5: PAC addition to a contact reactor, adapted from DWA (2019)

2 Objective

The main focus of this thesis is laid on the abatement of refractory organic micropollutants (OMPs) found in wastewater effluent samples. For this purpose, bench-scale ozonation and AC adsorption are applied as part of the fourth treatment stage.

Thematically, this thesis consists of three main parts. The first part addresses the effect of ozonation as a single-step procedure, which involves the application of three different specific O_3 doses. The second part deals with a combination of ozonation at a relatively low specific dose with a consecutive PAC (Epibon A) adsorption step at different specific PAC doses.

The third part studies the adsorption capacity of a novel product which is a part of an ongoing feasibility study. The product is composed of a suspended PAC and is offered in two formulations: AQUACLEAR A and AQUACLEAR B with an AC fraction of 10 and 18 %, respectively. In this part, different specific AC doses are applied in effluent samples originating from different Austrian WWTPs. Moreover, the differences between the product and the PAC used in its manufacture (CARBOPAL®) are enquired.

In the framework of this thesis the following questions are addressed:

Ozonation

- ➢ How does the application of three different specific O_3 doses affect OMP abatement?
- ➢ How do they affect the potential of bromate formation?
- ➢ How is the sum parameter BOD_5 influenced by ozonation?
- ➢ How good is the correlation between OMP abatement and percentual increase of the surrogate parameter ΔSAC_{254}?

Ozonation + PAC

- ➢ How do three different specific AC doses affect OMP abatement?
- ➢ How does ozonation affect subsequent PAC adsorption?
- ➢ How good is the correlation between the percentual increase of ΔDOC and the surrogate parameter ΔSAC_{254}?
- ➢ Does the adsorption capacity of the selected OMPs fit the adsorption models described by Freundlich and Langmuir?

Product

- ➢ How does the application of different specific AC doses of a novel product containing suspended AC perform regarding OMP removal?
- ➢ How do different wastewater matrices behave in this regard?
- ➢ Is there a difference in performance between the product and the PAC involved in its manufacture?
- ➢ Does the adsorption capacity of the selected OMPs fit the adsorption models described by Freundlich and Langmuir?

3 Materials and Methods

3.1 Experimental overview and sample preparation

To investigate the removal potential of ozonation and AC adsorption, these techniques were applied on wastewater effluent samples as an advanced treatment stage for OMP abatement. Moreover, the transformation product bromate was analyzed.

Additionally, the application of a novel PAC-containing product was tested in further lab tests. The product combines properties of PAC and polyaluminum chloride (precipitating agent) and can therefore be used for simultaneous removal of OMPs and phosphorus.

A total of six samples from six different periods and three different WWTPs was treated, as shown in Table 2.

Table 2: Experimental scheme

Sample	Period	WWTP	Ozonation D_{spec} (g O_3 g^{-1} DOC)					AC adsorption PAC		AQUACLEAR Product	
			0.40	0.45	0.46	0.57	0.88	Epibon A	CARBOPAL®	A	B
A1	14.06.2021 20.06.2021	A			✓	✓	✓				
A2	21.06.2021- 27.06.2021	A		✓				✓			
A3	28.06.2021- 04.07.2021	A	✓					✓			
A4	14.06.2021- 27.06.2021	A								✓	✓
B	21.06.2021	B							✓		✓
C	09.08.2021	C								✓	✓

In Table 3, the WWTP capacity, as well as the availability of different treatment stages, are shown. The WWTP capacity is expressed by the parameter population equivalent (PE_{60}), which equates to 60 g of BOD_5 per person per day.

Table 3: WWTP capacity and treatment stages

WWTP	Capacity (PE_{60})	C removal	Nitrification	Denitrification	P removal
A	950.000	✓	✓	✓	✓
B	6.000	✓	✓	✓	✓
C	54.000	✓	✓	✓	✓

The samples were taken as grab samples. A1-A4 are composite samples of a one-week period (A1-A3) and a two-week period (A4). The relative volume was calculated according to the wastewater load of the given sampling date, and the absolute amount was calculated by estimating the total amount required for the experiment and successive analysis. An example of composite sample A1 is shown in Table 4.

Table 4: Preparation of weekly composite sample A1

Sampling date	Wastewater load (m^3)	Sample volume (L)
14.06.21	94320	1.00
15.06.21	97424	1.03
16.06.21	97848	1.04
17.06.21	100008	1.06
18.06.21	97640	1.04
19.06.21	89672	0.95
20.06.21	86064	0.91

For the calculation of the specific O_3 dose, the O_3 concentration was normalized to the DOC value and compensated by the nitrite-nitrogen. Similarly, the specific AC dose was calculated by normalizing the AC dose to the DOC concentration. DOC and NO_2-N values, including the averaged O_3 concentration in the stock solution with the corresponding dilution factor, are found in Table 5.

Table 5: Important parameters for the calculation of the specific O_3 and AC dose

Sample	DOC	NO$_2$-N	O$_3$ stock solution averaged	Dilution factor
	mg L^{-1}	mg L^{-1}	mg L^{-1}	
A1	17.55	0.66	40.4 (D$_{spec}$ 0.57) 37.7 (D$_{spec}$ 0.46, 0.88)	0.80 (D$_{spec}$ 0.46) 0.76 (D$_{spec}$ 0.57) 0.80 (D$_{spec}$ 0.88)
A2	13.20	0.74	44.5 (D$_{spec}$ 0.45)	0.84 (D$_{spec}$ 0.45)
A3	12.90	0.69	34.3 (D$_{spec}$ 0.40)	0.82 (D$_{spec}$ 0.40)
A4	15.38			
B	6.00			
C	5.90			

Before every ozonation experiment, the samples had to be relatively particle-free. Since ozonation is used for particle removal, the presence of suspended solids would falsify the calculated OMP abatement (Gottschalk et al., 2009). Therefore, some of the samples with a higher content of particles were pre-filtered (A2 and A3) or decanted (A1) before the ozonation experiments.

3.2 Data evaluation

Data evaluation for removal percentage was realized under the following conditions:

- Concentrations of the raw data (dilution factor not included), which lie below the LOQ, were assigned 0.
- Removal percentage was only evaluated if the effluent concentration was at least ten times higher than the LOQ. This did not apply to IBP and DIU in all conducted experiments.
- Negative concentrations were assigned 0.
- Negative removal percentage was assigned 0.

The Freundlich and Langmuir parameters for the selected OMPs were determined under the following conditions:

- Data points at all three different concentrations must be present.
- Coefficient of determination R^2 higher than 0.50.
- The slope of the linearized function is positive.

3.3 Chemical analysis

3.3.1 Conventional wastewater parameters

DOC and NO_2-N were determined before the ozonation for the calculation of the nitrite-compensated specific O_3 dose. For the DOC measurement, the samples were filtered with a rinsed cellulose acetate filter with a pore size of 0.45 μm. BOD was measured in the initial effluent sample and every day after ozonation up to day 5 (BOD_5) and day 6 (BOD_6). All measurements were performed according to international standards. The parameters, measurement principle, and applied norms are given in Table 6.

Table 6: Wastewater parameters including measurement principle and norms

Parameter Abb.	Measurement principle	Norm
Dissolved organic carbon DOC	High-temperature combustion (complete conversion to CO_2) with non-dispersive infrared sensor	DIN EN 1484
Nitrite NO_2-N	Azo-dye formation in a flow injection analysis with colorimetric measurement	DIN EN ISO 15705
Biological oxygen demand BOD_5	Optical oxygen analyzer	DIN EN 1899-2

3.3.2 BOD_5

300 mL BOD bottles were washed thoroughly three times with water and three times with DI water. For every sample, a triplicate was prepared. Because the BOD parameter measures the demand to break down organic material, 300 μL of the nitrification inhibitor ATU (1 g/L) was added to the bottles. The ATU inhibits the conversion of ammonia to nitrate by nitrifying microorganisms which would affect the BOD measurements. After the batch experiments, the ozonated samples and the non-ozonated control samples were gradually and slowly filled in the bottles, making sure to avoid air bubble formation. To further remove small air bubbles, the brimful bottles were knocked with the stopper a few times for trapped air bubbles to escape. Finally, when no air bubbles were visible the stopper was slowly inserted into the bottle and turned. The measurement of the dissolved oxygen concentration was conducted with the Fiberobtic Oxygen Meter, Fibox 3 LCD-trace (Presence Precision Sensing). The measurement was carried out by attaching the luminophore to the outer surface of the BOD bottle, and the dissolved oxygen concentration was computed based on oxygen quenching. Measurement of dissolved oxygen and temperature was carried out immediately after the O_3 batch tests and the

samples were incubated at 20° C in the dark. Dissolved oxygen and temperature were measured in the following days up to day 5 or 6 and BOD in mg L^{-1} was calculated by the difference of day 0 and day x.

Figure 6: Used BOD flasks; the bleaching effect by O_3 is visible: three left BOD flasks contain sample, three right BOD flasks contain ozonated sample with a specific O_3 dose of 0.40 g O_3 g^{-1} DOC

Nonlinear regressions analysis was performed in SigmaPlot 14 (Systat Software, Inc.) with global curve fitting. To fit the BOD_5 data, the equation "Single, 2 Parameters" from the equation category "Exponential Rise to Maximum" was selected, as denoted in Equation (21).

$$y = a(1 - e^{-bx}) \tag{21}$$

3.3.3 SAC_{254}

The spectral absorption coefficient at 254 nm (SAC_{254}) is a surrogate parameter that measures the EfOM content in a water sample. The parameter was calculated according to DIN 38404-3:2005, which defines it as the quotient of the absorbance at 254 nm and the optical path length. The high absorption coefficient at 254 nm arises most likely due to intramolecular charge transfer transitions between electron donors and electron acceptors co-localized within a dissolved humic acid macromolecule. In contrast, low molecular weight conjugated molecules such as benzoic acid and toluene absorb at 254 nm with much lower absorption coefficients (Blough & Del Vecchio, 2004).

SAC_{254} can be used for both ozonation and PAC adsorption as a surrogate parameter for the specific O_3 dose and the specific PAC dose. Therefore, it can also be used as a surrogate parameter for OMP abatement (Bahr et al., 2007). Following ozonation, the decrease of the SAC_{254} results from structural changes of the EfOM, whereas with PAC adsorption EfOM is removed by adsorption (Altmann et al., 2014). The parameter is calculated as a percentage decrease of SAC_{254} or percentage increase of ΔSAC_{254}.

The biggest advantage of the SAC_{254} parameter in ozonation is its practicability for online monitoring. It can be used for feedback process control of O_3 dosing, which is relevant for fluctuating nitrite levels (Rizzo et al., 2019). By adhering to a specific SAC_{254} reduction, which corresponds to a specific O_3 dose, nitrite is considered automatically (Stapf et al., 2013). For control and regulation, the presence of dissolved O_3 should be considered since it absorbs at 258 nm. Wastewaters with low DOC values may have a lower O_3 decomposition. This can result in higher SAC_{254} reduction and, misleadingly, a higher set value for the O_3 dose. Therefore, SAC_{254} should be measured either including the O_3 absorption or after O_3 has been removed from the wastewaters.

3.3.4 Determination of OMPs and bromate

OMPs and bromate were determined by high-performance liquid chromatography (HPLC) - mass spectroscopy in electrospray ionization mode (ESI-MS). For OMP determination an additional online solid-phase extraction (SPE) was connected upstream to the separation column. Sample preparation consisted of sample filtration with VWR glass microfibres with a pore size of 1 µm.

3.3.4.1 OMPs

The HPLC system used for the elution was Agilent System (USA) and consisted of two binary pumps, a degasser, CTC PAL autosampler with Peltier cooler, and a Rheodyne 2-position, and a 6-port switching valve. For online SPE the Phenomenex Strata X On-Line extraction cartridge (20 x 2.0 mm; 25 µm) was used. For HPLC separation the analytical columns used were Phenomenex Luna C-18 (150 x 3.0 mm; 5 µm) and Phenomenex C18-Security guard cartridges (40 x 3.0 mm).

Sample injection volumes of 10 mL were used for SPE. For a gradient elution, two eluents were used: 0.1 % (v/v) acetic acid and 0.1 % (v/v) acetonitrile in DI water and the elution program was carried out according to Table 7.

Table 7: Gradient elution program for online SPE and HPLC

Time	Online SPE			HPLC		
	Flow	Gradient		Flow	Gradient	
min	mL/min	% A	% B	mL/min	% A	% B
0	1.0	100	0	0.8	100	0
5.6	1.0	100	0	0.8	100	0
0	1.0	100	0	0.8	80	20
5	1.0	100	0	0.8	90	10
8	0.5	0	100	0.8	90	10
8.2	1.0	0	100	0.8	0	100
8.5	1.0	0	100	0.8	60	40
17	1.0	0	100	0.8	60	40
19	1.0	100	0	0.8	5	95
25	1.0	100	0	0.8	80	20

The MSMS system consisted of a Hybrid triple quadrupole linear trap ion trap tandem mass spectrometer Q Trap 6500 from Applied Biosystems (USA). The ion spray voltage was -4500 V and the temperature was 400° C. OMP concentration was determined by an external calibration, using different concentrations of multicomponent standards. Details regarding the compounds involved in the standard preparation are found in Table 8.

Table 8: List of OMPs analyzed

Compound	CAS	Company	Formula	Molar mass
BZF	41859-67-0	Sigma-Aldrich	$C_{19}H_{20}ClNO_4$	361.8
BTA	95-14-7	Sigma-Aldrich	$C_6H_5N_3$	119.1
CBZ	298-46-4	Sigma-Aldrich	$C_{15}H_{12}N_2O$	236.3
DIU	330-54-1	Sigma-Aldrich	$C_9H_{10}Cl_2N_2O$	233.1
DCF	15307-79-6	Sigma-Aldrich	$C14_{4}H_{10}Cl_2NO_2Na$	318.1
IBP	31121-93-4	Sigma-Aldrich	$C_{13}H_{17}O_2Na$	228.3
MTP	37350-58-6	RTC, Sigma-Aldrich	$C_{15}H_{25}NO_3 \cdot C_4H_6O_6$	267.4
SMX	723-46-6	Sigma-Aldrich	$C_{10}H_{11}N_3O_3S$	253.3
TMP	738-70-5	Sigma-Aldrich	$C_{14}H_{18}N_4O_3$	290.3

Details regarding ionization mode used, mass-to-charge ratios of precursor ions (Q1), mass-to-charge ratio of qualifying and quantifying product ions (Q3) and LOQ are listed in Table 9.

Table 9: Parameters regarding OMP detection

Compound abb.	Molar mass	Polarity	Q1 mass	Q3 mass	Identifying mass				LOQ
	Da		m/z	m/z	m/z	DP	CE	CXP	ng L^{-1}
DIU	233.1	+	234.047	72.1/46.1	72.1	36	31	4	62.8
BZF	361.8	-	359.99	153.9/274.1	274.1	-25	-26	-2	1.0
BTA	119.1	+	120.097	65.1/92.2	65.1	46	31	4	1.6
CBZ	236.3	+	237.727	193.3/194.3	194.3	51	25	4	0.2
DCF	296.2	+	296	214/215	214.0	30	45	4	0.4
IBP	206.3	-	204.972	159.0/161.0	161.0	-20	-12	4	6.7
MTP	267.4	+	267.810	74.0/77.1	77.1	41	75	4	6.0
SMX	253.3	+	254.171	156.2/92.25	92.2	41	33	4	0.6
TMP	290.3	+	292.305	231.2/262.2	231.2	51	31	4	1.7

3.3.4.2 Bromate

Bromate was analyzed according to DIN EN ISO 10304. For HPLC separation the analytical column Synergi MAX-RP (250 x 4.6 mm; 4 µm C12) was used. The separation was carried out by gradient elution with two eluents: 0.1 % (v/v) formic acid in DI water (A) and 0.1 % (v/v) formic acid in acetonitrile (B) according to Table 10. An injection volume of 50 µL and a flow rate of 0.7 mL/min was applied.

Table 10: Gradient elution program

Time	Gradient	Gradient
min	% A	% B
1.2	95	5
3.5	95	5
7.0	20	80
7.1	20	80
12.1	95	5

The mass spectrometer used was QTRAP 3200 from AB Sciex (USA). The ion spray voltage was -4500 V and the temperature was 400° C. Due to the matrix effect bromate was determined according to DIN 32633 by spiking the sample with different bromate concentrations. Details regarding ionization mode used, retention time, mass-to-charge ratios of precursor ions (Q1), mass-to-charge ratio of qualifying and quantifying product ions (Q3) and LOQ are listed in Table 11.

Table 11: Parameters regarding bromate detection

Compound	Molar mass	Polarity	t_R	Q1	Q3	LOQ
	Da		min	m/z	m/z	$\mu g\ L^{-1}$
Bromate	127.9	-	5.1	126.7	110.8	6

Bromide was detected by HPLC coupled with a conductivity detector. The analytical column used was Metrosep A Supp 5; 5 µm C12; 250 x 4,0 mm and the eluent was 1mM $NaHCO_3$ + 3,2 mM Na_2CO_3. The eluent program was isocratic with a flow rate of 0.70 mL/min, injection volume of 50 µL, and pressure of circa 110 bar. The conductivity detector was coupled with a suppressor (Eco IC) from Metrohm (Switzerland).

Table 12: Parameters regarding bromide detection

Compound	t_R	LOQ
	min	$\mu g\ L^{-1}$
Bromide	11	45

3.4 Ozonation experiments

3.4.1 Preparation

O_3 generation was performed according to the set-up scheme shown in Figure 7. The O_3 generator was OZ500/5 from Fischer Technology (Germany) with an O_3 production capacity of 5 g/h and based on silent electric discharge with power set to 35 W. The oxygen cylinder was set to 1 bar and the airflow meter at the O_3 generator was set to 10 L/h. The generated O_3 was led through polytetrafluorethylene tubes and a stainless-steel three-way valve into a 2 L glass flask filled with DI water (O_3 reactor) and sealed with a silicone seal. O_3 flow was led through an O_3 diffusor air stone to produce fine bubbles and thus increase the solubility. Because O_3 solubility increases at lower temperatures the O_3 reactor was placed in an ice tank and the set-up ran for 4-5 hours for the O_3 concentration to equilibrate. Since O_3 does not completely dissolve in the water medium, gaseous O_3 must be led into a residual O_3 destructor. Therefore, the gas space of the O_3 reactor was led into a KI solution and non-absorbed O_3 could be quenched. The KI solution was prepared by dissolving 50 g KI in 450 mL DI water. As a preventive measure for a potential crystallization and clogging of the tube, the three-way valve was connected to a manganese (Mn) catalyst, which served as a second residual O_3 destructor. The dissolved O_3 concentration could be directly determined by circulating the aqueous O_3 solution through an L-7100 pump set to 1.5 mL/min and a UV/Vis photometer with an L-7400 UV detector, both from Merck Hitachi. From the absorbance at 258 nm the mass concentration ($mg\ L^{-1}$) could be calculated by multiplication with 22.2. However, the direct photometric measurement was used merely as a rough estimate, while the exact measurement was performed by implementing the indigo method.
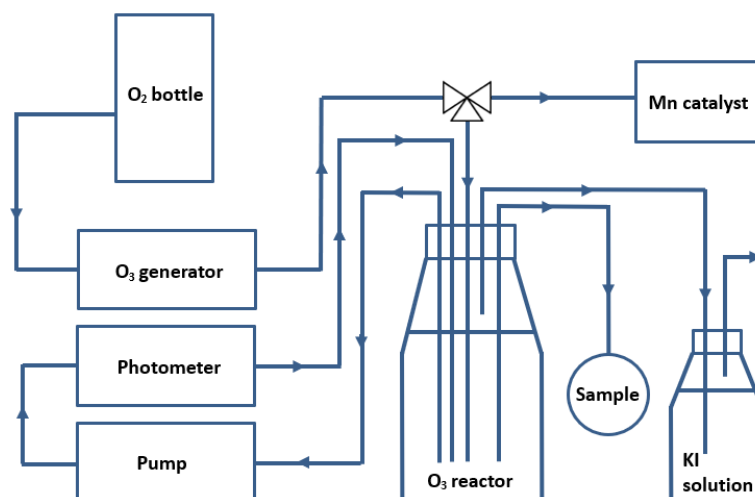
Figure 7: Scheme of the experimental set-up used for O$_3$ generation

When the absorbance was close to two (~40 mg L^{-1}), the glass syringe was connected to a stainless steel Luer lock valve and the stock solution was withdrawn for concentration measurement. For both the indigo method and the batch experiment, the O$_3$ stock solution was slowly withdrawn with a glass syringe to prevent bubbling of the O$_3$. For every withdrawal, the syringe and the needle were flushed with O$_3$ stock solution, which was discarded in a glass beaker. Ultimately, the needle was immersed into the sample/indigo solution and the solution was rapidly injected.

Figure 8: Experiment set-up in the lab

3.4.2 Ozone measurement

The indigo method for O$_3$ measurement is based on the decolorization of the indigo molecule. It is considered a fast, selective, and sensitive technique for the determination of the O$_3$ concentration. The method is based on the absorbance at 600 nm of a potassium indigotrisulfonate solution with ε_{600} = 20,000 M^{-1} cm^{-1}. The indigo molecule contains a C=C bond which is cleaved upon ozonation, producing two isatine sulfonic acid molecules. Those have an extinction coefficient of zero at 600 nm,

which leads to a stoichiometric decolorization of the indigo solution (Bader & Hoigné, 1981; Gottschalk et al., 2009). Indigo reagent solution was prepared according to DIN 38408-3(2011) under the modification of Zappatini & Götz (2015), which included the addition of an acid stock solution. The preparation of the reagents and their composition are listed in Table 13.

Table 13: Preparation of solution required for the indigo method

Reagents	Preparation and composition
Indigo stock solution	0.5 mL phosphoric acid (H_3PO_4) + 385 mg potassium indigotrisulfonate ($C_{16}H_7K_3N_2O_{11}S_3$) + DI water in a 500 mL volumetric flask
Acid stock solution	8.9 g sodium dihydrogen phosphate monohydrate ($NaH_2PO_4 \cdot H_2O$) + 7 mL H_3PO_4 + DI water in a 1000 mL volumetric flask
Indigo reagent solution (0.1 mM)	100 mL indigo stock solution + 900 mL acid stock solution in a 1000 mL volumetric flask

A reference solution (A) and a sample solution (B) were prepared in duplicates according to Table 14. For B, 10 mL indigo solution was first pipetted into a 50 mL beaker, which was circa ¾ filled with DI water. 0.5 mL O_3 stock solution was withdrawn and rapidly injected inside the beaker while stirring. The beaker was poured into a 100 mL volumetric flask and then washed three times with DI water. Then the volumetric flask was filled with DI water until the 100 mL mark. The measurement was performed with the UV/Vis spectral photometer Dr. Lange – Cadas 100 at 600 nm. For that, a 4 cm quartz cell was pre-washed with DI water and sample. The absorbance for each stock solution was determined, from which the mass concentration was calculated according to Equation (22) (DIN 38408-3, 2011). Since the O_3 concentration in the stock solution may change over time, the indigo method was carried out before and after the batch tests, and the mean O_3 concentration was determined.

Table 14: Preparation and composition of reference and sample solutions

Solutions	Preparation and composition
Reference solution (A)	Duplicates of 10 mL indigo reagent solution + 90 mL DI water in a 100 mL volumetric flask
Sample solution (B)	Duplicates of 10 mL indigo reagent solution + 0.5 mL O_3 stock solution + 89.5 mL Di water in 100 mL volumetric flask

$$p = \frac{(A_A - A_B) \cdot f \cdot V_{max}}{s \cdot V_p} \quad (22)$$

p O_3 mass concentration of B (mg L^{-1})

A_A absorbance of A

A_B absorbance of B

f   calibration function (2.4 mg cm L^{-1})

V_{max} total volume of B (100 mL)

s   optical path length of cell (3 cm)

V_p volume of the reference solution (0.5 mL)

3.4.3 Ozone batch test

Once the O_3 mass concentration in the O_3 reactor was sufficient, the required volume of O_3 stock solution and the composite effluent solution was calculated according to the desired nitrite-compensated specific O_3 dose. For the batch tests 500 mL Schott bottles were washed three times with water and three times with DI water. The samples were poured into 500 mL Schott bottles and placed under a magnetic stirrer, which was turned on for circa three seconds during the injection. The batch test was performed in triplicates for every specific O_3 dose and one triplicate for the non-ozonated sample. The bottles were immediately capped and after a contact time of one-hour O_3 was bubbled out for one minute with a diaphragm air pump. One shortcoming of the batch test lies in the different dilutions required. For a given O_3 mass concentration, a higher specific O_3 dose implies a higher dilution of the sample. To keep the dilution differences at bay, Zappatini & Götz (2015) recommend using an O_3 mass concentration higher than 48 mg L^{-1} (> 1 mmol L^{-1}). However, in this thesis, a maximal concentration of ~40 mg L^{-1} could be reached after 4-5 hours.

3.5 AC-adsorption batch tests

In the adsorption tests, three different PAC-containing products were used. The samples A1-3 were treated with commercially available "Epibon A" PAC. Moreover the samples A4 and C were treated with the product "AQUACLEAR A" and "AQUACLEAR B", while sample B was treated with the product "AQUACLEAR B" and the PAC "CARBOPAL®". All PAC-containing products were supplied by Donau Chemie AG (Austria).

The adsorption experiments were conducted by the shaking technique using the orbital benchtop shaker CERTOMAT® U from the company B. Braun (Germany). These experiments were carried out in Erlenmeyer flasks containing a fixed volume of effluent sample and a known adsorbent mass, which was calculated as the specific AC dose. Each sample was prepared either in duplicates or triplicates. The tested products AQUACLEAR A and AQUACLEAR B contained an AC percentage of 10 % and 18 %. Therefore, the specific AC dose was calculated regarding the contained AC portion in the product.

The cleaning procedure of the Erlenmeyer flasks involved rinsing 500 mL/200 mL with denatured ethanol, then thoroughly washing them with water, and finally with DI water. The samples were poured into each flask and the applied adsorbent was weighted in a precision balance using a plastic weighing pan. The weighing pan content was emptied into the corresponding flask and then washed with the sample a few times.

The added amount of the novel product was initially measured by the weight difference of a slightly filled and an ejected 1 mL plastic syringe. As the first attempt to measure the suspension for sample A4, this turned out to be too unprecise to achieve relatively similar triplicate results because of the following reasons. Firstly, the product was weighted in the tens of milligram range, which made it difficult to reach similar results by injecting small amounts into a syringe. This resulted in standard deviations ranging from 0.4 to 6.9 % in the four triplicates. Secondly, ejection into the sample led to small residues of the product in the syringe, which further led to variations. For the next two experiments, the product was weighted by ejecting small drops on a glass weighing pan using a plastic pipette. The content was washed with the sample a few times until no suspension was visible.

Finally, the flasks were sealed with parafilm and mounted to the shaker platform. The shaking was carried out at an adjusted lab temperature of 23° C and a shaking speed of 120 rpm for an equilibration time (t_{eq}) of 18 hours. After equilibrium has been reached, the samples were filtered with a VWR glass fiber filter (pore size 1 µm, grade 698), followed by SAC_{254} and OMP measurement. In addition, DOC measurements were carried out for all A2 samples and two A3 samples (an A3 effluent blank and an A3 ozonated blank).

For modeling the adsorption capacity of OMPs at the AC, the adsorption models described by Langmuir and Freundlich were fitted to the obtained data. For this purpose, the 2-parametric equations were linearized, as shown in Equations (23)-(24). The coefficient of determination for each model, including the Langmuir and Freundlich parameters, were calculated for each OMP.

The linearized Langmuir Equation:

$$\frac{1}{q} = \frac{1}{q_m} + \frac{1}{q_m c}\frac{1}{c} \tag{23}$$

The linearized Freundlich Equation:

$$\ln(q) = \ln K_F + n \ln c \tag{24}$$

Figure 9: Adsorption experiments using the orbital benchtop shaker CERTOMAT® U; t_{eq} = 18 h; T = 23° C

4   Results

4.1 Ozonation

Ozonation was studied as an advanced treatment step for the abatement of OMPs in the WWTP effluent samples A1-A3. Additionally, the percentual increase of ΔSAC_{254} as a surrogate parameter for the effective specific O_3 dose, and the sum parameter BOD_{1-6} were considered. In total, three different specific O_3 doses were studied in sample A1: 0.46, 0.57, and 0.88 g O_3 g^{-1} DOC, while samples A2 and A3 were treated with a lower specific O_3 dose of 0.45 and 0.40 g O_3 g^{-1} DOC, respectively.

4.1.1 Effect of different specific ozone doses on OMP abatement

The removal percentages of different OMPs in the experiments conducted with samples A1-A3 are given in Figure 10. It shows an evident impact of an increasing O_3 dose on the OMP abatement. CBZ, TMP, and DCF had high removals of more than 80 % already at a low specific O_3 dose range of 0.40-0.46 g O_3 g^{-1} DOC. After ozonation, the concentration of these compounds was very low or even below the LOQ of the applied method. DCF had the highest removal of 93.5 ± 0.5 % at the lowest specific O_3 dose of 0.40 g O_3 g^{-1} DOC. The removal of CBZ was 52.4 ± 1.1 % at 0.40 g O_3 g^{-1} DOC and more than 95 % at higher doses. The removal of SMX oscillated between 73.9 % at 0.40 g O_3 g^{-1} DOC and 59.4 ± 5.3 % at 0.46 g O_3 g^{-1} DOC. At a higher dose of 0.57 g O_3 g^{-1} DOC its removal remained relatively constant with 73.4 ± 2.0 %, while a higher removal of 95.8 ± 7.3 % was reached at 0.88 g O_3 g^{-1} DOC. MTP had low to intermediate removals at the specific O_3 dose range applied. At the highest dose, it was removed by 63.7 ± 5.3 %. At 0.40-0.57 g O_3 g^{-1} DOC, BTA had low removals, ranging from 17.3 ± 3.2 % to 28.5 ± 3.4 %. The highest removal increase occurred between 0.57 and 0.88 g O_3 g^{-1} DOC, which peaked to 85.3 ± 3.4 % at the highest dose. BZF was gradually removed with increasing specific O_3 doses. At 0.40, 0.57, and 0.88 g O_3 g^{-1} DOC it was removed by 43.0 ± 1.7 %, 61.1 ± 1.3 %, and 96.2 ± 0.6 %, respectively.
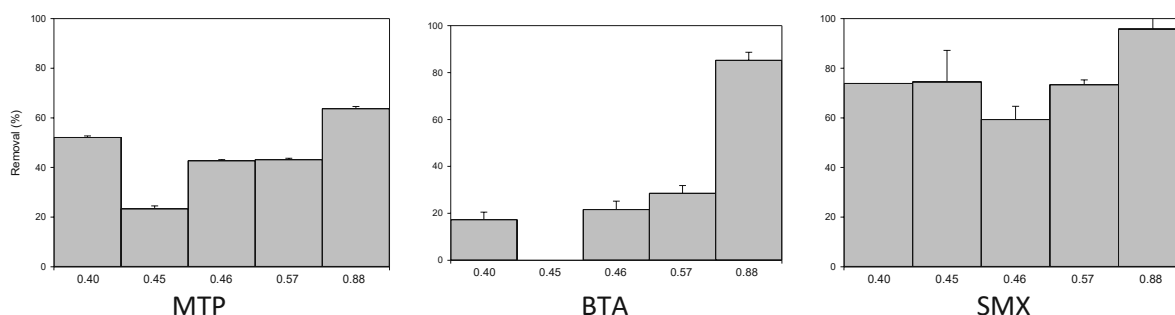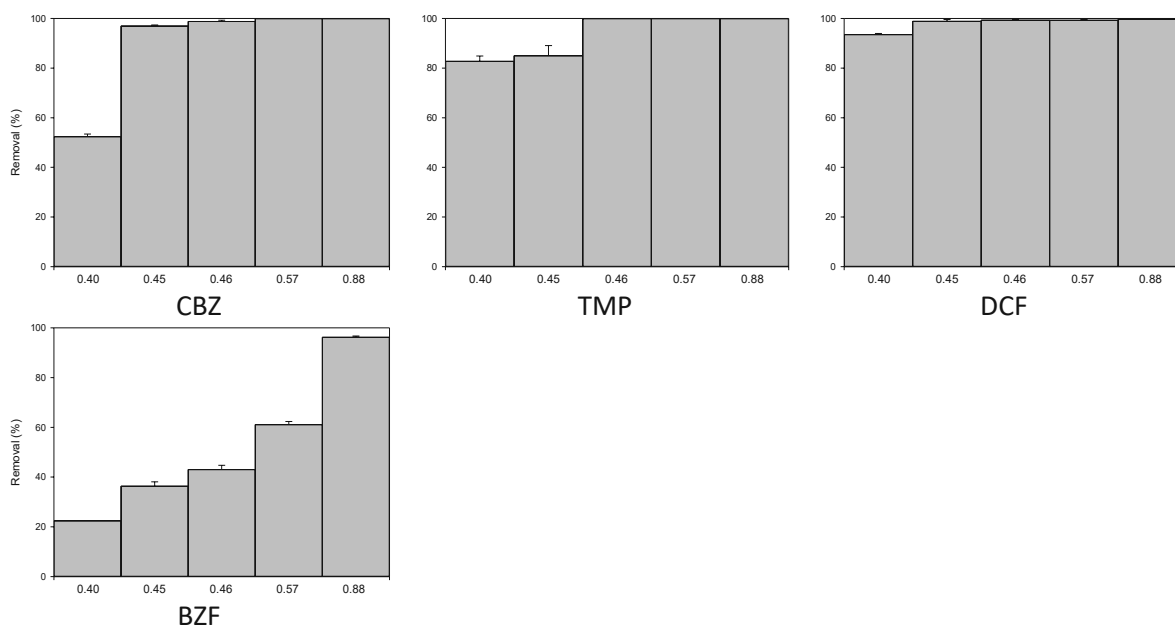
Figure 10: Removal percentage of OMPs at specific O_3 doses of 0.40, 0.45, 0.46, 0.57, and 0.88 g O_3 g^{-1} DOC in samples A1-A3

4.1.2 Potential of bromate formation

Bromate could only be detected in sample A1 at 0.88 g O_3 g^{-1} DOC at a concentration of 18.4 ± 1.2 µg L^{-1}, which exceeds the maximum contaminant level of 10 µg L^{-1} applied in drinking water. The effluent sample A1 had a bromide concentration of 40 µg L^{-1}, which indicates that 46 % of bromide was oxidized to bromate. At lower specific O_3 doses, bromate concentrations were below the LOQ (5 mg L^{-1}). Sample A2 had a higher bromide concentration of 100 µg L^{-1} but bromate was not detected at the corresponding specific O_3 dose (0.45 g O_3 g^{-1} DOC).

4.1.3 Correlation with ΔSAC_{254}

Figure 11 shows the calibration curve of the percentual reduction of SAC_{254} with the nitrite-compensated specific O_3 dose. The ΔSAC_{254} is caused by the structural changes of conjugated and aromatic moieties in the EfOM during ozonation. With a coefficient of determination R^2 of 0.94, the correlation between these parameters is fairly strong. A specific O_3 dose of 0.40 g O_3 g^{-1} DOC increased the ΔSAC_{254} by 38.6 ± 0.2 %, whereas the increase amounted to 68.7 ± 0.9 % at 0.88 g O_3 g^{-1} DOC.
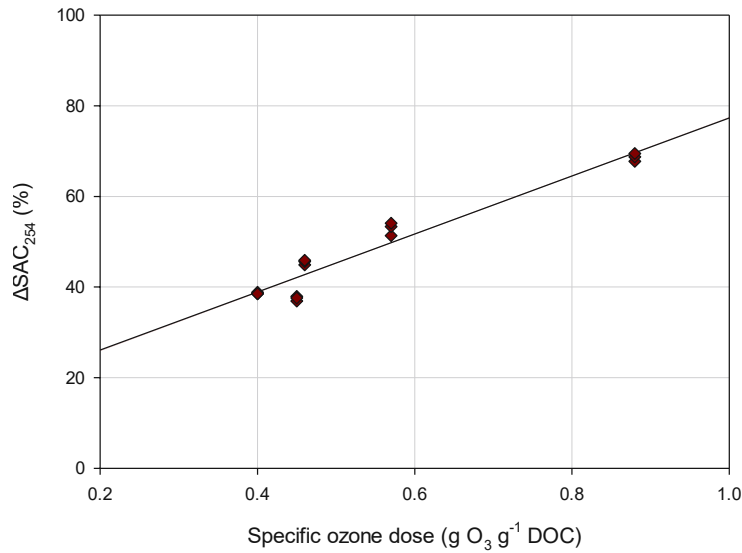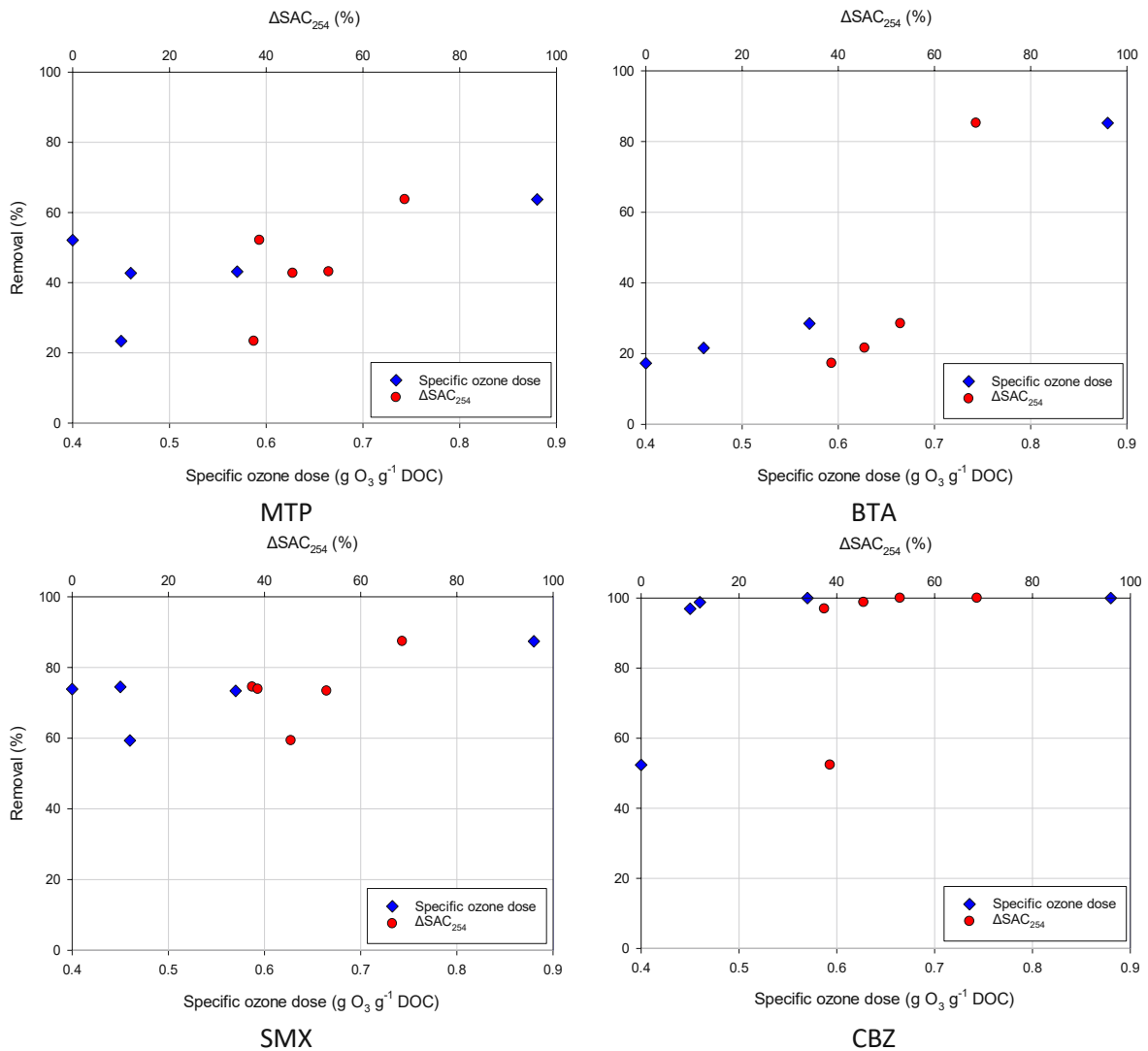
Figure 11: Linear correlation between ΔSAC₂₅₄ and specific O₃ dose; linear regression line (R² = 0.94)

Figure 12 illustrates the correlation regarding the removal of the single OMPs. Since the surrogate parameter correlates well with the specific O_3 dose it correlates also well with OMP removal.
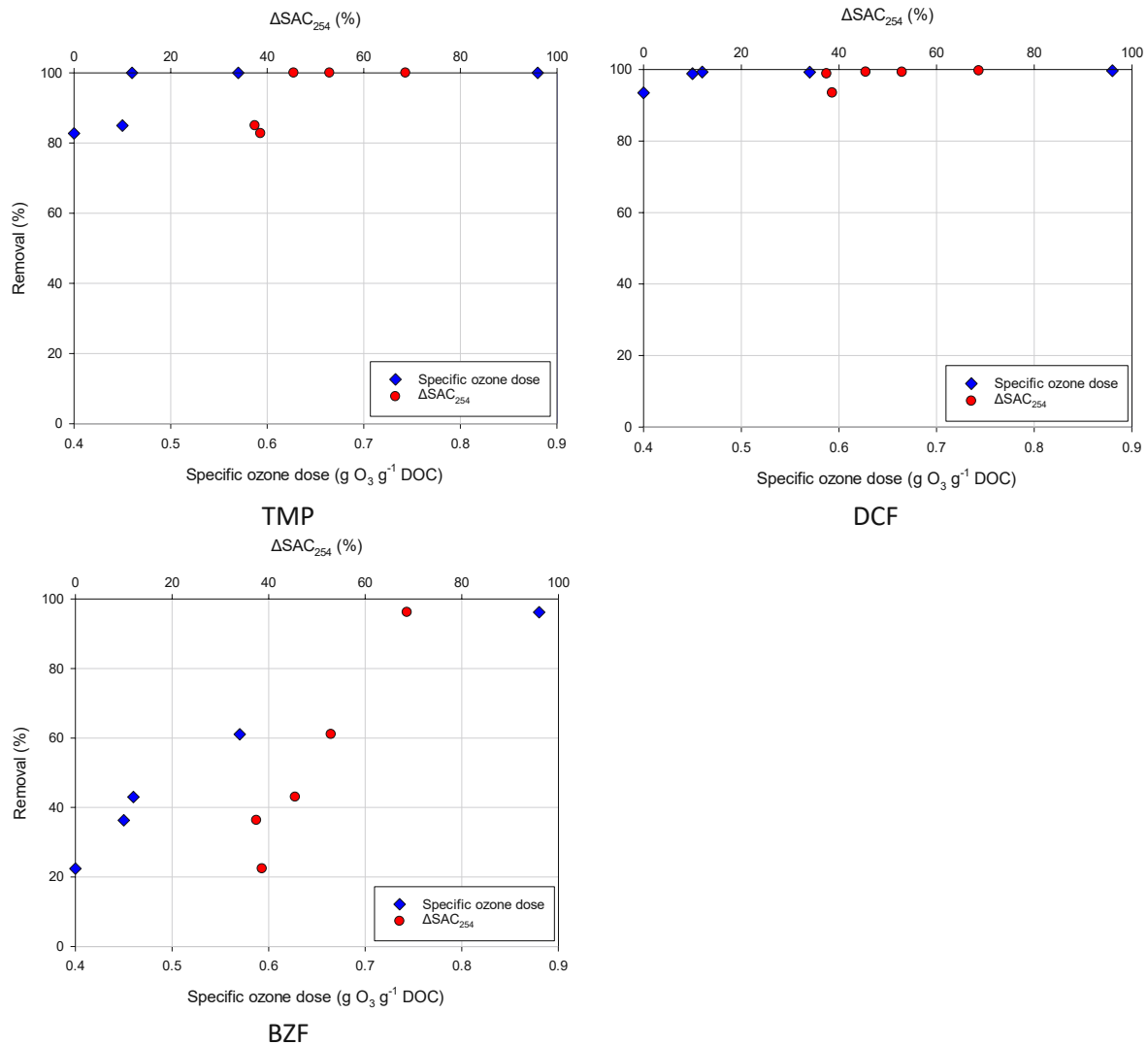
Figure 12: Removal percentage of OMPs as a function of both specific O₃ dose and ΔSAC₂₅₄

4.1.4 Effect of ozonation on biological oxygen demand (BOD₅)

During ozonation structural changes of the EfOM occur, which are characterized by an increased formation of more readily biodegradable organic matter, resulting in an increase of the sum parameter BOD_5 (Schaar et al., 2011). The increase of BOD_5 in A1 is depicted in Figure 13. Without ozonation, BOD_5 was 3.13 ± 0.27 mg L^{-1} while a specific O_3 dose of 0.46 g O_3 g^{-1} DOC increased it to 5.97 ± 0.48 mg L^{-1}. At 0.88 g O_3 g^{-1} DOC the increase relative to the effluent begins at day 2 and shows comparable values to the other A1 ozonated samples in the next days. A comparison of the A1 ozonated samples does not suggest a correlation between the applied specific O_3 doses and the BOD values. The BOD increase appears to be independent of the specific O_3 dose as the standard deviation in the single days overlap.
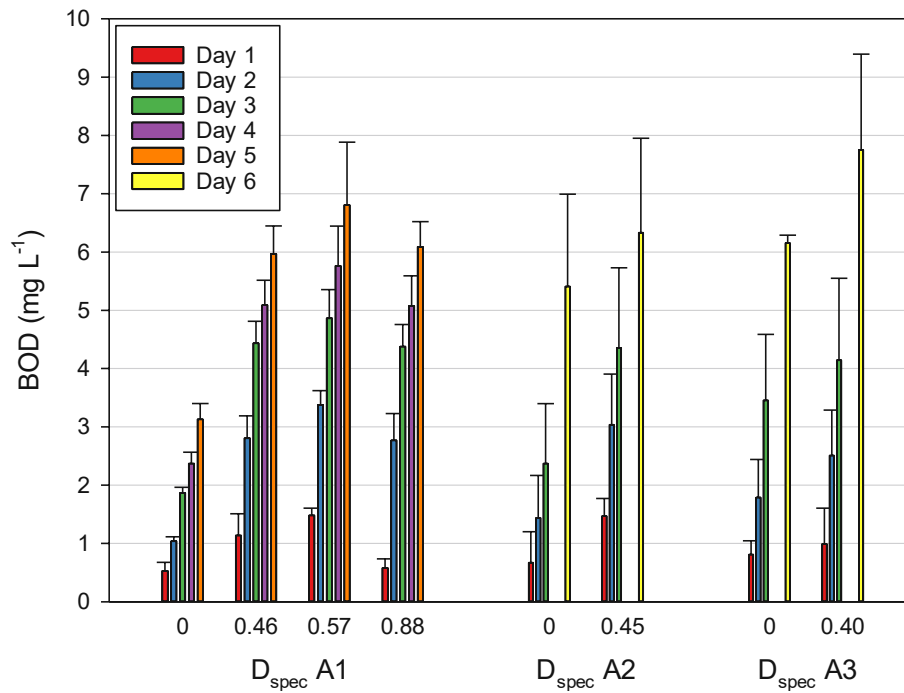
Figure 13: Increase of BOD concentration during the measuring days in samples A1-A3

Figure 14 shows the percentual increase of BOD_5 in respect to the initial concentration of the effluent sample. The largest increase occurred already at lowest specific O_3 dose of 0.46 g O_3 g^{-1} DOC. The relatively larger increase at 0.57 g O_3 g^{-1} DOC compared to 0.88 g O_3 g^{-1} DOC does not appear to be significant. It is apparent that there is a leveling-off effect in the analyzed range, which may suggest that respiration of biodegradable organic matter reached saturation. Therefore, the curve shape could be well fitted to a growth function with an exponential plateau.
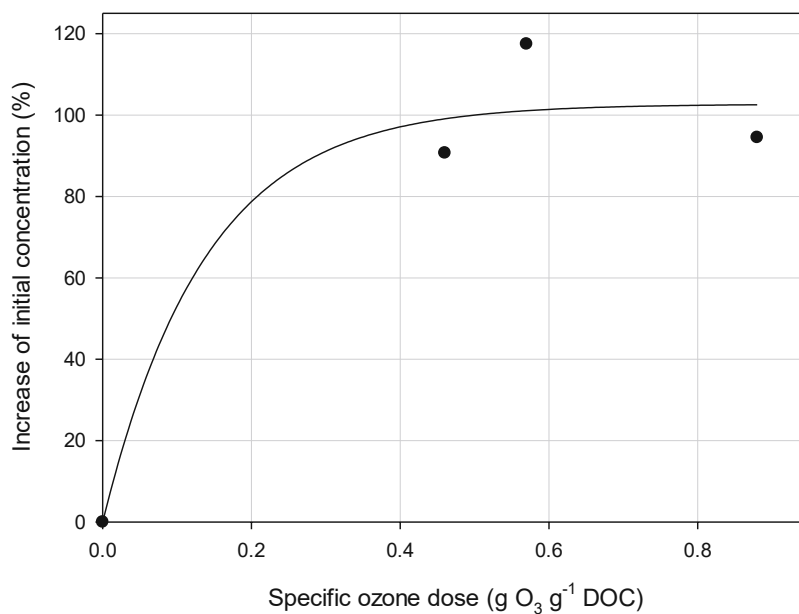
Figure 14: Increase of initial concentration in dependence of the specific O_3 dose; data were fitted using the dynamic fit wizard of SigmaPlot 14 (Systat Software, Inc.); $R^2 = 0.95$

In samples A2 and A3, the BOD_6 was measured instead of the BOD_{4-5}. In both samples, the increase of initial concentration was not as apparent anymore as in sample A1. At 0.45 and 0.40 g O_3 g^{-1} DOC, the BOD_6 increase of initial effluent concentration is 17.0 % and 25.8 % in samples A2 and A3, respectively. Noticeable in Figure 13 is a considerable standard deviation in both samples, which makes it hard to distinguish the effluent from the ozonated sample. BOD_6 of A2 effluent sample was 5.41 ± 1.58 mg L^{-1}, while it was 6.33 ± 1.62 mg L^{-1} in A2 ozonated sample. Likewise, BOD_6 of A3 effluent sample was 6.15 ± 0.14 mg L^{-1} and of A3 ozonated sample was 7.75 ± 1.64 mg L^{-1}. Moreover, two BOD flasks had no oxygen left after six days (an ozonated triplicate of sample A2 and an effluent triplicate of sample A3) and their values were not included in the BOD_6 calculation.

4.2 Combination of ozonation and PAC adsorption

This section contains data regarding OMP abatement by a combined O_3/PAC treatment of the samples. A2 and A3 effluent samples were first ozonated with the specific O_3 dose of 0.45 and 0.40 g O_3 g^{-1} DOC, respectively. The samples were then subjected to a PAC adsorption step using the commercially available PAC Epibon A with the specific AC doses 1.0, 1.5, and 2.0 g AC g^{-1} DOC. To investigate the effect of ozonation on a subsequent PAC adsorption step, non-ozonated A2 and A3 effluent samples were additionally treated with 1.5 g AC g^{-1} DOC.

4.2.1 Effect of PAC adsorption

Relative reductions of OMPs in ozonated samples A2 and A3 are depicted in Figure 15. To investigate the effect of PAC adsorption on OMP abatement the treated ozonated samples were normalized to the non-treated ozonated samples. Since TMP concentration in both ozonated samples, A2 and A3, was just above the LOQ its removal could not be evaluated. Similarly, MTP and SMX concentrations in the A3 ozonated samples were only five times higher than the LOQ, therefore, their removal was not evaluated as well. BTA shows an increased removal at higher specific AC doses. Following a PAC treatment from the lowest to the highest specific AC dose, BTA removal in sample A2 amounts to 43.7 ± 2.9, 55.5 ± 4.2, and 65.8 ± 2.6 g PAC g^{-1} DOC, whereas in sample A3 the removals are higher by circa 15 %. The removal of MTP and SMX at the tested specific AC doses is generally similar, whereas the highest removal increase occurred between 1.5 and 2.0 g AC g^{-1} DOC. MTP removal in sample A2 amounted to 73.4 ± 3.8, 76.4 ± 1.9, and 82.9 ± 0.8 g PAC g^{-1} DOC at the tested specific AC doses. Comparably, SMX had lower removals of 18.8 ± 9.5, 22.9 ± 2.3, and 49.2 ± 9.9 g PAC g^{-1} DOC. CBZ was mostly detected below the LOQ at all the applied specific AC doses, whereas an A2 triplicate at 1.0 and an A3 triplicate at 2.0 g AC g^{-1} DOC was detected slightly above the LOQ. DCF has different removals at 1.0 g AC g^{-1} DOC, which is 74.4 ± 22.2 and 90.7 ± 0.9 g PAC g^{-1} DOC in samples A2 and A3, respectively. At higher specific AC doses, DCF removal is above 80 %. BZF was detected below the LOQ in sample A2, while its removal was above 80 % at all tested specific AC doses in sample A3.
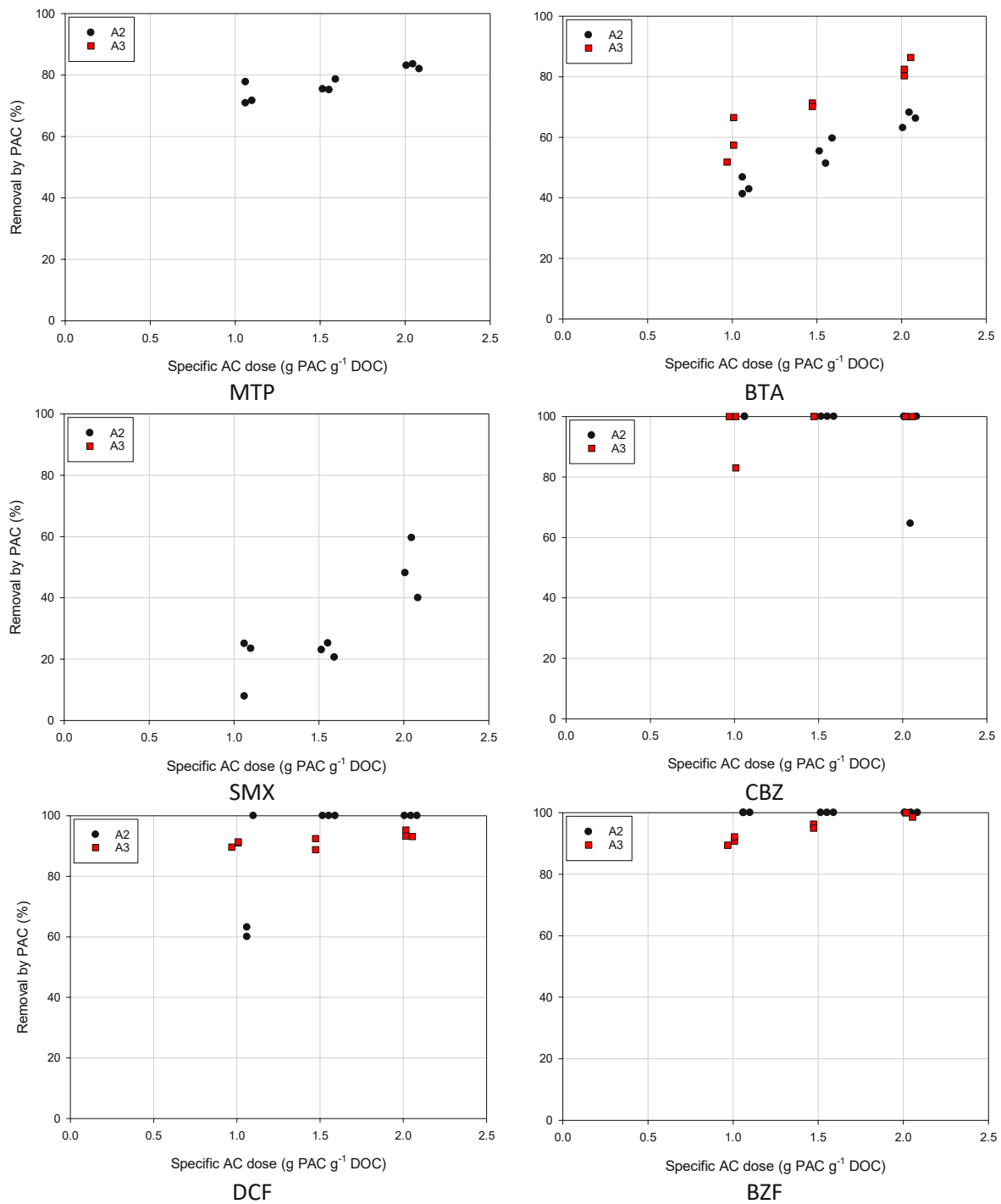
Figure 15: OMP removal from A2 and A3 ozonated samples at 1.0, 1.5, and 2.0 g PAC g^{-1} DOC

4.2.2 Comparison of OMP adsorption in ozonated and non-ozonated effluent

In addition to the combined treatment, the exclusive effect of PAC adsorption on the non-ozonated effluent was evaluated, as depicted in Figure 16. Therefore, the A2 and A3 ozonated and non-ozonated

samples were normalized to the effluent samples. For a full comparison, the exclusive effect of ozonation is additionally shown.

The compounds MTP, CBZ, TMP, DCF, and BZF were efficiently removed when ozonation and subsequent PAC adsorption were applied. DCF and BZF showed rather lower removals when PAC was exclusively applied, whereas MTP and TMP had similar removals in both cases. Notable is the difference in removal of DCF from effluent A3, which was 99.3 % in the ozonated effluent compared to 62.9 % in the non-ozonated effluent. This amounts to an improvement of 36.4 % when both steps were applied. Similarly, the removal of BZF from A3 effluent was increased from 86 % to 95 % by the combined treatment. BTA showed removals of 60-70 % in both A2 and A3 samples with no discernible differences between the two cases. For both BZF and BTA the removal is mainly driven by PAC adsorption. SMX was removed solely by ozonation while a subsequent PAC treatment with 1.5 g PAC g^{-1} DOC did not affect its removal.
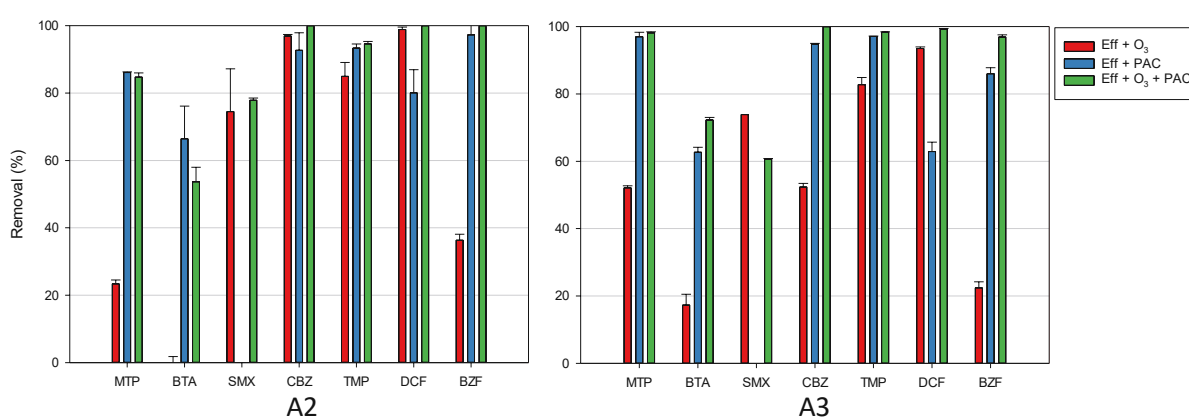
Figure 16: OMP removal from A2 and A3 effluent samples after ozonation with 0.45 and 0.40 g O_3 g^{-1} DOC, respectively (red bar), after PAC adsorption with 1.5 g PAC g^{-1} DOC (blue bar), and after combined treatment (green bar)

4.2.3 Correlation with ΔSAC_{254}

Similarly to ozonation, the parameter ΔSAC_{254} can be applied as a surrogate parameter for OMP abatement during PAC adsorption. This is based on EfOM adsorption to PAC, which also results in the decline of absorbance (Altmann et al., 2014; Rizzo et al., 2019).
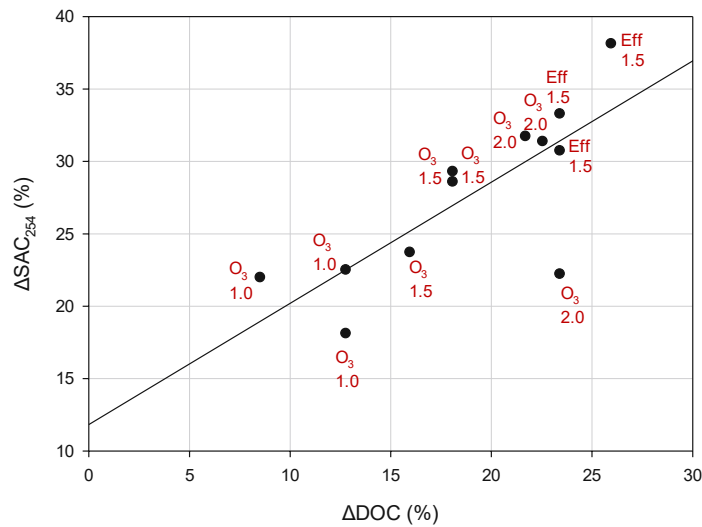
Figure 17: Linear correlation between ΔSAC$_{254}$ and DOC in sample A2; linear regression line (R^2 = 0.6)

Figure 17 shows a linear correlation between ΔDOC and ΔSAC$_{254}$ in ozonated and non-ozonated effluent samples following PAC treatment. Among the ozonated samples, higher specific PAC dose resulted in higher ΔDOC and higher ΔSAC$_{254}$ values. A comparison of ozonated and non-ozonated samples reveals that both parameters, ΔDOC and ΔSAC$_{254}$, increased stronger in the non-ozonated samples than in the ozonated ones. At a specific PAC dose of 1.5 g PAC g^{-1} DOC the non-ozonated sample features greater DOC reduction than ozonated samples treated with a higher specific PAC dose of 2.0 g PAC g^{-1} DOC. The mean ΔDOC values of the ozonated and non-ozonated samples were 17.4 ± 0.1 % and 23.4 ± 0.3 %, respectively. The corresponding increase of ΔSAC$_{254}$ at 1.5 g AC g^{-1} DOC of the ozonated and non-ozonated samples amounts to 27.2 ± 3.0 % and 33.8 ± 3.8 %.

4.2.4 EfOM adsorption and adsorption models

As shown in Figure 18, the removal of EfOM in ozonated and non-ozonated samples was different. Since EfOM can compete with the analyzed OMPs on the active sites of the adsorbent it additionally affects their adsorption capacity. In the analyzed range of the tested AC doses, the DOC loading of the PAC in the ozonated effluent was independent of the concentration in the liquid phase. Assuming that the data point at 8.6 mg L^{-1} is an outlier (triangle symbol), the AC applied in sample A2 shows relatively constant loadings of 70-85 mg DOC g^{-1} PAC, whereas the loadings of the non-ozonated samples lie distinctly higher at 110 to 125 mg DOC g^{-1} PAC. This agrees with the observed higher ΔSAC$_{254}$ values of the non-ozonated sample.
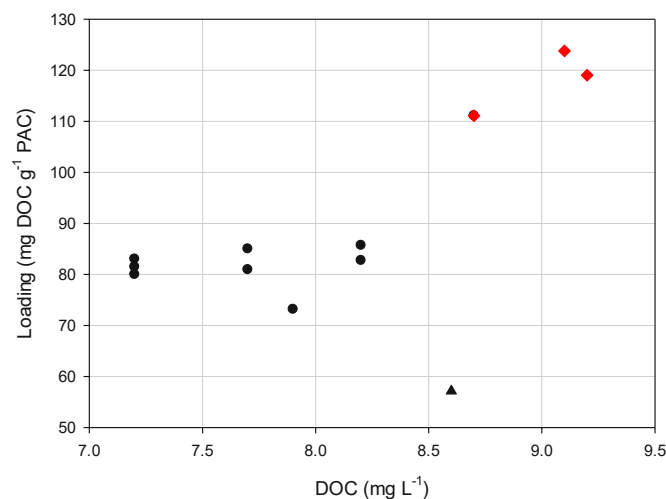
Figure 18: DOC adsorption isotherm of ozonated (black points) and non-ozonated (red diamonds) A2 samples; 0.45 g O_3 g^{-1} DOC; T = 23° C; t_{eq} = 18 hours

To analyze the adsorption capacity of the selected OMPs in the ozonated samples, the calculated loadings were linearized to fit the Langmuir and Freundlich models. However, only the Langmuir model could be fitted with a coefficient of determination above 0.54. The obtained isotherm constants can be found in Table 15. The concentrations of the compounds CBZ, DCF, and BZF were below the LOQ in most of the samples, therefore, their adsorption capacity could not be modeled.

Table 15: Regressed Langmuir adsorption parameters of MTP, BTA and BZF obtained for samples A2 and A3; T = 23° C; t_{eq} = 18 hours

| Sample | Compound | Langmuir | | |
| | | q_{max} | b | R^2 |
		ng g^{-1}	L ng^{-1}	-
A2	MTP	2.5×10^4	5.3×10^6	0.66
	BTA	5×10^3	8.7×10^5	0.54
A3	MTP	2.5×10^4	2.7×10^8	0.72
	BTA	1.0×10^4	5.0×10^6	0.63
	BZF	1.3×10^3	6.3×10^5	0.89

Figure 19: Adsorption isotherms of OMPs in sample A2 with (black points) and without (red diamonds) a pre-ozonation step; 0.45 g O_3 g^{-1} DOC; T = 23° C; t_{eq} = 18 hours

Figure 20: Adsorption isotherms of OMPs in sample A3 with (black points) and without (red diamonds) a pre-ozonation step; 0.40 g O_3 g^{-1} DOC; T = 23° C; t_{eq} = 18 hours

4.3 Adsorption potential of a novel product

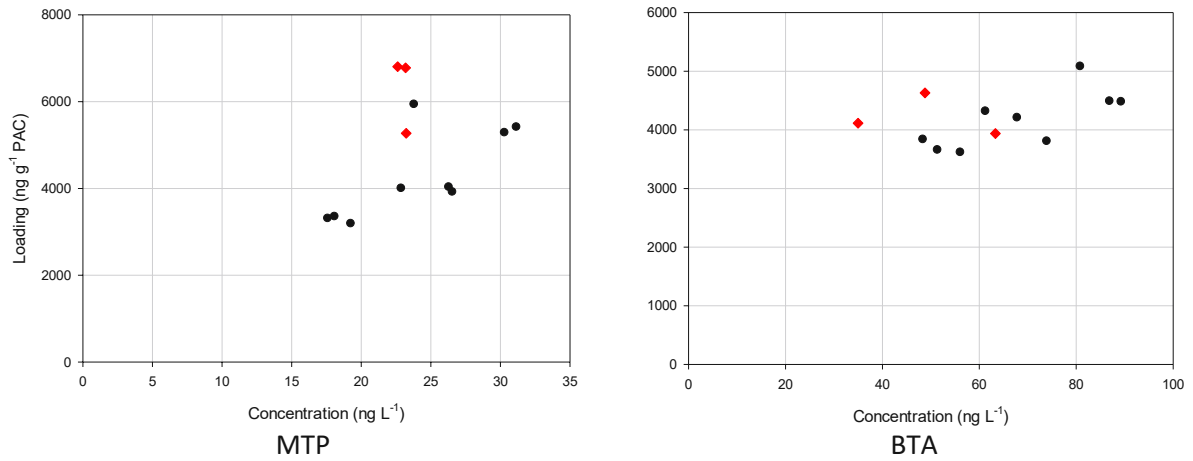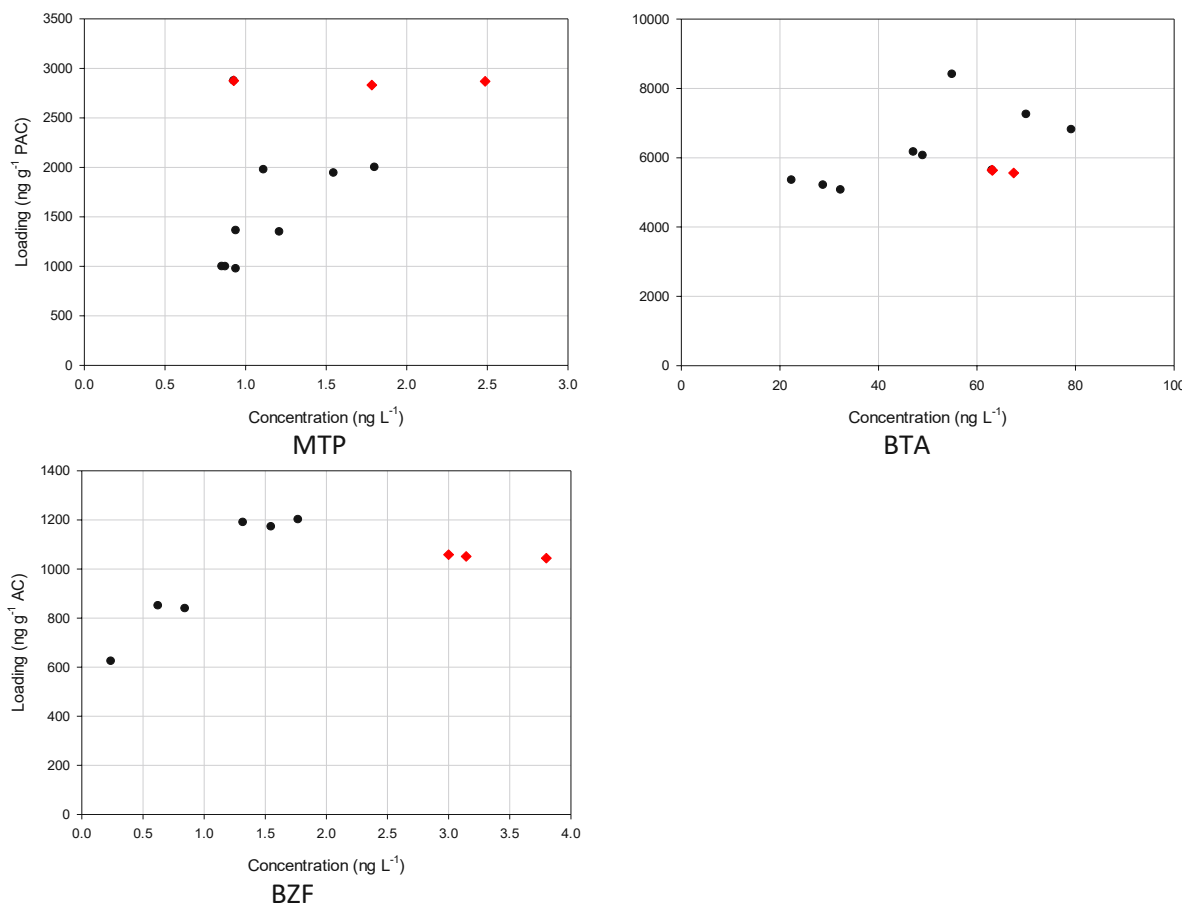In the following section, the adsorption potential of a novel product is analyzed. The product is a suspension containing PAC and polyaluminum chloride, combining precipitating and adsorbing properties. A clear advantage lies in its suspended form, which enables it to be dosed via pumps in WWTPs. Within an ongoing feasibility study, its removal potential of phosphorous and OMPs is investigated in different WWTP effluent matrices. The product is offered in two formulations: AQUACLEAR A and AQUACLEAR B with an AC fraction of 10 % and 18 %, respectively. In the framework of this thesis, the adsorption capacity of the product for OMPs is studied in three different Austrian WWTP effluent samples: A, B, and C. In addition, the product is compared with the PAC CARBOPAL®, which is the PAC ingredient involved in its manufacture.

4.3.1 OMP removal

A comparison of OMP removal in the different WWTPs shows a trend of higher removal with a higher specific AC dose, as depicted in Figure 21. In sample A4, the increased removal at the lower range is evident for all five compounds. Higher specific AC doses in the range 0.69 to 1.3 g AC g^{-1} DOC increased the MTP removal from 53.5 % to 68.4 %. BTA removal increased even more from 53.9 % to 77.5 %. At the same specific AC doses, CBZ was removed from 60.8 % to 77.6 %. DCF shows a relatively low removal of 24.6 % at the specific AC dose of 1.3 g AC g^{-1} DOC. At specific AC doses higher than 1.5 g AC g^{-1} DOC no increase of OMP removal is observed. Instead, the removal levels off and slightly decrease at the highest specific AC dose.

In sample B there is a large scatter in the MTP removal, which results in high standard deviations at all tested specific AC doses. From the lowest to the highest specific AC dose, MTP removal by the product is 55.6 ± 34.3, 42.9 ± 28.0, and 90.22 ± 15.3 %. In comparison, BTA, CBZ, and DCF did not reach high removals by the product also at the highest applied specific AC dose. BTA and CBZ were removed by 70.6 ± 3.2 % and 64.7 ± 4.4 % at 2.25 g AC g^{-1} DOC. DCF had low-intermediate removals at all specific AC doses applied. From the lowest to the highest specific AC dose, DCF removal by the product amounted to 34.0 ± 5.7, 29.9 ± 5.2, and 42.6 ± 3.1 %.

Compared to sample A4 and B, higher removals were accomplished in sample C. The removals of the compounds MTP, BTA, CBZ, and TMP were above 80 % already at 1.51 g AC g^{-1} DOC. The relatively low removal of BTA, CBZ, and TMP at 0.84 and 1.28 g AC g^{-1} DOC indicates that the largest removal increase occurred between 1.28 and 1.51 g AC g^{-1} DOC. MTP had intermediate removals of 49.8 ± 3.4 % and 46.0 ± 3.1 % at 0.84 and 1.28 g AC g^{-1} DOC, respectively. These increased to 94.8 ± 2.0 % and 99.0 ± 0.2 % at 1.51 and 2.28 g AC g^{-1} DOC, respectively. BZF was gradually removed stepping up from the lower to the higher specific AC dose. High BZF removal of 87.3 ± 1.3 % was reached at 2.28 g AC g^{-1} DOC. DCF showed low removals at the lower doses which jumped to 38.8 ± 3.4 % and 60.6 ± 2.5 % at the higher doses. SMX removal at all doses was very low with a maximal removal of 11.6 ± 5.1 % at the highest dose applied.
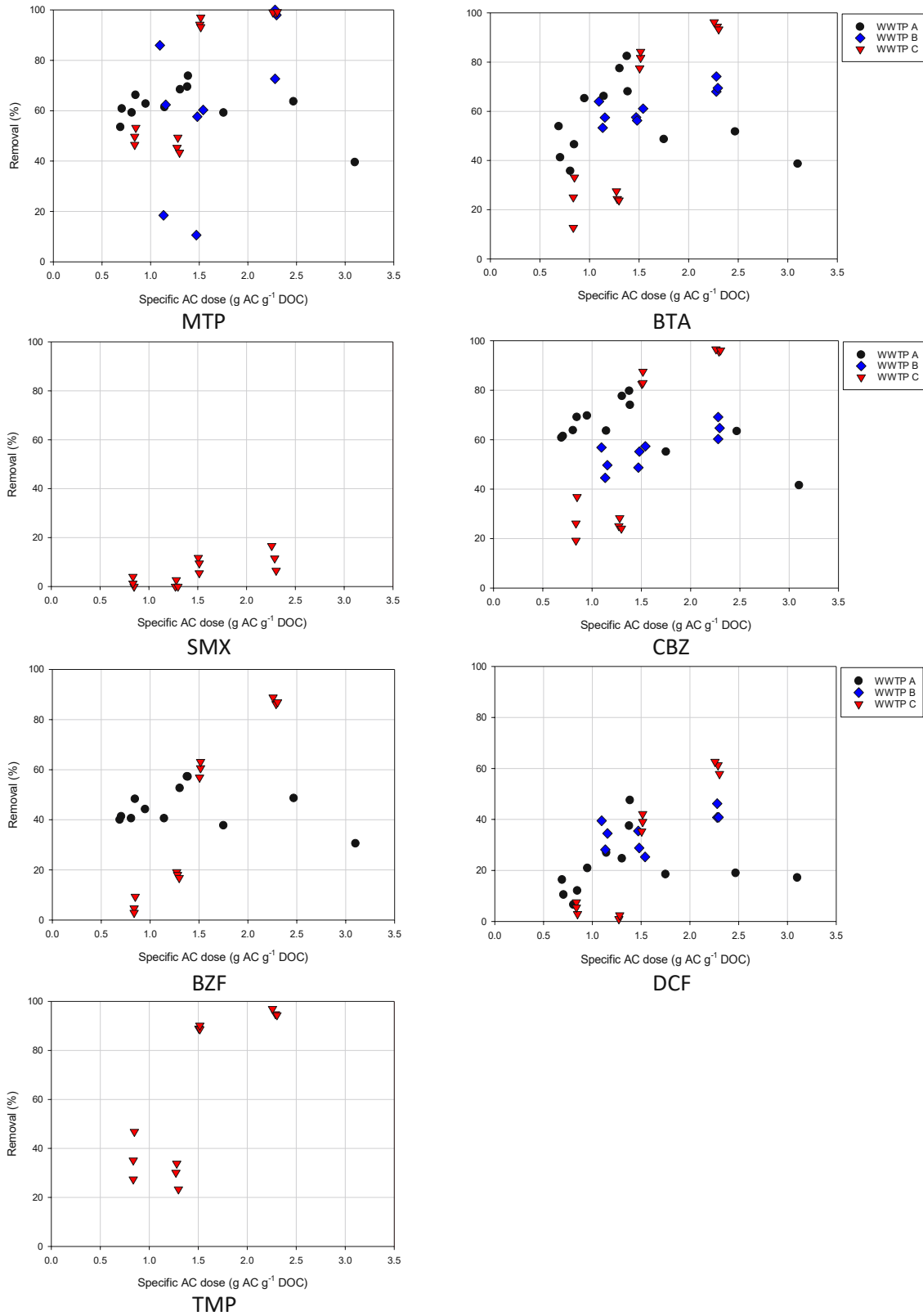
Figure 21: OMP removal from WWTPs A, B, and C

Figure 22 shows the increase of ΔSAC_{254} in WWTP B and C. It is evident that there is a larger data scatter concerning sample C compared to sample B. This makes it difficult to compare both WWTPs at 1.5 g AC g^{-1} DOC and lower. However, it seems that at 2.25 g AC g^{-1} DOC the product increases ΔSAC_{254}

stronger at sample C than at B. At this specific AC dose, sample C shows a ΔSAC_{254} of 31.7 ± 6.2 % whereas sample B shows a ΔSAC_{254} of 19.7 ± 2.3 %. Because the correlation between the specific AC dose and ΔSAC_{254} in sample A4 shows a low coefficient of determination of 0.21 no comparison with WWTP A can be made.

Figure 22: Linear correlation between ΔSAC_{254} and specific AC dose; linear regression lines of the product AQUACLEAR B in sample B ($R^2 = 0.85$), and AQUACLEAR A and B in sample C ($R^2 = 0.73$)

Table 16 lists the minimal specific AC dose required to reach a high removal > 80 % in WWTP B, considering the removal at the biological treatment stage. The compounds SMX, DIU, TMP, BZF, and IBP could be completely removed at the biological treatment stage. Therefore, product application is not necessary for their removal. The compounds MTP and BTA showed intermediate removals at the biological treatment stage, therefore, a specific AC dose of 1 g AC g^{-1} DOC is sufficient to reach a high removal. For an 80 % removal of the biologically recalcitrant CBZ and DCF, the removal by the product was not established. At 2.25 g AC g^{-1} DOC, 64.7 ± 4.4 % of CBZ and 42.6 ± 3.1 % of DCF were removed. Therefore, a specific AC dose > 2.25 g AC g^{-1} DOC is necessary for their removal.

Table 16: Required product dose for an 80% OMP removal in WWTP B

	MTP	BTA	SMX	CBZ	DIU	TMP	DCF	BZF	IBP
Biological removal in WWTP B (%)	40	45	100	0	100	100	20	100	100
Product dose (g AC g^{-1} DOC)	1	1	0	> 2.25	0	0	> 2.25	0	0

4.3.2 Comparison between AQUACLEAR B and CARBOPAL®

Due to additional components in the product formulation, notably polyaluminum chloride, differences in the OMP adsorption capacity may occur. To compare both adsorbents, three different specific AC doses of the product AQUACLEAR B and the PAC CARBOPAL® were applied in effluent sample B.

As shown in Figure 23, the PAC performed better at removing the analyzed OMPs. MTP removal by both adsorbents is similar at the low and intermediate doses with a high standard deviation. At 1.25 g AC g^{-1} DOC, it was removed by 55.6 ± 34.3 % by the product, and by 92.4 ± 2.6 % by the PAC. At 1.5 g AC g^{-1} DOC, the removal by the product was 42.9 ± 28.0 %, while a complete removal was reached by the PAC. With a higher specific AC dose of 2.25 g AC g^{-1} DOC the removal by the product increased to 90.2 ± 15.2 %. At the lowest dose, BTA had a similar removal by both adsorbents of 58.3 ± 5.4 % by the product and 62.5 ± 5.7 % by the PAC. At the medium dose, the removal by the product and by the PAC amounted to 58.3 ± 2.5 % and 81.6 ± 0.5 %, respectively. At the highest dose, the removal by the product increased to 70.6 ± 3.2 % and slightly decreased to 78.0 ± 1.3 % with the PAC. CBZ and DCF removal by the product is the largest at the highest specific AC dose, whereas their removal by the PAC is largest at the medium specific AC dose applied.
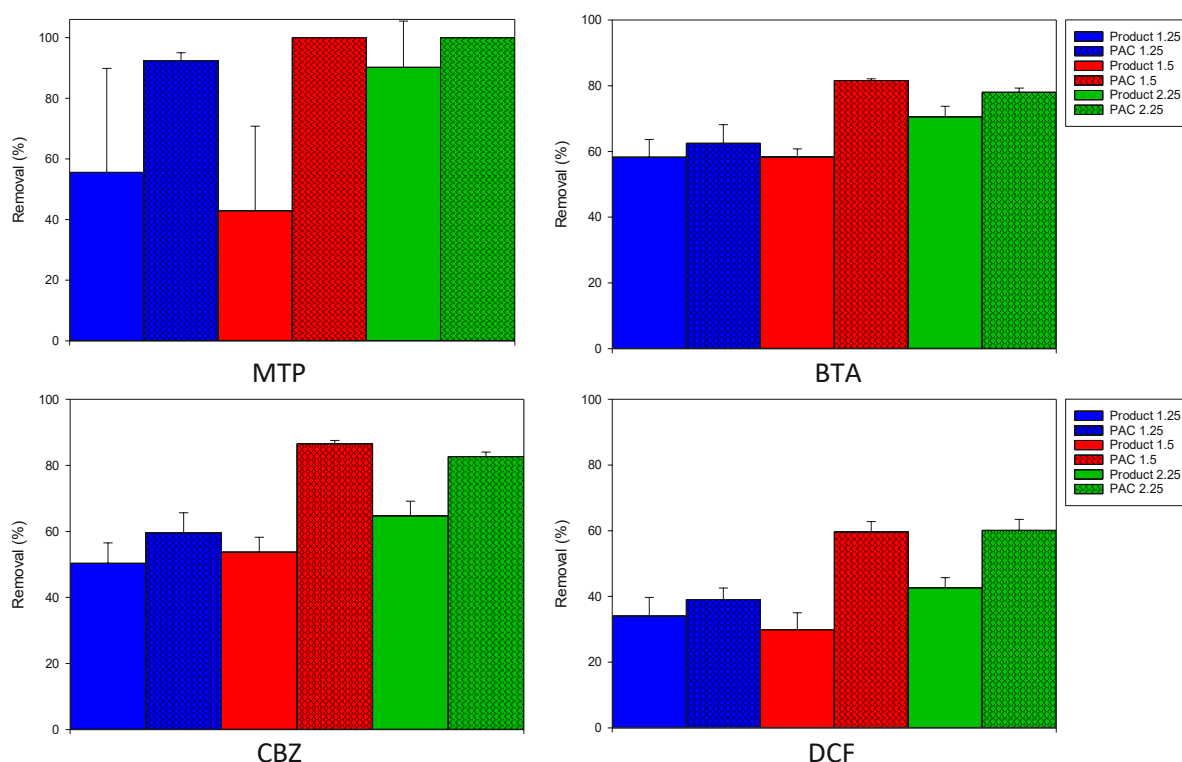
Figure 23: Percentual removal of the product AQUACLEAR B and the PAC CARBOPAL® in sample B at 1.25, 1.5, and 2.25 g AC g^{-1} DOC

A plot of the surrogate parameter ΔSAC_{254} against the specific AC dose shows a similar ΔSAC_{254} increase of both adsorbents, as depicted in Figure 24. This similar increase is noticeable both by the proximity of the y axis intercepts and the similar slope of the linear regression lines. The slightly higher ΔSAC_{254} increase at the same AC dose is in line with higher OMP removal achieved by the PAC.
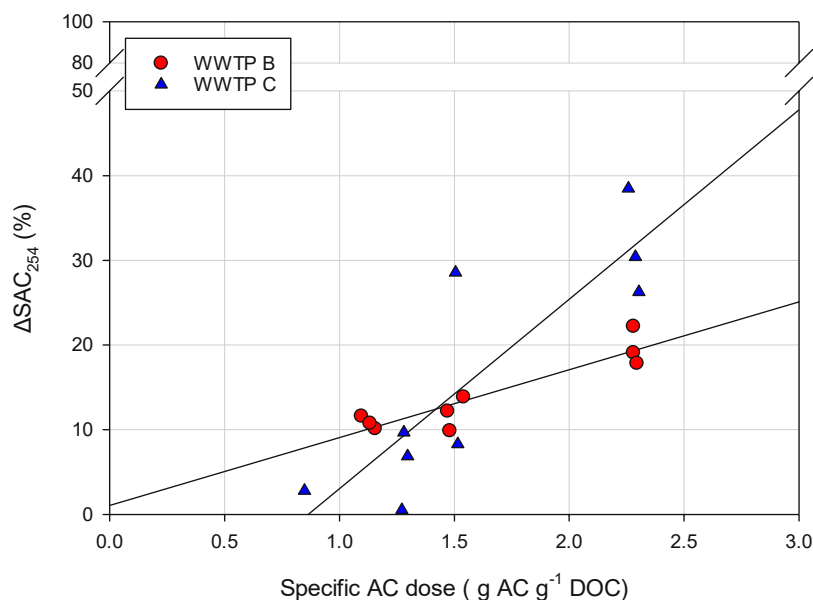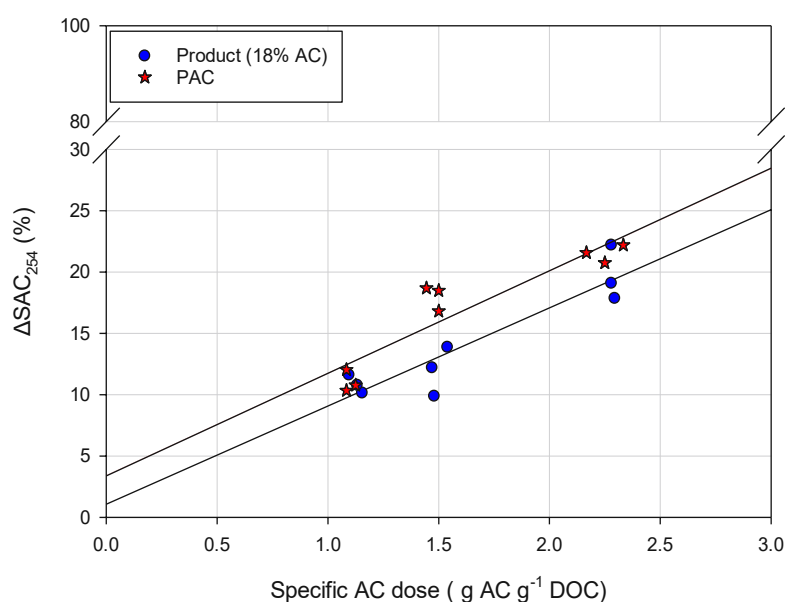
Figure 24: Linear correlation between ΔSAC₂₅₄ and specific AC dose; linear regression lines of the product AQUACLEAR B (R² = 0.85) and the PAC CARBOPAL® (R² = 0.84)

4.3.3 Adsorption models

The adsorption capacity according to the adsorption models of Langmuir and Freundlich could only be determined in samples A4 and B, as shown in Table 17.

In sample A4, CBZ was fitted to the linearized Langmuir model with a fairly high coefficient of determination of 0.92. In sample B, BTA could be fitted to the Freundlich model, albeit with a low coefficient of determination of 0.53, and CBZ could be fitted to both models with a low-intermediate coefficient of determination. Noticeable are the higher loadings at a similar concentration range shown for CBZ in sample B, as seen in Figure 26. These are higher by three orders of magnitude than in sample A4 (Figure 25).

Table 17: Regressed Langmuir and Freundlich adsorption parameters of CBZ and BTA obtained in samples A4 and B; T = 23° C; t_eq = 18 hours

Sample	Compound	Langmuir			Freundlich		
		q_{max}	b	R^2	K_F	n	R^2
		ng g^{-1}	L ng^{-1}	-	(ng^{1-n} L^n)/g	-	-
A4	CBZ	1.6×10^2	3.9×10^2	0.92			
B	BTA				9.1×10^2	0.85	0.53
	CBZ	3.3×10^5	8.0×10^{-4}	0.65	3.5×10^2	0.93	0.63

Figure 25: Adsorption isotherm of CBZ with AQUACLEAR A in sample A4; T = 23° C; t$_{eq}$ = 18 hours

BTA

CBZ

Figure 26: Adsorption isotherm of BTA and CBZ with AQUACLEAR B in sample B; T = 23° C; t$_{eq}$ = 18 hours
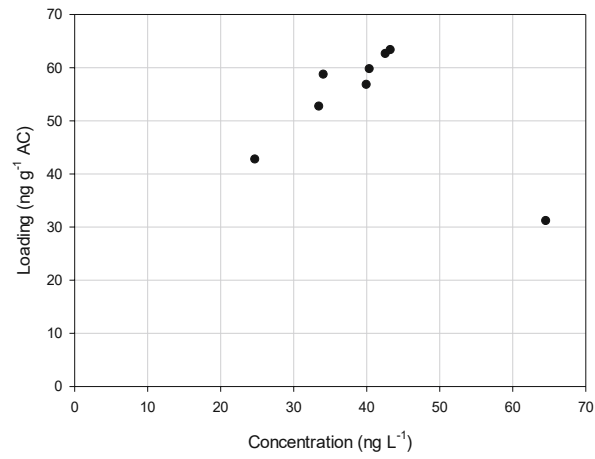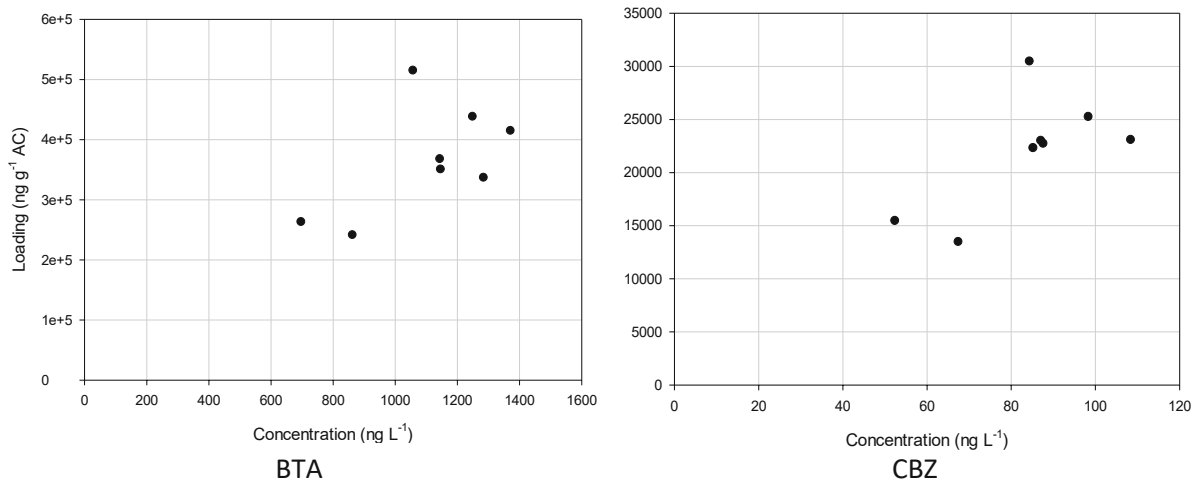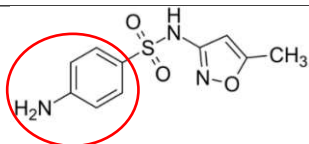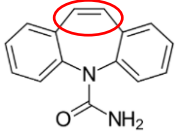
5 Discussion

5.1 Ozonation
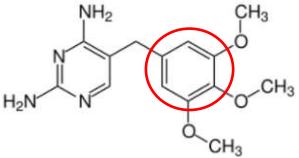
5.1.1 Effect of different specific ozone doses

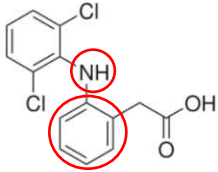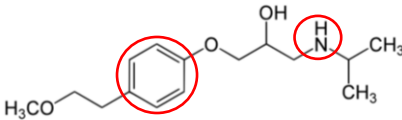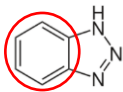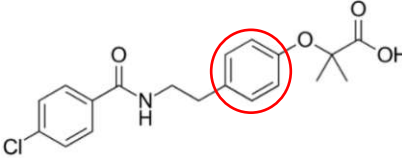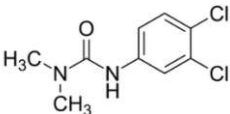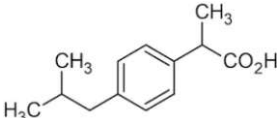Two main parameters should be considered when assessing the kinetics of OMP abatement via ozonation. These are compound reactivity, and O_3, and $\cdot OH$ exposures (Lee et al., 2013). The latter is influenced by the presence of nitrite, and EfOM, which was considered in terms of DOC. To take the effect of DOC and nitrite into account, the O_3 dose was normalized to the DOC concentration and compensated by nitrite. Variations of O_3 and $\cdot OH$ exposures induced by EfOM composition and nitrite were not measured as part of this thesis. The fact that the treated samples originate from the same WWTP as well as their temporal proximity, suggests that the EfOM composition should be similar. However, the effect of rainfall during the A2 and A3 sampling periods on EfOM composition should be considered as well. Assuming that O_3 and $\cdot OH$ exposures are similar, then the different removals should only be caused by compound reactivity, expressed as the second-order rate constant.

Lee et al. (2013) analyzed effluent samples from nine different WWTPs worldwide and classified the OMPs into five groups, according to their O_3 and $\cdot OH$ reactivities. The highly reactive compounds from group I, with a k_{O_3} higher than 10^5 $M^{-1} s^{-1}$, were over 90 % eliminated with a specific O_3 dose of 0.2 g O_3 g^{-1} DOC (not nitrite-compensated). These include DCF, CBZ, SMX, and TMP, which were efficiently removed at 0.4 g O_3 g^{-1} DOC. However, below 0.3 g O_3 g^{-1} DOC some WWTPs showed lower removals, caused by either relatively high nitrite concentrations or a good reactivity of the EfOM with the O_3. Group II compounds have a moderate O_3 reactivity ($10 < k_{O_3} < 10^5$ $M^{-1} s^{-1}$). This group includes the β-blocker Atenolol, which is structurally similar to MTP. At 0.2-0.3 g O_3 g^{-1} DOC, Atenolol was reported to have removals of 20-40 %, whereas at 1 g O_3 g^{-1} DOC it could be fully removed. The next groups are classified according to their $\cdot OH$ second-order rate constant, owing to their poor O_3 reactivity. Group III compounds, which include IBP, have a $k_{\cdot OH}$ higher than 5×10^9 $M^{-1} s^{-1}$. Group IV has a $k_{\cdot OH}$ between 1×10^9 and 5×10^9 $M^{-1} s^{-1}$, while group V is considered refractory to both O_3 and $\cdot OH$ treatments with a $k_{\cdot OH}$ lower than 1×10^9 $M^{-1} s^{-1}$.

The reactive moieties of the analyzed OMPs, their second-order rate constants of O_3 and $\cdot OH$, and their group classification according to Lee et al. (2013) are listed in Table 18.

Table 18: O_3 and $\cdot OH$ second-order rate constants at pH 7 and O_3 reactivities; red circles indicate reactive O_3 moiety

Compound (Formula) [Acronym]	Structure	k_{O_3} $M^{-1} s^{-1}$	$k_{\cdot OH}$ $M^{-1} s^{-1}$	Group # (Lee et al., 2013)
Sulfamethoxazole ($C_{10}H_{11}N_3O_3S$) [SMX]		$2.50E+06^a$	$5.50E+09^a$	I
Carbamazepine ($C_{15}H_{12}N_2O$) [CBZ]		$3.00E+05^a$	$8.80E+09^a$	I

Compound	Structure	k_{O_3}	$k_{\cdot OH}$	Group
Trimethoprim ($C_{14}H_{18}N_4O_3$) [TMP]		$2.70E{+}05^{b}$	$6.90E{+}09^{b}$	I
Diclofenac ($C_{14}H_{11}Cl_2NO_2$) [DCF]		$1.00E{+}06^{a}$	$7.50E{+}09^{a}$	I
Metoprolol ($C_{15}H_{25}NO_3$) [MTP]		$3.30E{+}02$ / $8.60E{+}05^{c**}$	$7.30E{+}09^{c}$	II
Benzotriazole ($C_6H_5N_3$) [BTA]		$2.30E{+}02$ / $2.40E{+}03^{c**}$	$1.07E{+}10^{d*}$	II
Bezafibrate ($C_{19}H_{20}ClNO_4$) [BZF]		$5.40E{+}02$ - $6.30E{+}02^{d}$	$7.40E{+}09^{a}$	II
Diuron ($C_9H_{10}Cl_2N_2O$) [DIU]		$1.65E{+}01^{e}$	$6.60E{+}05^{e}$	II
Ibuprofen ($C_{13}H_{18}O_2$) [IBP]		$9.60E{+}00^{d}$	$7.40E{+}09^{a}$	III

[a](Von Gunten, 2003); [b](Dodd et al., 2006); [c](Stapf et al., 2017); [d](Huber et al., 2003); [e](Benitez et al., 2007); *at pH 6.5; **site of attack is pH-dependent, higher K_{O_3} at higher pH

As shown in Figure 10, CBZ, DCF, and TMP show a high removal already at the lower specific O_3 doses applied. This is consistent with their group classification and their high second-order reaction rate constant, as seen in Table 18. Surprisingly, although SMX accounts for the substances with a high O_3 reactivity it manifests intermediate removals at the lower specific O_3 doses.

Group II compounds consist of MTP, BTA, BZF, and DIU. Because of their intermediate O_3 reactivity, they are typically not efficiently removed by O_3. The ·OH pathway is the main driver to their removal considering their high reaction rate with ·OH (Benner & Ternes, 2009). At the lower specific O_3 doses of 0.40-0.46 g O_3 g^{-1} DOC MTP and BTA showed low and fluctuating removals while BZF had a relatively gradual removal. The removal differences within the medium reactive compounds were also reported by (Kreuzinger et al., 2015). Accordingly, a specific O_3 dose of 0.7 g O_3 g^{-1} DOC was required for a 70 % removal of BZF, while a dose higher than 0.9 g O_3 g^{-1} DOC was needed for a similar removal of BTA. Stapf et al. (2017) reported of highly fluctuating BTA removals at 0.2-0.4 g O_3 g^{-1} DOC at different WWTPs. These fluctuations between WWTPs are also related to the different protonation states of

MTP and BTA at different pH values, which changes their O_3 reactivity accordingly. For example, the second-order rate constant of MTP amounts to 330 $M^{-1}s^{-1}$ at lower pH and 8.6×10^5 $M^{-1}s^{-1}$ at higher pH (Stapf et al., 2017). On the contrary, the O_3 reactivity of BZF is constant and its fluctuations are not caused by different pH values.

While DIU is a group II compound, it has both a low O_3 and ·OH reactivity. However, it has also been suggested that DIU can undergo direct reaction (Feng et al., 2008; Von Sonntag & Von Gunten, 2012). In contrast, IBP is considered O_3-refractory and its removal is mostly dependent on the ·OH pathway (Von Sonntag & Von Gunten, 2012). As was mentioned, removals of DIU and IBP could be determined for neither of the samples analyzed. This has to do with the high LOQ of DIU (62.8 ng L^{-1}) and its low effluent concentrations, which were either below the LOQ or just above the LOQ. The same problem was encountered for IBP, with a LOQ of 6.7 ng L^{-1}. IBP had low effluent concentrations in samples A1 and A2 compared to its LOQ (10 and 14 ng L^{-1}), and higher, albeit fluctuating concentrations in sample A3 (26 ± 15 ng L^{-1}). In addition, the concentrations of the ozonated sample showed a similarly high fluctuation. Therefore, considering IBP removal also at effluent concentrations lower than 10 times its LOQ appears to be too unprecise.

5.1.2 Reactive moieties

Considering their chemical properties, CBZ, DCF, TMP, and SMX possess electron-rich moieties, which serve as the sites of O_3 attack. CBZ has a cinnamic acid-based structure at which the olefinic C-C bond builds an O_3 adduct, which further decomposes to aromatic intermediates (McDowell et al., 2005). DCF has a few sites of attack, including the activated aromatic ring and the bridged secondary amine. DCF may also produce ·OH during ozonation, which further drives its removal. ·OH production can result from an addition of O_3 with the nitrogen atom in the imino bridge followed by heterolytic cleavage and production of ozonide radical ions (Von Sonntag & Von Gunten, 2012). SMX has a few potential sites of attack including the deprotonated amine, the aniline ring, and the oxazole ring. However, the high reactivity probably arises from the activated aniline moiety (Dodd et al., 2006). TMP contains diaminopyrimidine and trimethoxytolyl moieties. Because the heterocyclic nitrogen at position 5 has a pKa of 7.16, its protonated form lowers O_3 reactivity. Instead, the high O_3 reactivity of TMP owes to the trimethoxytolyl moiety, which functions as an activated aromatic ring (Dodd et al., 2006).

MTP and BTA are compounds containing a secondary amine group with pKa values of 9.67 and 9.03, respectively. MTP possesses an activated aromatic ring, which is reactive towards the O_3 molecule (Benner & Ternes, 2009). Although the pKa of the secondary amine of MTP is rather high, the reactivity with O_3 begins at a pH of 6.3, well below the pKa value. The high reactivity at pH values lower than the pKa is referred to as the "reactivity pKa" (Von Sonntag & Von Gunten, 2012). Therefore, the main site of attack is the amine functional group at the wastewater pH range of 6.8-8.5, whereas a higher pH within the range leads to a higher reactivity. The reactivity of BTA also relies on its state of protonation, however, its high second-order reaction rate with ·OH may also play a role in its removal (Karpel Vel Leitner & Roshani, 2010). The reactive moiety for both direct and indirect reactions is the benzo-ring. Deprotonation of the triazole ring was reported to increase the reaction rate, likely because of increased activation of the benzo-ring (Mawhinney et al., 2012). BZF contains two aromatic moieties, one is deactivated due to the electron-withdrawing effect of the amide and chlorine functionalities, and the other one is activated by electron-donating alkyl and an R-oxy substituent. Therefore, the latter moiety is expected to participate in the direct reaction (Dantas et al., 2007; Huber et al., 2003). IBP and DIU do not have reactive moieties. IBP possesses only slightly activating substituents, whereas DIU contains two deactivated moieties, an amide and a dichlorinated ring.

5.1.3 Potential of bromate formation

At specific O_3 doses lower than 0.88 g O_3 g^{-1} DOC bromate was not formed at a bromide concentration of 40 µg L^{-1}. At 0.45 g O_3 g^{-1} DOC bromate was not formed also at a higher bromide concentration of 100 µg L^{-1}. Bromate could only be detected with a concentration of 18.4 ± 1.2 µg L^{-1} at the highest specific O_3 dose of 0.88 g O_3 g^{-1} DOC with a formation percentage of 46 %.

A similar formation percentage was reported by Bahr et al. (2007) at a higher specific O_3 dose of 1.4 g O_3 g^{-1} DOC. At 0.8 g O_3 g^{-1} DOC, 11 µg L^{-1} bromate was formed, which is approximately 10 % of the bromide concentration. Schindler Wildhaber et al. (2015) applied different specific O_3 doses on seven effluents and reported bromate concentrations ranging from below the LOQ and up to 291 µg L^{-1} for effluents treated with 1 g O_3 g^{-1} DOC.

Overall, comparison with the literature regarding the beginning of bromate formation yields different results for different specific O_3 doses. Generally, literature data agrees that up to a certain specific O_3 dose threshold there is a linear correlation between bromate formation and the specific O_3 dose until a plateau is reached, in which complete oxidation of bromide is reached.

At the conventional specific O_3 doses applied in urban WWTPs (0.4-0.6 g O_3 g^{-1} DOC) bromate formation is usually less than 3 % for bromide concentrations below 100 µg L^{-1} (Abegglen & Siegrist, 2012; Soltermann et al., 2016). This would result in bromate concentrations below the drinking water standard of 10 µg L^{-1}. Therefore, considering that at specific O_3 doses lower than 0.88 g O_3 g^{-1} DOC bromate concentration was below the LOQ (5 µg L^{-1}), the experimental results are in line with expectations.

5.1.4 Correlation with ΔSAC_{254}

During ozonation conjugated and aromatic compounds undergo structural changes, which results in a decrease of absorption at 254 nm with increasing specific O_3 dose. The percentual increase of the ΔSAC_{254} parameter enables it to be used as a surrogate parameter for OMP abatement (Bahr et al., 2007; Kreuzinger et al., 2015; McArdell et al., 2020). Correlating the specific O_3 doses with ΔSAC_{254} yielded a high coefficient of determination, which confirms the applicability of the parameter as a surrogate parameter.

5.1.5 Effect of ozonation on biological oxygen demand (BOD_5)

There is a high discrepancy between sample A1 and samples A2 and A3, as seen in Figure 13. A1 shows a significant BOD increase of initial concentration, which amounts to nearly 100 %, whereas samples A2 and A3 show a relatively low increase. The largest relative increase occurred already at a lower specific O_3 dose than the ones measured.

Phan et al. (2021) compared the BOD percentual increase of initial effluent concentration upon ozonation with 0.65 g O_3 g^{-1} DOC. Accordingly, the data is highly fluctuating, ranging from below 50 % to 200 %. The mean increase was 94.5 ± 58.2 %. The experimental data of the specific dose 0.57 g O_3 g^{-1} DOC revealed a 117.5 ± 1.1 % increase. Yet due to the lower increase at 0.88 g O_3 g^{-1} DOC (94.6 ± 0.4 %), it appears that the data is very close to the mean established by Phan et al. (2021).

Considering samples A2 and A3, the increase of initial concentration amounted only to 17 % and 26 %, respectively. These low values lie below the standard deviation range established by Phan et al. (2021). These results are surprising considering the temporal proximity of those samples and the fact that they originate from the same WWTP. However, another parameter that should be considered concerns the precipitation conditions, which may alter the EfOM. During the A1 sampling period, there were dry weather conditions, which changed immediately beginning with the A2 sampling period and continued during the A3 sampling period. Ávila et al. (2012) found a decrease of BOD_5 under wet conditions at the effluents of constructed wetlands. They attributed the decrease to dilution of the wastewater occurring after the first-flush event. In contrast, the experimental data shows higher BOD_5 levels of the effluent under wet conditions in both A2 and A3. The relatively low increase caused by ozonation indicates that more readily biodegradable organic matter was found in A2 and A3 compared to A1. This is reinforced by the fact that on day 6 two samples (an ozonated triplicate of sample A2 and an effluent triplicate of sample A3) were measured with zero oxygen. In addition, there is a considerable standard deviation in both samples, which makes it difficult to further distinguish between the effluent and the ozonated sample.

Overall, it seems that under dry weather conditions ozonation increases the BOD_5 values significantly. Under wet conditions, such an increase is dramatically reduced.

5.2 Combination of ozonation and PAC adsorption

5.2.1 Comparison of ozonated and non-ozonated effluent

The abatement proportion by either ozonation (0.4-0.45 g O_3 g^{-1} DOC) or PAC adsorption (1.5 g AC g^{-1} DOC) is different among the tested compounds, as depicted in Figure 16. MTP, BTA, and BZF show higher removals by PAC adsorption, while SMX is removed only by ozonation. Interestingly, SMX is removed by PAC adsorption after an ozonation step has been applied (Figure 15). The compounds CBZ, TMP, and DCF show high removals by both treatments, although DCF is better removed by PAC adsorption in sample A3. Overall, the combined treatment is superior to single-step ozonation or PAC adsorption.

An additional effect of ozonation besides OMP modification is the oxidation of EfOM to lower molecular weight, more hydrophilic, and polar molecules. The extent of the transformation depends on EfOM and the applied O_3 dose. These fractions can exert different effects on OMP abatement in AC treatment. On the one hand, lower molecular weight, smaller EfOM fractions may diffuse further into the pore sites of the AC and thus lead to site competition and pore blockage. On the other hand, hydrophilic and charged fractions may remain in the liquid phase, thereby, reducing competition with the OMPs (Bourgin et al., 2017; Treguer et al., 2010). According to the experimental data, the non-ozonated A2 effluent sample, treated with 1.5 g AC g^{-1} DOC, demonstrated a larger decrease of DOC and SAC_{254} percentages, meaning that ozonation reduced the adsorption capacity of the AC for the EfOM. This suggests that the specific O_3 dose applied of 0.45 g O_3 g^{-1} DOC increased the hydrophilicity of EfOM. Although the adsorption capacity of EfOM decreased upon ozonation, it does not appear to play a significant role in the adsorption of OMPs at the specific O_3 doses applied.

5.2.2 EfOM adsorption and adsorption models

The relatively constant loadings of the EfOM indicate that it exerts the same effect on OMP adsorption throughout the concentration range. Since the competition on the adsorption sites is constant, data variations should not be caused by the presence of EfOM. A direct effect of the DOC concentration on OMP adsorption was also not shown in data from Altmann et al. (2014). Contrary to expectation, they reported that WWTPs with lower DOC loadings did not show an increased OMP adsorption.

A comparison of the loadings of AC with MTP and BTA shows similar results in sample A2. Compared to MTP and BZF, higher loadings of BTA were observed in sample A3. This may be explained by the higher initial concentration of BTA compared to MTP and BZF. The BTA concentration in the ozonated sample was 164.3 ng L^{-1}, whereas MTP and BZF concentrations were 26.8 and 16.8 ng L^{-1}, respectively. The higher loadings at higher initial concentrations were also shown by Altmann et al. (2014) for the compounds DCF and iomeprol.

5.2.3 Physicochemical properties of adsorbates

Physicochemical properties relevant for OMP adsorption capacity are given in Table 19. No correlation was found between the charge of a compound or its size with the removal in the ozonated and non-ozonated samples. The positively charged MTP and TMP exhibited both high removal percentages. In contrast, the negatively charged compounds had clearly different removal percentages. BZF showed a high removal, DCF had an intermediate removal while SMX was hardly removed. As to the neutral compounds, BTA had a medium removal while CBZ had a high removal. This high variability of results suggests that the charge did not play a significant role in the adsorption of the OMPs.

The lack of adsorption shown by SMX can be explained by its relatively low hydrophobicity, expressed by a negative log D_{ow} value at pH 8. Hydrophobic interactions play a major role in AC adsorption, therefore low hydrophobicity results in lower adsorption (Nam et al., 2014). A further explanation underlies the sulfonamide moiety, which is strongly electron-withdrawing. This results in an electron-donating effect of the associated aromatic ring, which reduces the π-π EDA interactions of SMX with the graphene layers of the AC (Ji et al., 2010). In contrast, CBZ is moderately hydrophobic with a relatively high log D_{OW} value at pH 8, low aqueous solubility, and a high pKa. These properties correlate with the non-specific interactions and its high observed adsorption capacity.

Steric hindrance by size exclusion appears not to be an important factor as TMP (50.7 Å) exhibited better removal than the smaller BTA (20.1 Å). The lower adsorption capacity observed for BTA may actually result from its lower size. It was suggested that London molecular interactions are directly related to molecular weight (Aldeguer Esquerdo et al., 2021). In addition, its relatively low HMO π energy may reduce its π-π EDA interactions.

Table 19: Physical-chemical properties of the selected OMPs

Compound (Formula) [Acronym]	Structure	MW (g mol^{-1})	Log K_{ow}	Log D_{ow} at pH 8	pKa acidic (FG)[b]	pKa basic (FG)[b]	Charge	VdW volume (Å^3)[c]	Minimal projection area (Å^2)[c]	Aqueous solubility (mg/L)[c]	HMO π energy[c]
Metoprolol (C$_{15}$H$_{25}$NO$_3$) [MTP]		267.37	1.76	0.09	14.09 (sec. hydroxyl)	9.67 (sec. amine)	+1	274.24	33.1	537.85	20.67
Benzotriazole (C$_6$H$_5$N$_3$) [BTA]		119.13	1.30	1.21	9.04 (sec. amine)	0.22 (tert. Amine)	0	100.02	20.12	7.32	15.38
Sulfamethoxazole (C$_{10}$H$_{11}$N$_3$O$_3$S) [SMX]		253.28	0.79	-0.11	6.16 (sec. amine)	1.97 (aromatic amine)	-1	204.63	34.11	12.58	29.67
Carbamazepine (C$_{15}$H$_{12}$N$_2$O) [CBZ]		236.27	2.77	2.77	15.96 (amine)	-3.75 (carboxylic O)	0	210.04	39.57	0.04	29.14
Diuron (C$_9$H$_{10}$Cl$_2$N$_2$O) [DIU]		233.09	2.53	2.53	13.18 (sec. amine)	-3.24 (carboxylic O)	0	186.92	31.15	0.46	24.21
Trimethoprim (C$_{14}$H$_{18}$N$_4$O$_3$) [TMP]		290.32	1.28	1.28		7.16 (heterocyclic N, pos. 5)	+1 / 0	261.36	50.70	1.12	37.32
Diclofenac (C$_{14}$H$_{11}$Cl$_2$NO$_2$) [DCF]		296.15	4.26	0.85	4.00 (carboxylic acid)	-2.08 (sec. amine)	-1	236.79	44.52	15.08	31.58
Bezafibrate (C$_{19}$H$_{20}$ClNO$_4$) [BZF]		361.82	3.99	0.55	3.83 (carboxylic acid)	-0.84 (carboxylic O)	-1	319.42	39.31	7.38	36.43
Ibuprofen (C$_{13}$H$_{18}$O$_2$) [IBP]		206.29	3.84	0.69	4.85 (carboxylic acid)		-1	211.74	31.19	8.37	14.06

[a]all data were calculated with MarvinSketch 21.13 by ChemAxon; [b]the strongest pKa is given; [c]charge, aqueous solubility, and HMO π energy are calculated at pH 7

5.2.4 Comparison between ozonation and PAC adsorption

In Figure 27 data obtained in the framework of this thesis is compared with literature data using similar specific O_3 and PAC doses (Bourgin et al., 2017; Zwickenpflug et al., 2009). The experimental data generally agrees with the literature data that SMX, CBZ, and DCF are efficiently removed at the relatively low specific O_3 dose applied. There is less agreement regarding the removal of BTA and BZF through ozonation. This can be explained by a combination of their intermediate O_3 reactivity and a relatively low applied specific O_3 dose, which may cause fluctuating results depending on the water matrix. As mentioned in section 5.1.1., BTA showed high variations of removal percentages in urban WWTPs ranging from 0-80 % (Stapf et al., 2017). Regarding removal by PAC, the tested compounds show intermediate and high removals except for SMX, which had a low removal by PAC in the A2 ozonated sample of 18.8 ± 0.6 %. A comparison with the literature of the compounds BTA, SMX, DCF, and BZF shows relatively low deviations below 15 %. In contrast, the obtained removal of CBZ is 26 % higher in the experimental results than in the literature.
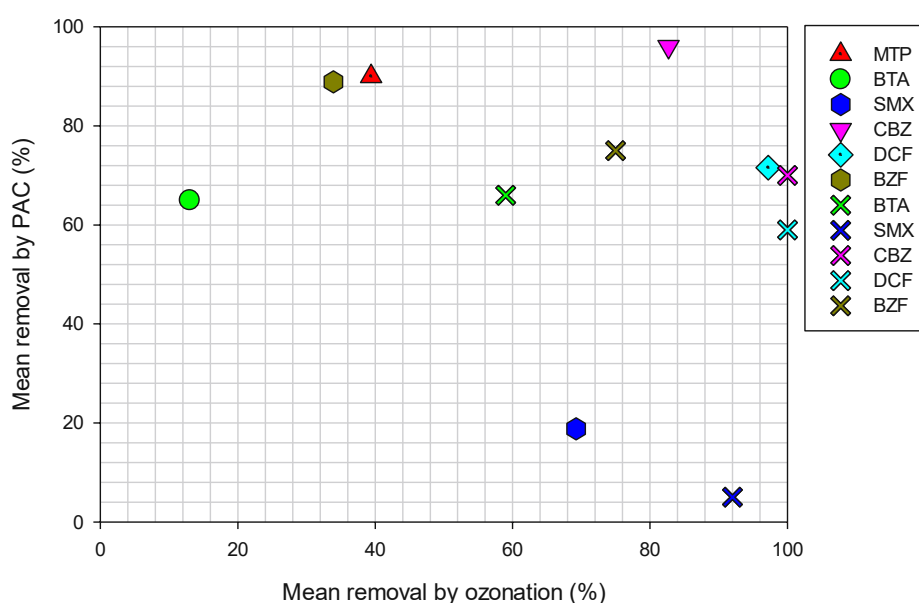

Figure 27: Mean removal by ozonation (D_{spec} = 0.43 g O_3 g^{-1} DOC) vs. mean removal by PAC adsorption (1.0 g PAC g^{-1} DOC); literature ozonation and PAC data were obtained from Bourgin et al. (2017) and Zwickenpflug et al. (2009), respectively; literature specific O_3 dose is 0.44 g O_3 g^{-1} DOC and specific PAC dose is 1-1.25 g PAC g^{-1} DOC

5.3 Adsorption potential of a novel product

5.3.1 OMP removal

The general trend of increased OMP abatement with increased specific AC dose is evident in samples A4, B, and C, whereas the removal increase began to plateau approximately at 1.5 g AC g^{-1} DOC. A comparison of samples B and C shows a more efficient removal in sample C. To remove MTP, BTA, CBZ, and TMP above 80 % in sample C, a minimal specific AC dose of 1.5 g AC g^{-1} DOC was necessary. A higher specific AC dose of 2.2 g AC g^{-1} DOC was required for the removal of BZF. In contrast, sample B required the highest specific AC dose of 2.25 g AC g^{-1} DOC for the removal of MTP. Removals above 80 % were not observed for BTA and CBZ, while DCF had low-intermediate removals. At the applied

doses no high removals were reached for DCF, which indicates that higher doses are necessary. As to SMX, from sample C it is clear that also at 2.2 g AC g^{-1} DOC its removal is very low. These results suggest that the general adsorption behavior of OMPs on the novel product is similar to the adsorption behavior, which can generally be seen for OMPs on activated carbon.

A comparison of the calibration curves of ΔSAC_{254} with the specific AC dose shows a higher slope of sample C. Below a value of approximately 1.5 g AC g^{-1} DOC, the increases of ΔSAC_{254} in sample C is less than in sample B. On the contrary, above 1.5 g AC g^{-1} DOC, the opposite applies.

This shows that different wastewater matrices exert different effects on OMP removal under the same experimental conditions and at similar specific AC doses. This owes to the EfOM characteristics, which display different affinities to the adsorbents in different WWTPs. Clearly, a direct comparison between WWTPs using the surrogate parameter is not possible.

5.3.2 Comparison between AQUACLEAR B and CARBOPAL®

A comparison of the performance of both adsorbents shows that generally, the PAC removed the OMPs better than the product, although the difference was not always high. This difference in performance might arise from the presence of the precipitating agent and coagulant PACl. The main goal of coagulants is to destabilize colloidal particles, thereby causing them to agglomerate to settable flocks. During coagulation soluble inorganic and organic molecules are adsorbed to the flocks and removed (Nam et al., 2017). In addition, PACl functions as a precipitating agent for the removal of phosphate.

According to some authors, the effect of coagulation-flocculation on OMP removal is considered to be low. Adams et al. (2002) applied the coagulants aluminum sulfate and ferric sulfate on samples spiked with an antibiotic mix and river water. They reported that no significant removal of the antibiotics was reached. Zhang & Emary (1999) studied Atrazine removal in drinking water treatment plants by enhanced coagulation. They tested different factors such as PAC dose, pH, contact time, mixing energy, and alum dosage. Accordingly, there is a synergistic effect of PAC and alum on Atrazine removal at a low pH. This owes to the fact that at the tested pH, Atrazine possesses a charge, which allows it to undergo electrostatic interactions with the coagulant. In addition, increasing the PAC dose resulted in increased removals. Nam et al. (2017) tested the removal of caffeine, SMX, MTP, and CBZ in spiked distilled water samples by changing the operating condition and PACl dose. At pH 7, SMX had the highest removal of over 50 % at 30 mg L^{-1} alum. In comparison, MTP was not removed at all while CBZ and caffeine removal lay below 20 % at the same alum dose. This was explained by the negative charge of SMX, which can undergo electrostatic interactions with the positively charged coagulant salts.

Comparing the literature data with the experimental data, the large difference in removal of MTP in favor of the PAC could be explained by electrostatic repulsion of the positively charged MTP with Al^{3+} cations. Conversely, a higher removal by the product caused by electrostatic interactions with the negatively charged DCF is not observed. If the removal increase by the PAC is significant, it appears that it involves other physicochemical properties.

5.3.3 Correlation with ΔSAC$_{254}$

Based on the experimental data, the coefficient of determination for the correlation of the specific AC dose with ΔSAC$_{254}$ was 0.85 in sample B and 0.73 in sample C. Overall this indicates that application of ΔSAC$_{254}$ as a surrogate parameter for the specific AC dose is more reasonable for sample B.

High removals above 80 % were not reached in sample B except for MTP. Complete removal of MTP by the product corresponds to an approximate ΔSAC$_{254}$ of 20 %. At the same ΔSAC$_{254}$, BTA and CBZ could be removed by more than 60 % while the removal of DCF lay by 40 %. Altmann et al. (2014) reported of a high correlation between OMP removal and increase of ΔSAC$_{254}$ in effluent samples from four different WWTPs. After a 48-hour equilibration time, they found a similar correlation between ΔSAC$_{254}$ and the removal of CBZ, BTA, and DCF, however, not SMX.

5.3.4 Adsorption models

As was shown in Figures 25 and 26, CBZ could be modeled to the Langmuir model in sample A4 and to both of the adsorption models in sample B, while BTA could be modeled to the Freundlich model in sample B. However, from the form of the isotherms, it is evident that no classical Langmuir or Freundlich isotherms were obtained. For a better model description, more data points are necessary.

Noticeable is the higher q$_{max}$ of CBZ in sample B, which is higher by three orders of magnitude than in sample A4. A possible reason for this difference could be the high DOC level of sample A4 (15.38 mg L^{-1}) compared to sample B (6 mg L^{-1}). EfOM can hinder the adsorption of OMPs by direct competition for adsorption sites and by pore blockage (Worch, 2012).

6 Summary

6.1 Ozonation

- At the range of specific O_3 doses used, higher doses resulted in increased abatement of OMPs.
- Generally, the percentual OMP abatement corresponds to compound reactivity, predicted with the second-order rate constant.
- Bromate was detected only at the highest specific O_3 dose applied (0.88 g O_3 g^{-1} DOC).
- The surrogate parameter ΔSAC_{254} showed a high linear correlation with the applied specific O_3 doses and with OMP abatement.
- There is conflicting information regarding the increase of the sum parameter BOD_5 by ozonation, which appears to result from the weather conditions and their effect on wastewater characteristics. During dry weather conditions, the parameter was increased by more than 90 %, while BOD_6 was increased by 17 % and 26 % during rain events. In addition, no correlation between the specific O_3 dose and the sum parameter BOD_5 could be established.

6.2 Combination of ozonation and PAC adsorption

- A combination of ozonation and PAC adsorption proved to be superior to single-step ozonation or single-step PAC adsorption for most compounds.
- There is a moderate fit between the surrogate parameters ΔSAC_{254} and ΔDOC.
- DOC is decreased upon ozonation, but the decrease did not appear to impact OMP abatement during the following adsorption step.
- BZF showed a high fit, whereas MTP and BTA showed a moderate fit to the Langmuir model.

6.3 Adsorption potential of a novel product

- The OMP removal is mainly influenced by the DOC of the WWTP effluent matrix.
- There is a high correlation between the specific AC dose and ΔSAC_{254} in sample B, and an intermediate correlation in sample C.
- The adsorption capacities obtained by CARBOPAL® were higher than the ones of the PAC included in the product.
- The product reached higher removals in WWTP C. A dose of approximately 1.5 g AC g^{-1} DOC is required to reach a high removal for most compounds in WWTP C, while a dose higher than 2.2 g AC g^{-1} DOC is required for WWTP B.
- Although BTA and CBZ could be correlated to the adsorption models in samples B and A4, the correlation was low-intermediate in sample B. More data points are required for model application.

7 Bibliography

Abegglen, C., & Siegrist, H. (2012). *Mikroverunreinigungen aus kommunalem Abwasser*. Bundesamt für Umwelt.

Adams, C., Wang, Y., Loftin, K., & Meyer, M. R. (2002). Removal of Antibiotics from Surface and Distilled Water in Conventional Water Treatment Processes. *J. Environ. Eng.*, 253–260. https://doi.org/10.1061/(ASCE)0733-9372(2002)128:3(253)

Aldeguer Esquerdo, A., Varo Galvañ, P. J., Sentana Gadea, I., & Prats Rico, D. (2021). *Carbamazepine and Diclofenac Removal Double Treatment: Oxidation and Adsorption*. https://doi.org/10.3390/ijerph18137163

Altmann, J., Ruhl, A. S., Zietzschmann, F., & Jekel, M. (2014). Direct comparison of ozonation and adsorption onto powdered activated carbon for micropollutant removal in advanced wastewater treatment. *Water Research*, 185–193. https://doi.org/10.1016/j.watres.2014.02.025

Alvarino, T., Suarez, S., Lema, J., & Omil, F. (2018). Understanding the sorption and biotransformation of organic micropollutants in innovative biological wastewater treatment technologies. *Sci Total Environ.*, 297–306. https://doi.org/10.1016/j.scitotenv.2017.09.278

Ávila, C., Salas, J., Martín, I., Aragón, C. A., & García, J. (2012). Integrated treatment of combined sewer wastewater and stormwater in a hybrid constructed wetland system in southern Spain and its further reuse. *Ecological Engineering*. https://doi.org/10.1016/j.ecoleng.2012.08.009

Bader, H., & Hoigné, J. (1981). Determination of ozone in water by the indigo method. *Water Research*, 449–456. https://doi.org/10.1016/0043-1354(81)90054-3

Bahr, C., Ernst, M., Jekel, M., Heinzmann, B., Luck, F., & Ried, A. (2007). *Pilotuntersuchungen zur kombinierten oxidativ-biologischen Behandlung von Klärwerksabläufen für die Entfernung von organischen Spuren- und Wirkstoffen und zur Desinfektion*. Schriftenreihe Kompetenzzentrum Wasser Berlin.

Bailey, P. S. (1958). The Reactions Of Ozone With Organic Compounds. *Chemical Reviews*, 925–1010. https://doi.org/10.1021/cr50023a005

Barbosa, M. O., Moreira, N. F., Ribeiro, A. R., Pereira, M. F., & Silva, A. M. (2016). Occurrence and removal of organic micropollutants: An overview of the watch list of EU Decision 2015/495. *Water Res*, 257–279. https://doi.org/10.1016/j.watres.2016.02.047

Benitez, F. J., Francisco, J. R., Juan, L. A., & Carolina, G. (2007). Kinetics of the transformation of phenyl-urea herbicides during ozonation of natural waters: Rate constants and model predictions. *Water Research*, 4073–4084. https://doi.org/10.1016/j.watres.2007.05.041

Benner, J., & Ternes, T. A. (2009). Ozonation of Metoprolol: Elucidation of Oxidation Pathways and Major Oxidation Products. *Environmental Science & Technology*, 5472–5480. https://doi.org/10.1021/es900280e

Blough, R., & Del Vecchio, N. V. (2004). On the Origin of the Optical Properties of Humic Substances. *Environmental Science & Technology*, 3885–3891. https://doi.org/10.1021/es049912h

Böhme, C. (2000). *Untersuchungen zur Aktivkohlefilterung und Analytik von Amino – und Nitroaromaten, Dissertation*.

Bourgin, M., Beck, B., Boehler, M., Borowska, E., Fleiner, J., & Salhi, E. (2017). *Evaluation of a full-scale wastewater treatment plant upgraded with ozonation and biological post-treatments: Abatement of micropollutants, formation of transformation products and oxidation by-products*. https://doi.org/10.1016/j.watres.2017.10.036

Buffle, M. O., Schumacher, J., Meylan, S., Jekel, M., & von Gunten, U. (2006). Ozonation and Advanced Oxidation of Wastewater: Effect of O3 Dose, pH, DOM and HO•-Scavengers on Ozone Decomposition and HO• Generation. *Ozone: Science & Engineering*, 247–259. https://doi.org/10.1080/01919510600718825

Buffle, M. O., Schumacher, J., Salhi, E., Jekel, M., & von Gunten, U. (2006). Measurement of the initial phase of ozone decomposition in water and wastewater by means of a continuous quench-flow system: Application to disinfection and pharmaceutical oxidation. *Water Res*, 1884–1894. https://doi.org/10.1016/j.watres.2006.02.026

Çeçen, F., & Aktaş, Ö. (2011). *Activated Carbon for Water and Wastewater Treatment: Integration of Adsorption and Biological Treatment*. John Wiley & Sons, Inc.

Chavoshani, A., Hashemi, M., Amin, M. M., & Ameta, C. S. (2020). *Micropollutants and Challenges, Emerging in Aquatic Environments and Treatment Processes*. Elsevier.

Cheremisinoff, N. P. (2002). *Handbook of Water and Wastewater Treatment Technologies; Chapter 10—Ion exchange and carbon adsorption*. Butterworth-Heinemann. https://doi.org/doi.org/10.1016/B978-075067498-0/50013-9

Chon, K., Salhi, E., & von Gunten, U. (2015). Combination of UV absorbance and electron donating capacity to assess degradation of micropollutants and formation of bromate during ozonation of wastewater effluents. *Water Research*, 388–397. https://doi.org/10.1016/j.watres.2015.05.039

Cirja, M., Ivashechkin, P., & Schäffer, A. (2008). Factors affecting the removal of organic micropollutants from wastewater in conventional treatment plants (CTP) and membrane bioreactors (MBR). *Rev Environ Sci Biotechnol*, 61–78. https://doi.org/10.1007/s11157-007-9121-8

Coughlin, R. W., & Fouad, S. E. (1968). Role of surface acidity in the adsorption of organic pollutants on the surface of carbon. *Environmental Science & Technology*, 291–297. https://doi.org/10.1021/es60016a002

Dantas, R. F., Canterino, M., Marotta, M., Sans, C., Esplugas, S., & Andreozzi, R. (2007). Bezafibrate removal by means of ozonation: Primary intermediates, kinetics, and toxicity assessment. *Water Research*, 2525–2532. https://doi.org/10.1016/j.watres.2007.03.011

Dauenhauer, P. J., & Omar, A. A. (2018). A Universal Descriptor for the Entropy of Adsorbed Molecules in Confined Spaces. *ACS Central Science*, 1235–1243. https://doi.org/10.1021/acscentsci.8b00419

Daughton, C. G., & Ternes, T. A. (1999). Pharmaceuticals and personal care products in the environment: Agents of subtle change? *Environ Health Perspect*, 907–938. https://doi.org/10.1289/ehp.99107s6907

Dodd, M. C., Buffle, M. O., & von Gunten, U. (2006). Oxidation of Antibacterial Molecules by Aqueous

Ozone: Moiety-Specific Reaction Kinetics and Application to Ozone-Based Wastewater

Treatment. *Environmental Science & Technology*, 1969–1977.

https://doi.org/10.1021/es051369x

DWA. (2019). *Aktivkohleeinsatz auf kommunalen Kläranlagen zur Spurenstoffentfernung—*

Verfahrensvarianten, Reinigungsleistung und betriebliche Aspekte. Deutsche Vereinigung für

Wasserwirtschaft, Abwasser und Abfall.

Elovitz, M. S. (2000). Hydroxyl Radical/Ozone Ratios During Ozonation Processes. II. The Effect of

Temperature, pH, Alkalinity, and DOM Properties, Ozone. *Science & Engineering*, 123–150.

https://doi.org/10.1080/01919510008547216

Feng, J., Zheng, Z., Luan, J., Zhang, Z., & Wang, L. (2008). Degradation of diuron in aqueous solution

by ozonation. *Journal of Environmental Science and Health*, 576–587.

https://doi.org/10.1080/03601230802234450

Frédéric, O., & Yves, P. (2014). Pharmaceuticals in hospital wastewater: Their ecotoxicity and

contribution to the environmental hazard of the effluent. *Chemosphere*, 31–39.

https://doi.org/10.1016/j.chemosphere.2014.01.016

García-Araya, J., Beltrán, F., & Álvarez, P. (2003). Activated Carbon Adsorption of Some Phenolic

Compounds Present in Agroindustrial Wastewater. *Adsorption 9*, 107–115.

https://doi.org/10.1023/A:1024228708675

Giles, C. H., Smith, D., & Huitson, A. (1974). A general treatment and classification of the solute

adsorption isotherm. I. Theoretical,. *Journal of Colloid and Interface Science*, 755–765.

https://doi.org/10.1016/0021-9797(74)90252-5

Gottschalk, C., Libra, J. A., & Saupe, A. (2009). *Ozonation of Water and Waste Water: A Practical*

Guide to Understanding Ozone and its Applications. Wiley.

Grieshaber, C. A., Penland, T. N., Kwak, T. J., Cope, W. G., Heise, R. J., Law, J. M., & Kullman, S. W.

(2018). Relation of contaminants to fish intersex in riverine sport fishes. *Sci Total Environ*,

73–89.

Huber, M. M., Canonica, S., Park, G. Y., & von Gunten, U. (2003). Oxidation of Pharmaceuticals during Ozonation and Advanced Oxidation Processes. *Environmental Science & Technology*, 1016–1024. https://doi.org/10.1021/es025896h

Imai, A., Onuma, K., Inamori, Y., & Sudo, R. (1998). Effects of Pre-Ozonation in Refractory Leachate Treatment by the Biological Activated Carbon Fluidized Bed Process. *Environmental Technology*, 213–221. https://doi.org/10.1080/09593331908616673

Inglezakis, V. J., Poulopoulos, S. G., & Kazemian, H. (2018). *Insights into the S-shaped sorption isotherms and their dimensionless forms*. https://doi.org/10.1016/j.micromeso.2018.06.026

Inyang, M. I., Gao, B., Yao, Y., Xue, Y., Zimmerman, A., & Mosa, A. (2016). A review of biochar as a low-cost adsorbent for aqueous heavy metal removal. *Critical Reviews in Environmental Science and Technology*, 406–433. https://doi.org/10.1080/10643389.2015.10968

Jekel, M., & Dott, W. (2013). *Polare organische Spurenstoffe als Indikatoren im anthropogen beeinflussten Wasserkreislauf, Ergebnisse des Querschnittsthemas „Indikatorsubstanzen"*. W. B. d. B.-F. r. R. v. n. S. u. K. i. W. (RiSKWa).

Ji, L., Liu, F., Xu, Z., Zheng, S., & Zhu, D. (2010). Adsorption of Pharmaceutical Antibiotics on Template-Synthesized Ordered Micro- and Mesoporous Carbons. *Environmental Science & Technology*, 3116–3122. https://doi.org/10.1021/es903716s

Kamaz, M., Wickramasinghe, S. R., Eswaranandam, S., Zhang, W., Jones, S. M., Watts, M. J., & Qian, X. (2019). *Investigation into Micropollutant Removal from Wastewaters by a Membrane Bioreactor*. https://doi.org/10.3390/ijerph16081363

Karpel Vel Leitner, N., & Roshani, N. (2010). Kinetic of benzotriazole oxidation by ozone and hydroxyl radical. *Water Research*, 2058–2066. https://doi.org/10.1016/j.watres.2009.12.018

Kreuzinger, N., Haslinger, J., Kornfeind, L., Schaar, H., Saracevic, E., & Winkelbauer, A. (2015). *KomOzAK Endbericht—Weitergehende Reinigung kommunaler Abwässer mit Ozon sowie Aktivkohle für die Entfernung von organischen Spurenstoffen*. Bundesministerium für Land- und Forstwirtschaft.

Lapworth, D. J., Baran, N., Stuart, M. E., & Ward, R. S. (2012). Emerging organic contaminants in groundwater: A review of sources, fate and occurrence. *Environmental Pollution*, 287–303. https://doi.org/10.1016/j.envpol.2011.12.034

Lee, Y., Gerrity, D., Lee, M., Bogeat, A. E., Salhi, E., Gamage, G. A., Trenholm, R., Wert, E., Snyder, S. A., & von Gunten, U. (2013). Prediction of Micropollutant Elimination during Ozonation of Municipal Wastewater Effluents: Use of Kinetic and Water Specific Information. *Environmental Science & Technology*, 5872–5881. https://doi.org/10.1021/es400781r

Li, Q., Snoeyink, V. L., Mariñas, B. J., & Campos, C. (2003). Pore blockage effect of NOM on atrazine adsorption kinetics of PAC: the roles of PAC pore size distribution and NOM molecular weight. *Water*, 4863–4872. https://doi.org/10.1016/j.watres.2003.08.018

Luo, Y., Guo, W., Ngo, H. H., Nghiem, L. D., Hai, F. I., & Zhang, J. (2014). A review on the occurrence of micropollutants in the aquatic environment and their fate and removal during wastewater treatment. *Sci Total Environ.*, 473-474:619-41. https://doi.org/10.1016/j.scitotenv.2013.12.065

Mawhinney, D. B., Vanderford, B. J., & Snyder, S. A. (2012). Transformation of 1H-Benzotriazole by Ozone in Aqueous Solution. *Environmental Science & Technology*, 7102–7111. https://doi.org/10.1021/es300338e

McArdell, C., Böhler, M., Hernandez, A., Oltramare, C., Siegrist, H., & Büeler, A. (2020). *Pilotversuche zur erweiterten Abwasser-behandlung mit granulierter Aktivkohle (GAK) und kombiniert mit Teilozonung (O3/GAK) auf der ARA Glarnerland (AVG)*. EAWAG.

McDowell, D. C., Huber, M. M., Wagner, M., von Gunten, U., & Ternes, T. A. (2005). Ozonation of carbamazepine in drinking water: Identification and kinetic study of major oxidation products. *Environ Sci Technol.*, 8014–8022. https://doi.org/10.1021/es050043l

Muñoz, F., Mvula, E., & von Sonntag, C. (2001). Singlet dioxygen formation in ozone reactions in aqueous solution. *Journal of The Chemical Society*. https://doi.org/10.1039/B101230O

Nam, S. W., Choi, D. J., Kim, S. K., & Her, N. &. (2014). Adsorption characteristics of selected hydrophilic and hydrophobic micropollutants in water using activated carbon. *J Hazard Mater*, 144–152. https://doi.org/10.1016/j.jhazmat.2014.01.037

Nam, S., Yoon, Y., Chae, S., Kang, J., & Zoh, K. (2017). Removal of Selected Micropollutants During Conventional and Advanced Water Treatment Processes. *Environmental Engineering Science*, 752–761. https://doi.org/10.1089/ees.2016.0447

Naumov, S., Mark, G., Jarocki, K., & von Sonntag, C. (2010). The Reactions of Nitrite Ion with Ozone in Aqueous Solution – New Experimental Data and Quantum-Chemical Considerations. *Ozone: Science & Engineering*, 430–434. https://doi.org/10.1080/01919512.2010.522960

Newcombe, G., Morrison, J., Hepplewhite, C., & Knappe, D. R. (2002). Simultaneous adsorption of MIB and NOM onto activated carbon: II. Competitive effects. *Carbon*, 2147–2156. https://doi.org/10.1016/S0008-6223(02)00098-2

Ngo, H. N., Cheng, D., Guo, W., Pandey, A., Lee, D., & Deng, L. (2020). Chapter 8—Biotransformation of organic micro-pollutants in biological wastewater. *Current Developments in Biotechnology and Bioengineering*, *185*, 5990–5995. https://doi.org/10.1016/B978-0-12-819594-9.00008-5

Nöthe, T., Fahlenkamp, P., & von Sonntag, C. (2009). Ozonation of Wastewater: Rate of Ozone Consumption and Hydroxyl Radical Yield. *Environmental Science & Technology*, 5990–5995.

Paraskeva, P., & Graham, N. J. (2002). Ozonation of municipal wastewater effluents. *Water Environ Res.*, 569–581. https://doi.org/10.2175/106143002x140387

Park, H. S., Hwang, T. M., Kang, J. W., Choi, H., & Oh, H. J. (2001). Characterization of raw water for the ozone application measuring ozone consumption rate. *Water Res*, 2607–2614. https://doi.org/10.1016/s0043-1354(00)00564-9

Phan, L., Schaar, H., Saracevic, E., Krampe, E., & Kreuzinger, N. (2021). Effect of ozonation on the biodegradability of urban wastewater treatment plant effluent. *Science of the Total Environment*, *in submission*.

Pinkernell, U., & von Gunten, U. (2001). Bromate minimization during ozonation: Mechanistic considerations. *Environ Sci Technol.*, 2525–2531. https://doi.org/10.1021/es001502f

Rizzo, L., Malato, S., Antakyali, D., Beretsou, V. G., Đolić, M., & Gernjak, W. (2019). Consolidated vs new advanced treatment methods for the removal of contaminants of emerging concern from urban wastewater. *Science of The Total Environment*, 986–1008. https://doi.org/10.1016/j.scitotenv.2018.11.265

Rogowska, J., Cieszynska-Semenowicz, M., & Ratajczyk, W. (2020). Micropollutants in treated wastewater. *Ambio*, 487–503. https://doi.org/10.1007/s13280-019-01219-5

Sahoo, T. R., & Prelot, B. (2020). In *Chapter 7—Adsorption processes for the removal of contaminants from wastewater: The perspective role of nanomaterials and nanotechnology,*. Elsevier.

Santos, L. H., Araújo, A. N., Fachini, A., Pena, A., Delerue-Matos, C., & Montenegro, M. C. (2010). Ecotoxicological aspects related to the presence of pharmaceuticals in the aquatic environment. *J Hazard Mater*, 45–95.

Schaar, H. (2015). *Ozonung von Kläranlagenablauf zur weitergehenden Abwasserreinigung*. Wien.

Schaar, H., Knasmueller, S., Ferk, S., Misik, M., Sommer, R., Schürhagl, R., Grillitsch, R., & Altmann, D. (2011). *KomOzon—Technische Umsetzung und Implementierung einer Ozonungsstufe für nach dem Stand der Technik gereinigtes kommunales Abwasser—Heranführung an den Stand der Technik.* Endbericht TU Wien.

Schindler Wildhaber, Y., Mestankova, H., Schärer, M., Schirmer, K., Salhi, K., & Von Gunten, U. (2015). Novel test procedure to evaluate the treatability of wastewater with ozone. *Novel test procedure to evaluate the treatability of wastewater with ozone*, 324–335. https://doi.org/10.1016/j.watres.2015.02.030

Schmidt, C. K., & Brauch, H. J. (2008). N,N-dimethylsulfamide as precursor for N-nitrosodimethylamine (NDMA) formation upon ozonation and its fate during drinking water treatment. *Environ Sci Technol.*, 6340–6346. https://doi.org/10.1021/es7030467

Schwaiger, J., Ferling, H., Mallow, U., Wintermayr, H., & Negele, R. D. (2004). Toxic effects of the non-steroidal anti-inflammatory drug diclofenac. Part I: histopathological alterations and bioaccumulation in rainbow trout. *Aquat Toxicol.*, 141–150. https://doi.org/10.1016/j.aquatox.2004.03.014

Soltermann, F., Abegglen, C., Götz, C., & von Gunten, U. (2016). Bromide Sources and Loads in Swiss Surface Waters and Their Relevance for Bromate Formation during Wastewater Ozonation. *Environmental Science & Technology*, 9825–9834. https://doi.org/10.1021/acs.est.6b01142

Stapf, M., Miehe, U., Lesjean, B., Wiedmann, B., & Jekel, M. (2013). *Vergleichende Untersuchungen von Steuerungskonzepten für nachgeschaltete Ozonanlagen*. Fulda.

Stapf, M., Schumann, P., Völker, J., & Miehe, U. (2017). *Studie über Effekte und Nebeneffekte bei der Behandlung von kommunalem Abwasser mit Ozon*. Kompetenzzentrum Wasser gGmbH.

Suarez, S., Lema, J. M., & Omil, F. (2009). Pre-treatment of hospital wastewater by coagulation-flocculation and flotation. *Bioresour Technol.*, 2138–2146. https://doi.org/10.1016/j.biortech.2008.11.015

Swenson, H., & Stadie, N. P. (2019). Langmuir's Theory of Adsorption: A Centennial Review. *Langmuir*, 5409–5426. https://doi.org/10.1021/acs.langmuir.9b00154

Tentscher, P. R., Bourgin, M., & von Gunten, U. (2018). Ozonation of Para-Substituted Phenolic Compounds Yields p-Benzoquinones, Other Cyclic α,β-Unsaturated Ketones, and Substituted Catechols. *Environmental Science & Technology*, 4763–4773. https://doi.org/10.1021/acs.est.8b00011

Trambarulo, R., Ghosh, S. N., Jr, B., A, C., & Gordy, W. (1953). *The Molecular Structure, Dipole Moment, and g Factor of Ozone from Its Microwave Spectrum*. https://doi.org/doi.org/10.1063/1.1699045

Treguer, R., Tatin, R., Couvert, A., Wolbert, D., & Tazi-Pain, A. (2010). Ozonation effect on natural organic matter adsorption and biodegradation – Application to a membrane bioreactor containing activated carbon for drinking water production. *Water Research*, 781–788.

Von Gunten, U. (2003). Ozonation of drinking water: Part I. *Oxidation kinetics and product formation*, 1443–1467. https://doi.org/10.1016/S0043-1354(02)00457-8

von Gunten, U., Salhi, E., Schmidt, C. K., & Arnold, W. A. (2010). Kinetics and Mechanisms of N-Nitrosodimethylamine Formation upon Ozonation of N, N-Dimethylsulfamide-Containing

Waters: Bromide Catalysis. *Environmental Science & Technology*, 5762–5768.

https://doi.org/10.1021/es1011862

Von Sonntag, C., & Von Gunten, U. (2012). *Chemistry of Ozone in Water and Wastewater Treatment.*
From Basic Principles to Applications. IWA Publishing.

Worch, E. (2012). *Adsorption Technology in Water Treatment-Fundamentals and Modeling Processes*.

Zappatini, A., & Götz, C. (2015). *Testverfahren zur Beurteilung der Behandelbarkeit von Abwasser mit*
Ozon—Anleitung und Durchführung von Laborversuche. ENVILAB AG.

Zhang, T. C., & Emary, S. C. (1999). Jar tests for evaluation of atrazine removal at drinking water
treatment plants. *Environmental Engineering Science*, 417–432.

https://doi.org/10.1089/ees.1999.16.417

Zwickenpflug, B., Böhler, M., Siegrist, H., Gujer, W., Behl, M., & Neuenschwander, S. (2009). *Einsatz*
von Pulveraktivkohle zur Elimination von Mikroverunreinigungen aus kommunalem
Abwasser. 3. Zwischenbericht. EAWAG.

8 Appendix
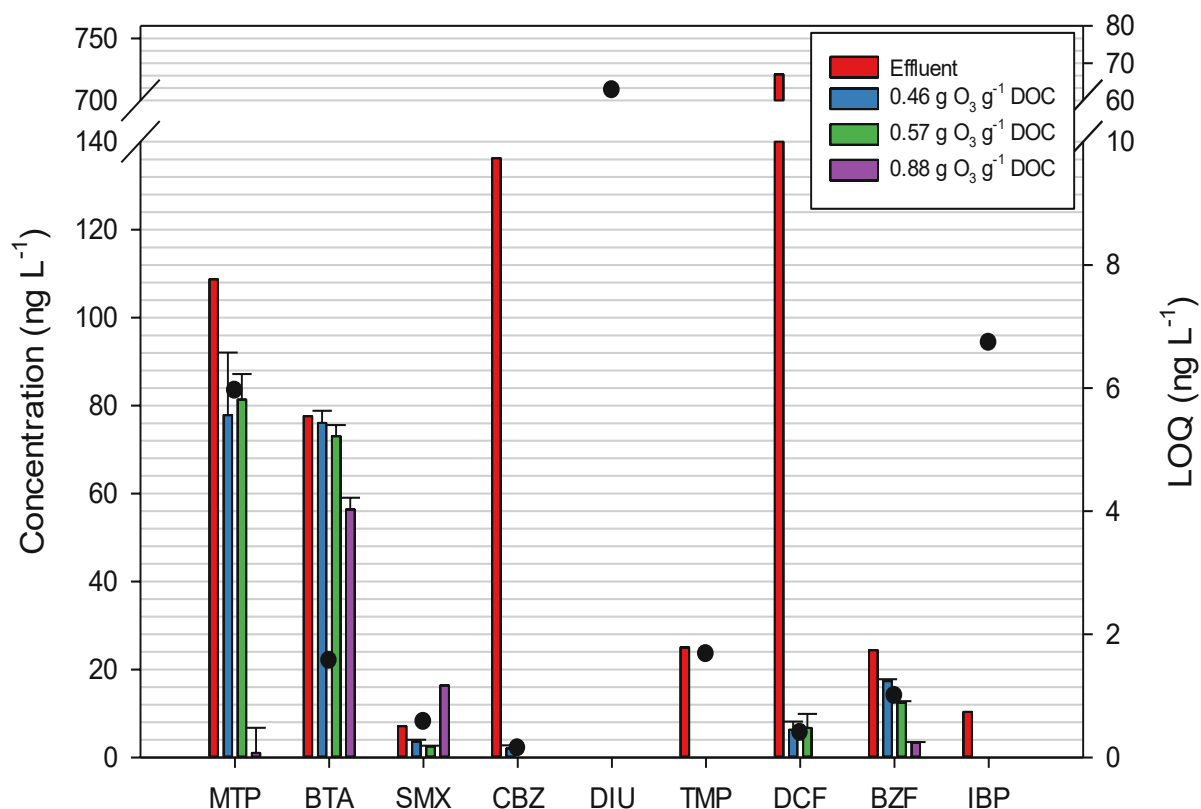
8.1 Samples A1-A3: Ozonation

Figure 28: Detected OMP concentration before and after ozonation including calculated LOQs (black points) in sample A1; dilution factor is taken into account

Figure 28 illustrates the absolute reduction of OMP concentrations in sample A1 for the specific O_3 dose of 0.46, 0.57, and 0.88 g O_3 g^{-1} DOC.

It is evident that some substances are highly removed at the lowest specific O_3 dose. These include DCF, CBZ, and TMP. The first two are reduced from 721 ng L^{-1} and 136 ng L^{-1} to 5 and 2 ng L^{-1}, respectively, after ozonation with 0.4 g O_3 g^{-1} DOC. Other compounds require higher doses to achieve a better removal. These include MTP and BTA. The latter is reduced from 78 ng L^{-1} to 11 ng L^{-1} after ozonation with a specific O_3 dose of 0.88 g O_3 g^{-1} DOC.

Figure 29 depicts the absolute reduction of OMP concentration in all studied samples at the specific O_3 dose range 0.40-0.46 g O_3 g^{-1} DOC. The effluent concentration of a given sample is highly variable between the analyzed compounds. Relatively high variability of effluent concentrations is seen for the compounds BTA, CBZ, DIU, and DCF. DCF showed relatively high values while DIU was detected only in sample A3.
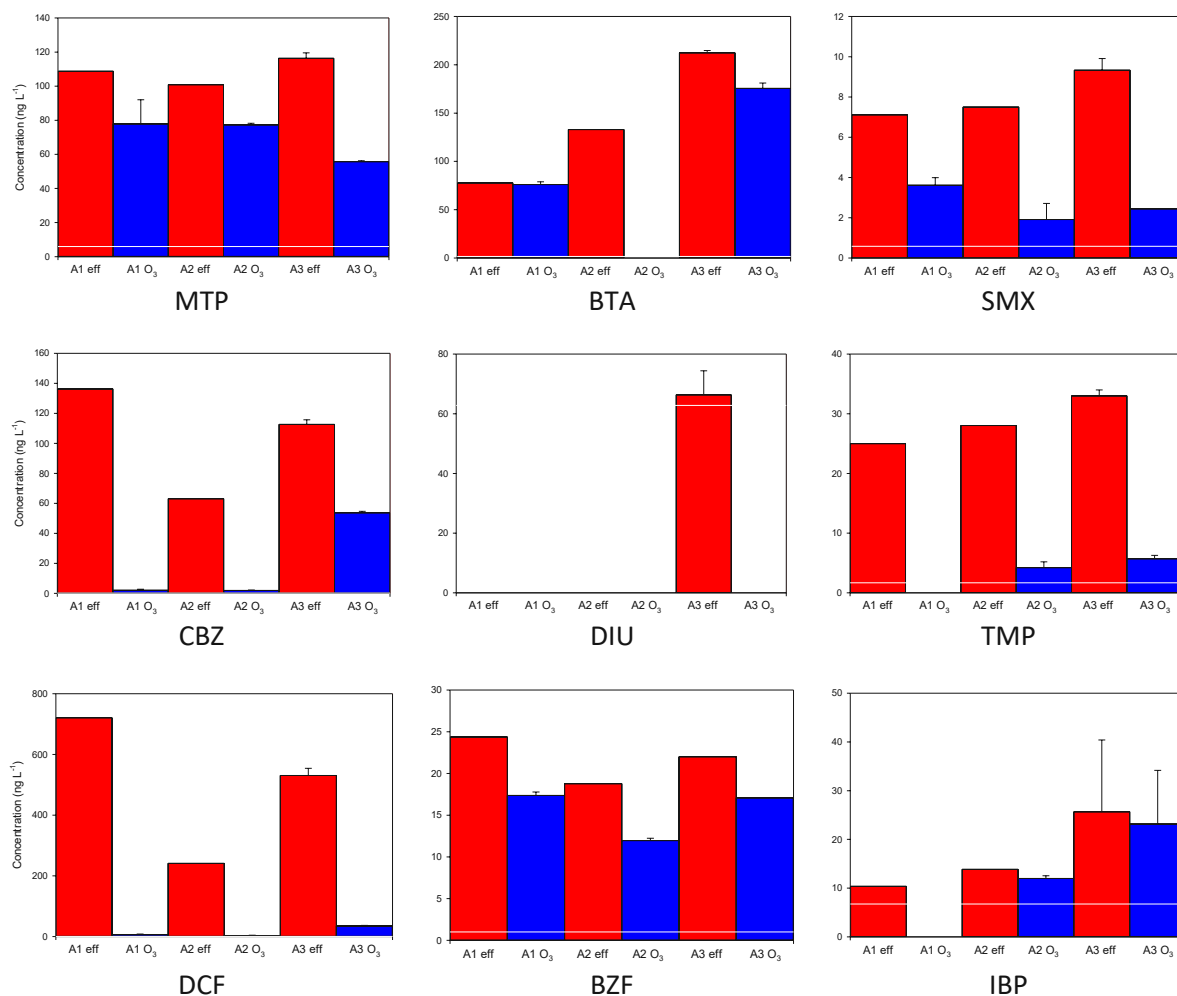
Figure 29: Detected OMP concentration before and after ozonation at the specific O₃ dose of 0.46, 0.45, and 0.40 g O₃ g⁻¹ DOC in samples A1-A3, respectively; white solid line represents the LOQ; effluent samples A1 and A2 did not have replicates; dilution factor is taken into account

8.2 Samples A1-A3: Combination of ozonation and PAC adsorption

Figures 30 and 31 show the absolute removal of OMPs from the effluent via ozonation with a subsequent PAC treatment. The effluent samples A2 and A3 were ozonated with a specific O₃ dose of 0.45 and 0.40 g O₃ g⁻¹ DOC, respectively. Following ozonation, each sample was treated with the specific PAC doses 1.0, 1.5, and 2.0 g PAC g⁻¹ DOC.

From that, the contribution of the adsorption step is low in substances with high O₃ affinity such as DCF and TMP, as the ozonation step resulted in an already significant reduction in concentration. For example, DCF was reduced from 292.3 ng L⁻¹ to 5.5 ng L⁻¹ in sample A2, and a similar trend was observed in sample A3. The subsequent PAC treatment reduced the DCF concentrations to below the LOQ. Substances with an intermediate O₃ reactivity such as MTP, BTA, and BZF are largely affected by the adsorption step. For the removal of BTA, the specific O₃ doses applied were too low to observe a reduction by ozonation. Instead, a reduction was achieved by adsorption to PAC, with higher PAC doses

yielding higher removals. BTA in effluent sample A2 was reduced from 146 ng L^{-1} to 85.7 ng L^{-1} with a PAC dose of 1 g PAC g^{-1} DOC. A similar reduction was observed for BTA in effluent sample A3, which was reduced from 173.1 ng L^{-1} to 68 ng L^{-1} at the same PAC dose. BZF in effluent sample A2 was reduced by ozonation from 20.9 ng L^{-1} to 11.6 ng L^{-1}, and further PAC treatment resulted in concentrations below the LOQ.
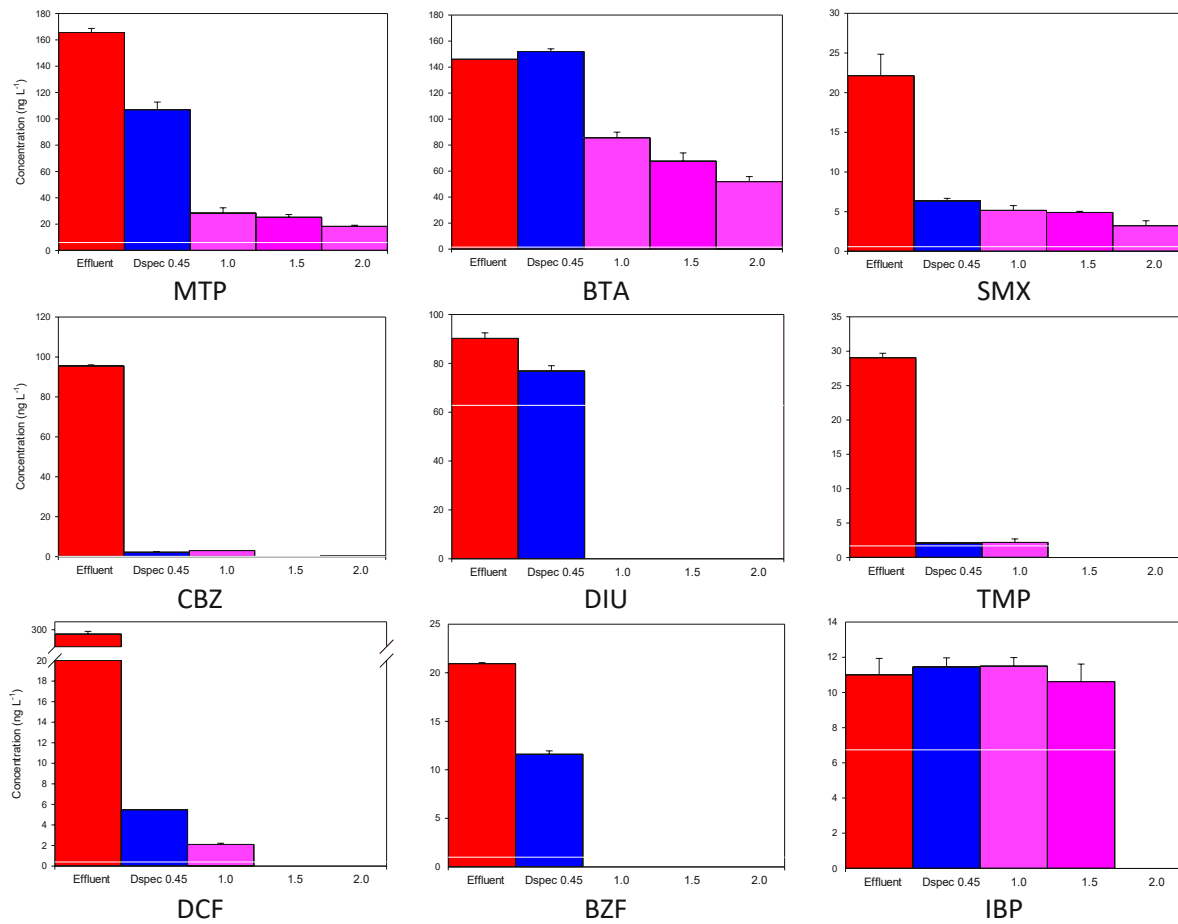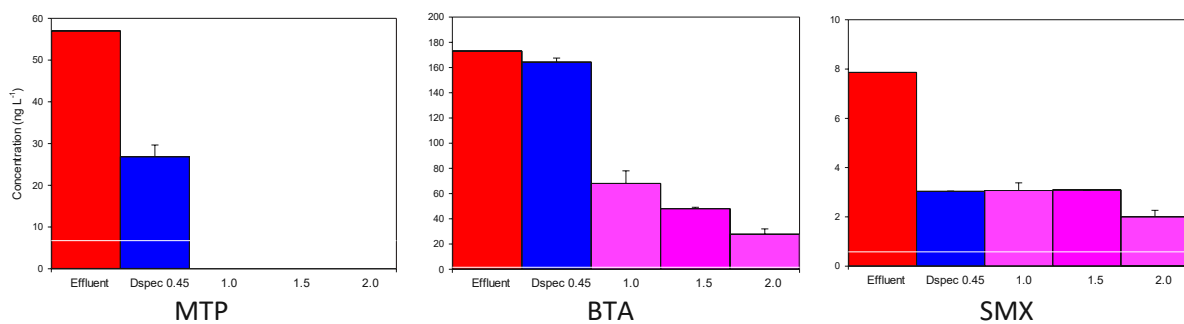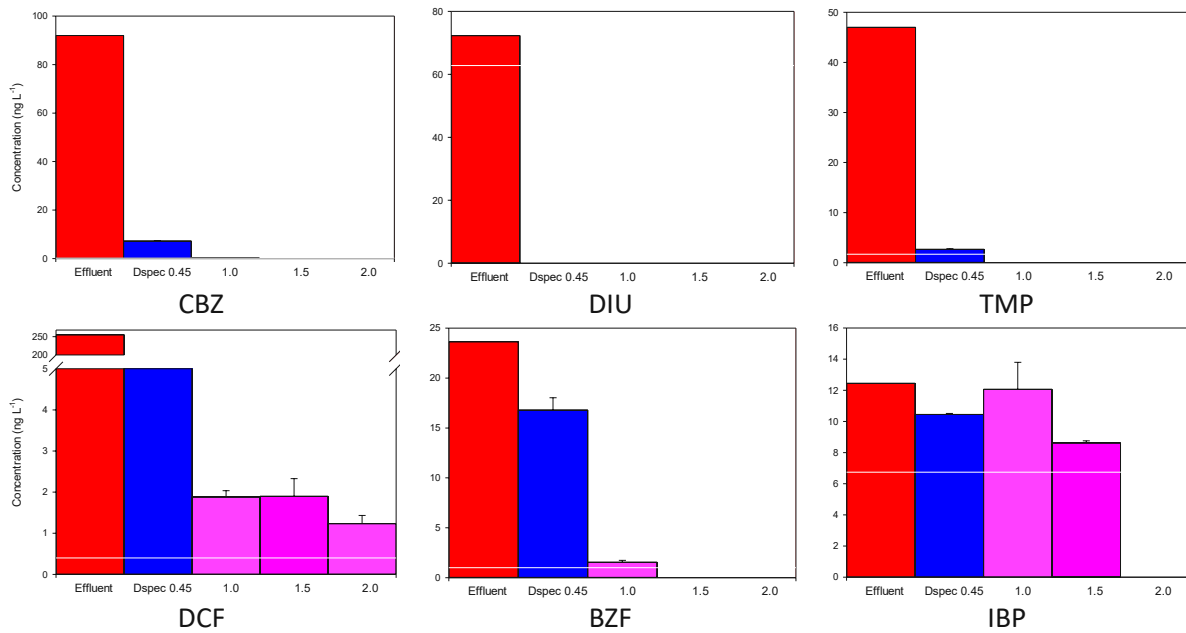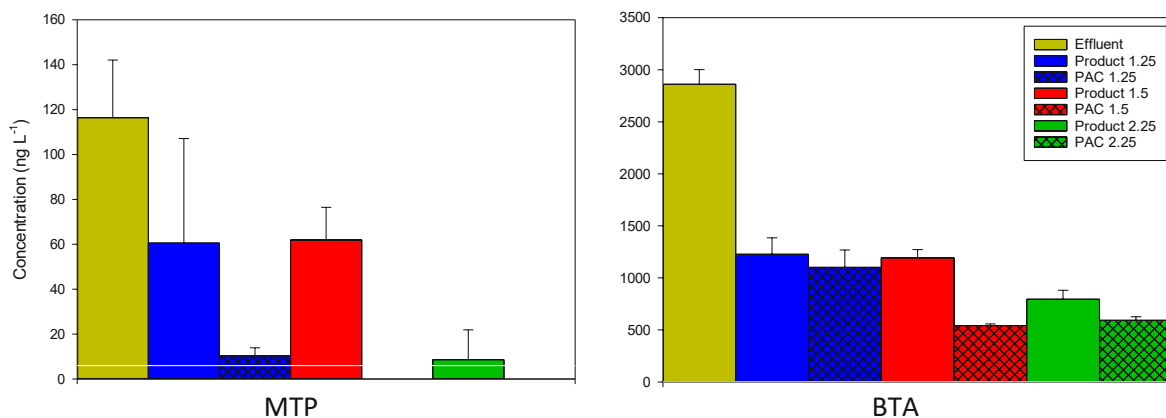

Figure 30: Detected OMP concentration in the A2 effluent (red), ozonated sample (blue), and ozonated sample after treatment with PAC with the doses 1.0, 1.5, and 2. 0 g PAC g^{-1} DOC (green); white solid line represents the LOQ

Figure 31: Detected OMP concentration in the A3 effluent (red), ozonated sample (blue), and ozonated sample after treatment with PAC with the doses 1.0, 1.5, and 2.0 g PAC g^{-1} DOC (green); white solid line represents the LOQ

8.3 Sample B: Comparison between AQUACLEAR B and CARBOPAL®

Figure 32 shows the concentrations in sample B, before and after treatment with either the product AQUACLEAR B or the PAC CARBOPAL®. Clearly, the effluent concentration range of BTA and DCF are higher than MTP and CBZ by an order of magnitude, and higher than SMX by two orders of magnitude. The better performance of the PAC is evident especially for MTP, which was completely abated after a treatment with 1.5 g AC g^{-1} DOC. A treatment of SMX with the product showed no effect. In contrast, the PAC performed better. However, due to the low effluent concentration in comparison to the LOQ its removal wasn't evaluated.
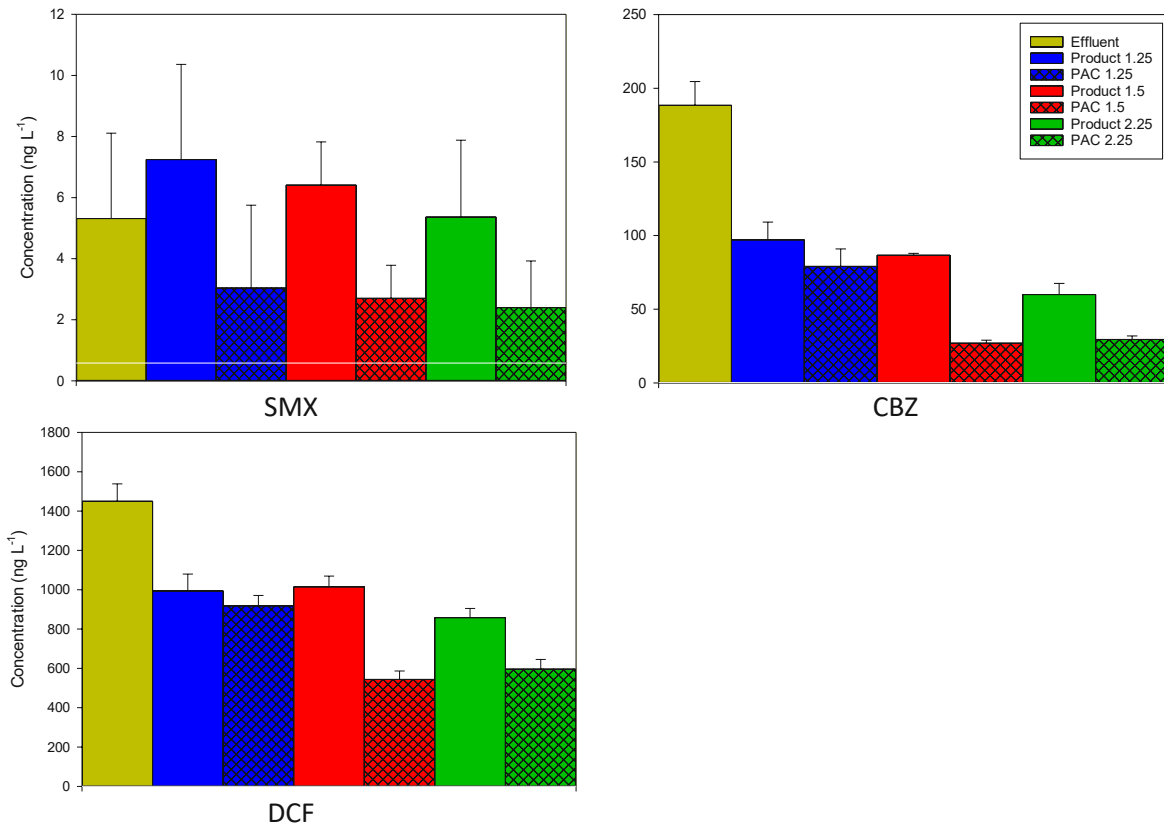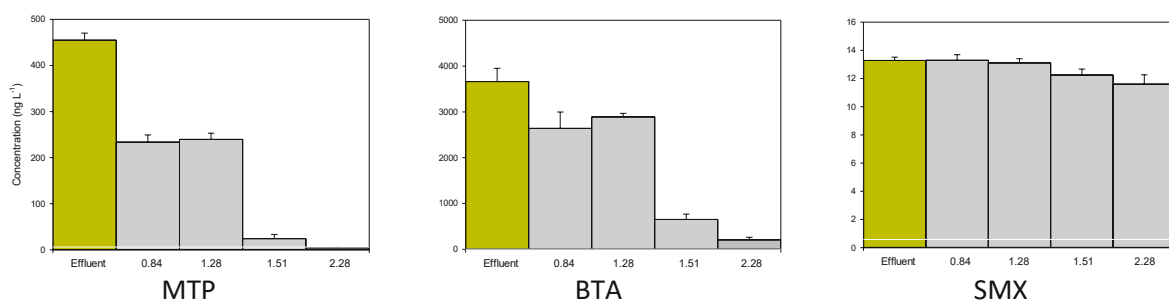
Figure 32: Detected OMP concentration in the B effluent (beige) and the B effluent samples treated with AQUACLEAR B (open bars) and CARBOPAL® (cross-hatched bars) with the doses 1.25, 1.5 and 2.25 g AC g^{-1} DOC; white solid line represents the LOQ

8.4 Sample C: AQUACLEAR A and B

As with sample B, also sample C shows high BTA concentrations, which are in the low single-digit µg L^{-1} range. In comparison, the concentrations of MTP, CBZ, TMP, and DCF are lower by an order of magnitude, while the concentrations of SMX and BZF are lower by two orders of magnitude. The concentration reduction with the specific AC dose is visible when 0.84 g AC g^{-1} DOC was applied. However, no further reduction was achieved at 1.28 g AC g^{-1} DOC. Instead, an increase of the specific AC dose to 1.51 g AC g^{-1} DOC resulted in a further reduction, which is most noticeable for MTP, BTA, CBZ, and TMP. The concentration reduction of SMX by AQUACLEAR throughout the specific AC dose range is clearly very low.
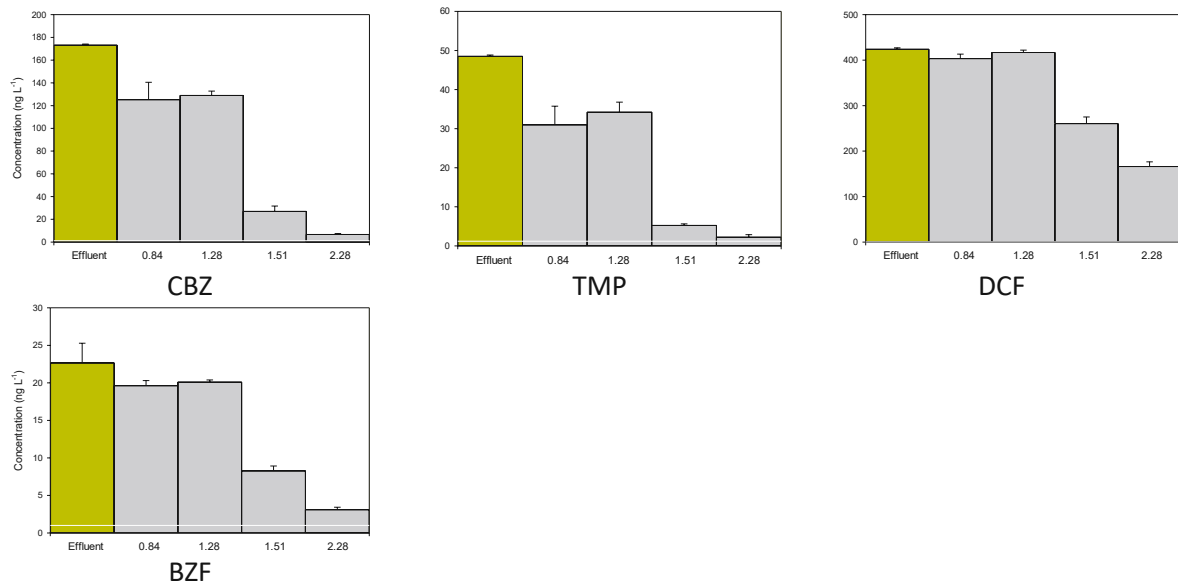
Figure 33: Detected OMP concentration in the C effluent (beige) and in the C effluent samples treated with AQUACLEAR A (0.84-1.28 g AC g^{-1} DOC) and AQUACLEAR B (1.51-2.28 g AC g^{-1} DOC); white solid line represents the LOQ

8.5 Wastewater load and weather conditions

Table 20: Wastewater load and weather conditions during the A1-A3 sampling period

| Sample	Period	Wastewater load (m³/day)	Weather conditions
A1	14.06.2021	94320	Dry
	15.06.2021	97424	Dry
	16.06.2021	97848	Dry
	17.06.2021	100008	Dry
	18.06.2021	97640	Dry
	19.06.2021	89672	Dry
	20.06.2021	86064	Dry
A2	21.06.2021	103904	Rain
	22.06.2021	330712	Rain
	23.06.2021	317408	Rain
	24.06.2021	217280	Rain
	25.06.2021	219192	Rain
	26.06.2021	116560	Rain
	27.06.2021	98520	Rain
A3	28.06.2021		Dry
	29.06.2021	144200	Rain
	30.06.2021	224576	Rain
	01.07.2021	141600	Rain
	02.07.2021	184088	Rain
	03.07.2021	103984	Rain
	04.07.2021	97520	Rain

8.6 BOD$_5$ equation fit
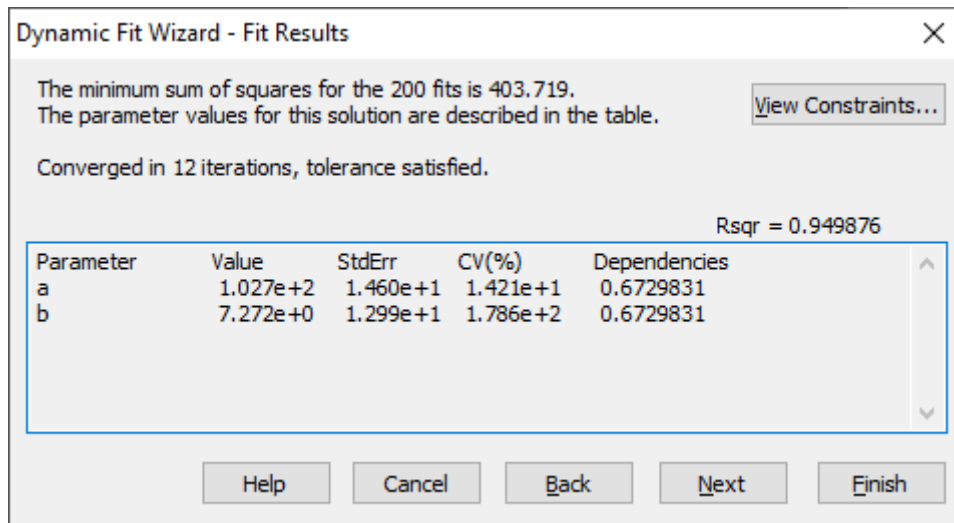
Figure 34: Fitting parameters to the obtained data